Optimization of Passive Solar Design and Integration of Building Integrated
Photovoltaic/Thermal (BIPV/T) System in Northern Housing

Li Ma

A Thesis

in

The Department

of

Building, Civil and Environmental Engineering

Presented in Partial Fulfillment of the Requirements

for the Degree of Master of Applied Science (Building Engineering) at

Concordia University

Montreal, Quebec, Canada

December 2019

CONCORDIA UNIVERSITY

School of Graduate Studies

This is to certify that the thesis prepared

By: Li Ma

Entitled: Optimization of Passive Solar Design and Integration of Building Integrated Photovoltaic/Thermal (BIPV/T) System in Northern Housing

and submitted in partial fulfillment of the requirements for the degree of

Master of Applied Science (Building Engineering)

complies with the regulations of the University and meets the accepted standards with respect to originality and quality.

Signed by the final Examining Committee:

_____ Chair
Dr. Radu Zmeureanu

_____ Examiner
Dr. Luiz A. C. Lopes

_____ Examiner
Dr. Andreas Athienitis

_____ Supervisor #1
Dr. Hua Ge

Approved by _____
Dr. M. Nokken, GPD
Department of Building, Civil and Environmental Engineering

December 5 2019 _____
Dr. Amir Asif, Dean
Gina Cody School of Engineering and Computer Science

ABSTRACT

Optimization of Passive Solar Design and Integration of Building Integrated Photovoltaic/Thermal (BIPV/T) System in Northern Housing

Li Ma

With the growing concerns about climate change, Northern Canada is aiming to adopt a "net-zero ready" model building code by 2030. Northern Canada has its unique environmental loads and challenges – namely, the extremely cold climate and the high expense, as the north imports most of its materials and fuel from the south. Significant energy savings could be achieved by optimizing the design of building envelopes and integrating solar design strategies, with a little added construction cost. This thesis focuses on optimizing the passive solar design parameters and the use of thermal and electrical energy from building integrated photovoltaic/thermal (BIPV/T) system as moves toward net-zero energy housing in northern Canada. A reference house representing the typical residential building in northern regions is modeled in EnergyPlus software to study the building design parameters, including thermal resistance of the building envelope, thermal mass, window-wall ratio, shading schedule and ventilation rate. The optimization is carried out by coupling EnergyPlus and Matlab using a multi-objective genetic algorithm. The optimal house under a 25-year life cycle in Yellowknife, NWT, could achieve a 46% energy savings with an initial construction cost increase of 10%. Based on this optimized house, the optimal use of thermal energy produced by a BIPV/T system is evaluated by integration with the space heating system, heat recovery ventilation (HRV) and air-source heat pump (ASHP). Simulation results show that a BIPV/T system with a space heating system can reduce total energy consumption by 15.5%, a BIPV/T system with a HRV could decrease the frost risk time by 8.8% and defrost time by 7.8%, and a BIPV/T system with an ASHP could extend the ASHP working period by 128 hours and increase the annual COP about 2.5%.

ACKNOWLEDGMENTS

I would like to start my acknowledgments by expressing my sincere gratitude to my supervisor, Dr. Hua Ge. She has provide me with a really interesting research topic in energy conservation in residential buildings, and this is the area I would like to work on in my future career. During my research, her expertise and patience supported me greatly from the very beginning and step by step until I completed the research. She also let me join the Solar Decathlon 2018 project to see how a low-energy building being designed, constructed and operated. It was a precious and enjoyable experience.

Special thanks to Dr. Bruno Lee, not only for his passive solar building design course, which provided me with a general understanding of building design parameters that lower the energy demand/consumption, but also because in meeting during my reaserch operation period he shared valuable information that led me to develop the optimization process for my study.

My sincere thanks also goes to Dr. Lin Wang, the postdoctoral scholar with Dr. Ge. He first supported me during the verification of my BIPV/T Matlab code and later on helped me with the thesis structure and reviewing. I really appreciate all his efforts and time spent on my research. And I send my gratitude to Asok Thirunavukarasu, M.A.Sc. He helped me understand his research and passed me useful material before his graduation to support me in continuing research based on his.

I would like to thank Ph.D. students Stratos Rounis and Zissis Ioannidis for helping with my BIPV/T simulation code in Matlab, master's student Daniel Baril for sharing building construction information for northern Canada, and master's student Felipe Andres Merino Gordo for helping me solve some modeling questions in EnergyPlus.

I would like to say thank you to my friends and colleagues in the office, Fangwei Pu, Firouzeh Souri, Cheng Zhang and Xin Zhang, for bringing happiness during the school years. They are the people I felt comfortable turning to and talking about the difficulties I was facing during the research.

Finally, I want to send my appreciation to my parents, who support me, comfort me and encouraged me during my master's years.

Table of Contents

List of Figures

List of Tables

Nomenclature

Symbols

A_{surf}	area of surface	m^2
A_{pv}	area of BIPV/T, also refer to the project area of the bottom/back surface	m^2
$Area_{window}$	window area	m^2
c_p	specific heat of the air	J/kg·K
C_i	thermal capacity of node i	J/K
D_h	hydraulic diameter	m
E_{elec}	electricity generated by BIPV/T	W
f_{activ}	fraction of surface area with active BIPV/T collector	-
f_{bypass}	fraction of the airflow rate that bypasses BIPV/T collector	-
G_T	solar radiation on BIPV/T surface	W/m^2
h_c	convective coefficient	W/m^2·K
$h_{c,b}$	convective coefficient between the cavity air and cavity bottom surface	W/m^2·K
$h_{c,p}$	convective coefficient between PV panels and the cavity air	W/m^2·K
h_o	exterior air film coefficient	W/m^2·K
h_r	radiation coefficient	W/m^2·K
$I_b/I_{ds}/I_{dg}$	Beam diffuse or ground-reflected solar radiation	W/m^2
I_t	solar radiation falls on the south roof	W/m^2
k	thermal conductivity	W/m·K
$\dot{m}$	entire mass flow of the air through the BIPV/T	kg/s
M	volume flow rate of the air	m^3/s
Nu	Nusselt number	-
Pr	Prandtl number, ν/α	-
q_i	Heat source ay node i	W/m^2
Q_{therm}	thermal energy collected by BIPV/T	W
Q_{window}	total solar energy transmitted through the window	W
$R_{(i,j)}$	Thermal resistance value between node i and j	m^2·K /W
$R_{i,j}^f/R_{j,i}^b$	window front and the back reflectance from layer i to layer j	-
$R_{ins+roof}$	the thermal resistance contains the extra RSI 1 insulation on the bottom surface and the thermal resistance of the roof	m^2·K/ W
Re	Reynold number, $\rho V D_h/\mu$	-
$SHGC_b(\theta)/$ $SHGC_{ds+dg}$	solar heat gain coefficient of beam radiation, diffuse and reflect radiation	-
T_a	temperature of the air in BIPV/T cavity	˚C
$T_{a(mean)}$	average temperature of T_a at each section	˚C
T_{attic}	temperature of the attic	˚C
T_{bot}	temperature of the bottom surface of PV/T cavity	˚C
$T_b(\theta)/T_{diff}$	window beam and diffuse transmittance	-
T_i^{p+1}/T_i^p	Temperature of node i in time steps	˚C
$T_{i,j}$	window transmittance from layer i to layer j	-
T_{in}	temperature of the air entering the BIPV/T	˚C
T_m	mean temperature of PV temperature and bottom surface temperature	˚C
T_o	temperature of outdoor air	˚C
T_{out}	temperature of the air leaving the BIPV/T	˚C
T_{pv}	temperature of the BIPV/T panel	˚C
$T_{set,out}$	temperature set-point at the node of the air leaving the BIPV/T	˚C
Δt	time step	
V	air velocity	m/s
V_{wind}	wind speed on building surface	m/s
w	width of the PV/T cavity	m
x	distance from the air inlet vent in BIPV/T	m

Greek letters

ρ	density of the air	kg/m^3
$\eta_{thermal}$	thermal conversion efficiency	-
η_{elec}	electrical efficiency	-
η_{total}	total efficiency	-
α_{pv}	absorptivity of PV panels	-
σ	Stefan-Boltzmann constant	W/m$^2 \cdot$K^4
ε_{pv}	emissivity of the inside face of the PV panels	-
ε_{pv}	emissivity of the inside face of the bottom surface	-
μ	dynamic viscosity of air	Pa$\cdot$s=N$\cdot$s/m^2= kg/(m$\cdot$s)
α	thermal diffusivity of air	m^2/s
ν	kinematic viscosity of air	m^2/s
θ	incident angle of solar radiation	°

Abbreviations and Acronyms

ACH	air change per hour
AFT	advanced framing techniques
ANN	artificial neural networks
ASHP	air-source heat pump
BIPV/T	building integrated photovoltaic/thermal
CCASHP	could climate air-source heat pump
CMHC	Canada mortgage and housing corporation
DG	double glazing
DG+SF	double glazing with suspended film
DHW	domestic hot water
EA	evolutionary algorithm
GA	genetic algorithm
GA-RF	genetic algorithm with refine process
GBP	good building practice for northern facility
GHG	greenhouse gas
HDD	heating degree-days
HP	heat pump
HRV	heat recovery ventilation
HVAC	heating, ventilation and air conditioning
IAQ	indoor air quality
IHA	Inuvik housing authority
MNECH	model national energy code for house
MOGA	Multi-objective genetic algorithm
NBCC	national building code of Canada
NECC	national energy code of Canada for building
NHC	Nunavut housing corporation
NRC	national research council of Canada
NRCan	natural resources Canada
NSGA-II	non-dominated sorting genetic algorithms
NSH	northern sustainable house
NU/NT	Nunavut (Canada)
NWT	Northwest Territories (Canada)
NWTHC	Northwest Territories housing corporation
PR-GA	preparation process and genetic algorithm
PSO	particle swarm optimization
QC	Quebec (Canada)
SA	simulated annealing optimization
SIPs	structural insulated Panels

SVM	support vector machines
TNM	thermal network model
TG	triple glazing
WWR	window-wall ratio
YHC	Yukon housing corporation
YT	Yukon (Canada)

Chapter 1   Introduction

1.1 Background

According to the International Energy Agency, across the globe, residential buildings account for 20% of all end-use energy, and half of which is consumed by space heating (International Energy Agency, 2018). In Canada, as Figure 1-1 (a) shows, 28% of all energy used is consumed by buildings, and residential buildings take the major part, consuming 17% of the total energy (Energy Resources Canada, 2019). Residential building energy consumption is significant, and reducing energy use in buildings will considerably reduce the total national energy consumption, which will also have a significant impact on lowering greenhouse gas (GHG) emissions. In 2017, Build Smart – Canada's Buildings Strategy – set a goal that provinces and territories will adopt a "net-zero energy ready" model building code by 2030 (Energy and Mines Ministers' Conference, 2017). To realize the net-zero energy building, reducing energy use is the first priority, as space heating account for 61% of residential energy used (Figure 1-1(b)), and a properly designed house is required to minimize the heating requirement.

2016 Canada Energy Use (PJ)
(Total: 8,786.4)

Total Transportation
2,617.9
30%

Agriculture
299.1
3%

Residential
1,458.2
17%

Industrial
3,413.8
39%

Commercial/
Institutional
997.4
11%

2016 Canada Residential Energy Use (PJ)   (Total: 1.458.2)

Water Heating
284.3
19%

Space Heating
885.1
61%

Appliances
198.3
14%

Lighting
53.6
4%

Space Cooling
37.0
2%
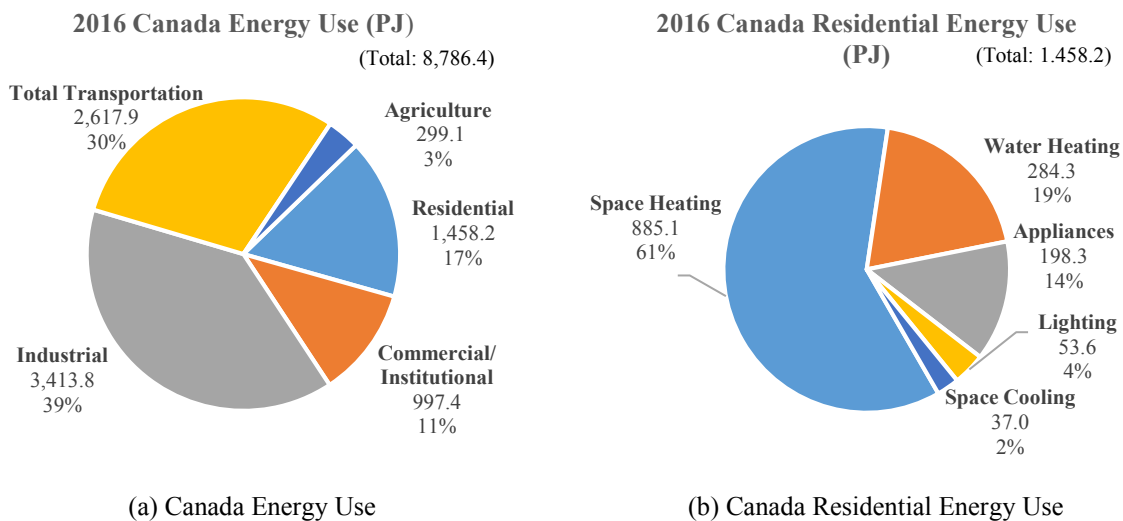
(a) Canada Energy Use   (b) Canada Residential Energy Use
Figure 1-1 Energy use in Canada 2016 (Energy Resource Canada, 2019)

The use of renewable energy is another way to move houses to net-zero. This self-sufficiency of the house has always been a key factor for survival in a harsh climate among the small, isolated communities in the far north of Canada (CMHC, 2007). In northern Canada, there is a large potential for using solar energy (Figure 1-2). A building integrated photovoltaic/thermal (BIPV/T) system not only could function as the outer layer of the envelope but also could generate electricity

and produce thermal energy. The generated electricity can be used on-site to reduce the amount of electricity from the grid and save money for the homeowner. The thermal energy from a BIPV/T system can be integrated with different mechanical systems, such as the space heating system, heat pump system (HP) and heat recovery ventilation system (HRV), for reducing heating demand or improving system efficiency.
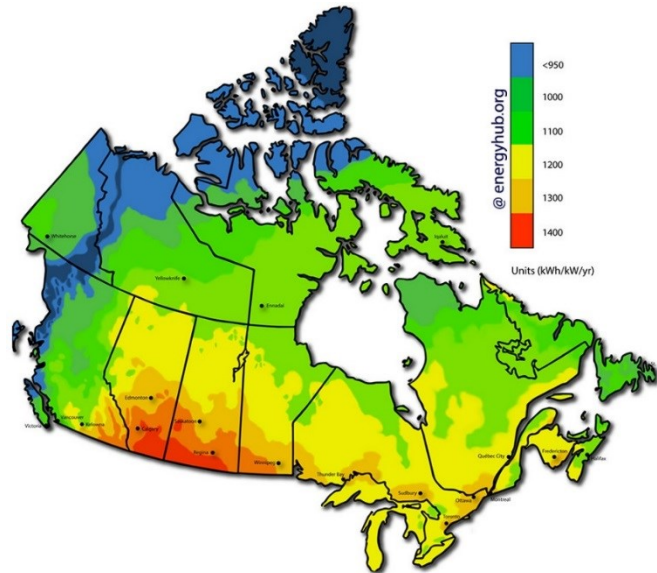
Solar irradiation was calculated using the "municip_kWh" spreadsheet from the *photovoltaic potential and insolation dataset* from Natural Resources Canada. Average annual irradiation where the installation angle equals degrees latitude -15 from the top five populated cities from each province was used. A 25% efficiency loss factor was then applied before getting the final kWh/kW/yr number.

Figure 1-2 Solar energy map of Canada (Energyhub)

1.2 Problem Statement

The Territories in the north of Canada occupy 4 million km^2, which account for 40% of Canada's landmass. Across this vast land, a population of 117,000, roughly 0.3% of Canada's population, is sparsely distributed in 72 communities, with most of the population gathered in capitals (Iqaluit, NU; Yellowknife, NWT; and Whitehorse, YT) (Canadian Northern Economic Development Agency, 2016; World Population Review, 2019). Nunavik, a Quebec region, which is the north of the 55th parallel, also faces the same situation, a vast land (500,000 km^2) with a small population distributed in 14 northern villages, with populations ranging from 200 to 2,400 (Société D'habiation du Québec, 2014).

Due to the sparse population and remoteness, northern communities have to deal with a lack of transportation infrastructure. Furthermore, in some areas, there are few or even no transportation alternatives. During an infrastructure failure, the northern communities would be cut off from goods from the south. Meanwhile, due to the extreme weather and remote location, constructing and operating transportation infrastructure becomes much more challenging and costly (Bristow & Gill, 2011). The lack of transportation infrastructure connecting with southern communities means the costs of all imported materials and fuels are higher than the Canadian average (Société D'habiation du Québec, 2014; National Energy Board of Canada, 2011).

The climate of northern Canada is particularly harsh; generally, the number of heating degree-days (HDD) for the north is over 8,000, and the further north region is much colder, with HDD reaching 12,000 or more (Canada Weather Stats; Government of Canada). The long and cold winter in the north leads to the requirements for a well-performing house: a super-insulated envelope to prevent heat loss during the heating season, with no penetrations serving as thermal bridges; a continuous and high-performing air and vapor barrier to stop air leakage and vapor diffusion, which not only lead to large heat losses but also create moisture problems in the building assembly; an elevated floor with ventilated air space beneath it to avoid heat transfer to the soil melting the permafrost; and a properly designed roof to deal with snow and ice dams as well as blown-in snow in the attic space, which would contribute moisture in the envelope when the temperature rises (Lstiburek, 2009). The long winter and harsh winter also results in a short house construction and material shipping period.

Laborers in the north are mostly at a low education level, and there is a limited number of skilled professionals (Canadian Northern Economic Development Agency, 2016). When hiring labor from the south, the logistics fees – which include travel, food and lodging – are much higher than the salaries.

The north needs a high-performing house against the extremely cold climate, while a lack of infrastructure, a short construction and shipping period, and construction labor from south all add hugely to the total construction cost. To provide a cost-effective low-energy house in the north, all the design parameters need to be balanced to ensure the add-on cost for better performance remains

a small portion of the total cost, one that could be offset by the energy savings over an acceptable period – namely, its life cycle.

1.3 Research Objectives

The objectives of this thesis are as follows:

- To optimize passive design to reduce house energy demand using a genetic algorithm method that balances the initial construction cost and operational energy cost. The optimal building envelope design parameters suitable for Canada's northern region are identified. These passive design parameters include the thermal resistance of walls, ceiling and floor; windows; window-wall ratio; thermal mass and strategies to avoid overheating.
- To investigate the potential benefits of integrating BIPV/T system with mechanical systems to generate energy, improve system efficiency and performance, and decrease energy consumption of the optimized house.

1.4 Outline of the Thesis

This thesis includes the following chapters.

Chapter 2 – Literature Review. This chapter includes four parts: northern house codes, northern house projects and research, optimization algorithm and BIPV/T system. The northern house codes and projects represent the current status of northern houses. The optimization algorithm section summarizes recent optimization research studies, mainly focusing on the simulation software and algorithm platforms of previous studies and the investigated parameters. The BIPV/T system section reviews the integration of an air-based BIPV/T system with other house systems and its effect on the energy performance of houses.

Chapter 3 – Optimization of Passive Design Parameters. A reference house prescribed by the National Building Code of Canada (2015) is modeled, and the multi-objective genetic algorithm (MOGA) method is used to optimize the reference house design to determine the optimal

combination of passive design parameters using EnergyPlus as simulation software and Matlab as an algorithm platform.

Chapter 4 – Solar Strategy Applied to the Optimized House. Based on the optimized house from Chapter 3, a BIPV/T system is integrated with the house's mechanical systems, including the space heating system, HRV system and HP system. This chapter presents an analysis of the energy performance of different integration strategies.

Chapter 5 – Conclusion. This chapter summarizes the key findings and main contributions of this thesis.

Chapter 2   Literature Review

This literature review chapter includes four sections. The first section presents the current codes and standards for Canada, especially for northern Canada. The current codes and standards do not explicitly involve solar strategies, and some requirements are not sufficient for the harsh climate in northern Canada. The basic requirements prescribed in codes and standards provide a baseline for the further optimization of houses. The second section analyzes some northern projects to introduce the features and energy systems used in high-performance northern houses that designed for the cold climate with low energy consumption and that are suitable for the local residents' lifestyle and culture. Also in this section, the review of recent research on northern housing presents the study of improving energy efficiency for northern housing. The chapter's third section is a review of recent literature on building optimization and covers the commonly used optimization methods including the algorithms, optimization tools and building performance assessment models, and the involved variables and objectives. These serve as a reference source for developing the optimization methodology used in this research that is appropriate for housing design in the far north region of Canada. The fourth section reviews the application of air-based building integrated photovoltaic/thermal (BIPV/T) system coupled with different energy systems to improve overall energy efficiency.

2.1 Codes and Standards for Northern Housing

2.1.1 National Building Code of Canada

The National Building Code of Canada (NBCC 2015) is published by the National Research Council of Canada (NRC) and developed by the Canadian Commission on Building and Fire Codes. It is an objective-based National Model Code that can be adopted by provincial or territorial governments without change or with modifications to suit the requirements within their jurisdictions.

The NBCC provides the requirements for each climate zone – namely, Zone 4, Zone 5, Zone 6, Zone 7A, Zone 7B and Zone 8. These zones are divided according to heating degree-days (HDD), and as the HHD for northern Canada is greater than 8000, it is all located in Zone 8. The Code

prescribes the minimum thermal resistance for different types of envelopes and fenestrations and also defines the required window types and ventilation rate for each type of room, such as kitchen, bedroom and basement. The Energy Performance Compliance section provides the temperature setpoints for heating and cooling in the energy performance simulation.

2.1.2 R-2000

The R-2000 standard (R-2000, 2012), developed by Natural Resources Canada (NRCan), is a voluntary national standard formalized in 1981 and periodically updated. The goal of the R-2000 standard is to improve the energy-efficiency of new houses without compromising either the interior or exterior environment. The standard also provides sections on construction techniques, building products, mechanical equipment, lighting and appliances to offer flexibility for builders.

The R-2000 standard addresses five areas to achieve a state-of-the-art energy-efficient house: building envelope requirements, mechanical system, energy performance targets, indoor air quality (IAQ) and water conservation and environmental features. For passive design parameters, the standard sets the minimum insulation levels that meet or exceed the provincial or local requirements. The airtightness requirements specified a maximum air infiltration rate is of 1.5 air change per hour (ACH) at 50 Pa. The standard also specifies the minimum requirements for windows, which must be double-glazed windows with a low-emissivity coating; an inert gas fill; and an insulated spacer with a wood, vinyl or fiberglass frame. For energy performance, the standard sets the energy target for space heating and domestic hot water (DHW), which should be 50% of the calculated results from the current version of HOT2000, an energy simulation and design tool for low-rise residential buildings, and it provides the energy target equations with detailed settings information.

The technical requirements of R-2000 are in addition to provincial or local building codes rather than being a substitute for them. If there is an absence of provincial or local building codes, then the requirements in R-2000 should refer to the current version of the National Building Code of Canada (NBCC).

2.1.3 Good Building Practice for Northern Facilities

The primary objective of Good Building Practice for Northern Facilities (GBP, 2011) is to serve as a reference handbook to support builders in developing the best value in northern buildings. By achieving the energy target in the National Energy Code of Canada for Buildings 2011 (NECC), efficient buildings in the north should use less energy, both fossil fuel and electricity, and use them as efficiently as possible. GBP highlights that during building design the envelope should be airtight and well insulated; the vapor and air barrier should be properly installed; thermal bridging should be minimized and other building features such as siting, orientation, daylighting, solar gain and shading should be optimized. It also recommends that the building system should be simple and easy to operate.

In GBP, detailed information is presented on five aspects of building: site work, architectural, structural, mechanical and electrical. To achieve a better-performing building, the insulation should be located on the cold side and should be continuous; a minimum envelope thermal resistance is also suggested. As the north has permafrost, the building floors are often elevated above ground to eliminate heat flow that might thaw susceptible soils. The maximum air leakage rate is set at different values based on the indoor air relative humidity. GBP recommends windows be double-glazed sealed units with low-"E" coating or triple-glazed sealed units.

Energy sources for northern buildings also need to be considered. GBP recommends using natural gas, propane or biomass as the heating source if they are available, since these energy sources are more economical than oil. It also recommends considering wind, solar and geothermal as alternative energy sources. Electricity can be considered as a primary heating fuel source where cheaper-rate interruptible power is available, when the house has a permanent heating system as a backup.

2.1.4 Summary

One of the objectives in this research is to minimize the energy demand of a residential house by optimizing the passive design parameters, including envelope thermal resistance, window type, airtightness, ventilation and temperature set-point. The current codes and standards for Canada

prescribe requirements for those parameters, although local codes may have stricter requirements than the national code. The detailed requirements are listed in Appendix A, and these provide the baseline for the reference house to be used for the optimization. However, the current codes and standards do not include suggestions or requirements for thermal mass and window-wall ratio, and passive solar strategies to fully use solar heat gain during the winter are also not mentioned. These two features are involved in the optimization in this research, and examples are provided to show how they could benefit the house's energy savings. Furthermore, active solar systems are also not addressed in the codes or standards.

2.2 Northern House Project and Research

2.2.1 Northern Sustainable House

The Northern Sustainable House (NSH) is a project funded by Canada Mortgage and Housing Corporation (CMHC) in collaboration with local housing corporation and construction. The two objectives of the project are to design and build northern houses with its energy consumption 50% less than that of similar housing specified by the 1997 Model National Energy Code for Houses (MNECH) and to promote culturally appropriate housing in the north (CMHC, 2009). The four buildings constructed under this project are located at Arviat, Nunavut (CMHC, 2014a); Dawson City, Yukon (CMHC, 2014b; CMHC, 2014c); and Inuvik, Northwest Territories (CMHC, 2014d). The features of these four projects are summarized in Table 2-1, and the locations are placed on the map in Figure 2-1.

Figure 2-1 Northern Sustainable House (NSH) locations

Table 2-1 Summary of Northern Sustainable House (NSH) features

	Arviat, Nunavut	Dawson City, Yukon E/2	Dawson City, Yukon E/9		Inuvik, Northwest Territories	
			Solar Unit	Flex Unit	Unit A	Unit B
Building Area	**142 m²** footprint and **105 m²** heated floor area	**141.41 m²** heated floor area	**150.3 m²** footprint and **138.8 m²** heated floor area	**150.3 m²** footprint and **120.9 m²** heated floor area	**247 m²** footprint and **210 m²** heated floor area	
Building Axis	Southwest-Northeast	East-West	South-North		Southwest-Northeast	
Wall	**RSI-8.0 (R-46)** Type: Double wall, 38 x 140 mm (2 x 6 in) exterior wall, 12-mm (1/2 in) air gap, 38 x 89 mm (2 x 4 in) interior wall and 38 x 38 mm (2 x 2 in) horizontal strapping with 38-mm (1.5 in) rigid insulation	**RSI-7.2 (R-41)** Type: Double-stud wall, 38 x 184 mm (2 x 8 in) stud with batt insulation, 38 x 89 mm (2 x 4 in) strapping with batt insulation	**RSI-8.4 (R-47.5)** Type: Structural insulated panel (SIP) with additional 38 x 89 mm (2 x 4 in) interior wall		**RSI-8.8 (R-50)** Type: Double-wall, 38 x 89 mm (2 x 4 in) exterior wall, 89-mm (3 1/2 in) insulation, 38 x 89 mm (2 x 4 in) interior wall	
Ceiling/Roof	**RSI-11.6 (R-66)** Type: Shed-style roof, deeper joist with one more batt insulation	**RSI-10.6 (R-60)** Type: Raised-heel engineered roof trusses with blown-in insulation	**RSI-14.1 (R-80)** Type: Roof truss with blown-in insulation		**RSI-14.1 (R-80)** Type: Raised-heel roof trusses with blown-in insulation	
Floor	**RSI-9.1 (R-52)** Type: Truss joist I-beams with batt and rigid insulation over crawlspace	**RSI-7.8 (R-44)** Type: Engineered floor joist with batt insulation over unheated crawlspace	**RSI-7.8 (R-44)** Type: Engineered floor joist with batt insulation over unheated crawlspace		**RSI-9.3 (R-53)** Type: Structural insulated panel (SIP) on a steel-space frame foundation	
Window	**RSI-0.92 (R-5.2)** Type: Triple-glazed, argon-filled, fiberglass-frames windows	**RSI-0.97 (R-5.5)** Type: Triple-glazed, low-E windows	**RSI-0.97 (R-5.5)** Type: Triple-glazed, low-E windows		**RSI-0.97 (R-5.5) - South** **RSI-0.74 (R-4.2) - North** Type: Duplex feature high-performance, triple-pane, fiberglass-framed window on south side. Quadruple-pane fiberglass window with higher thermal insulating value and lower solar heat gain coefficients on north side	

				19 m² in total South glazing-to-floor ratio: 9.0% (10.9 m²)		
Window Area	**9.64 m²** in total South glazing-to-floor ratio: 7.2% (7.57 m²)	**17.5 m²** in total South glazing-to-floor ratio: 4.5% (6.4 m²)	**19.4 m²** in total South glazing-to-floor ratio: 6.9% (9.6 m²)		**27.7 m²** in total South glazing-to-floor ratio: 5.29% (11.1 m²)	
Airtightness	**1.4 ACH at 50 Pa**	**1.7 ACH at 50 Pa**	**0.75 ACH at 50 Pa**	**0.83 ACH at 50 Pa**	**2.36 ACH at 50 Pa**	**2.7 ACH at 50 Pa**
HRV	**Yes** Type: 55% efficiency at -25 ˚C (-13 ˚F), and 62.5% efficiency at 0 ˚C (32 ˚F), two-speed 20 or 50 L/s (39 or 98 CFM). Inlet air preheated by a preheat coil	**Yes** Type: Inlet air preheated by a hot water coil from the boiler, 45 L/s (95 CFM) speed	**Yes** Type: 45 L/s (95 CFM) speed		**Yes** Type: Inlet air preheated by a preheat coil. Heat recovery has 89% efficiency at -25 ˚C (-13 ˚F), and 83% efficiency at 0 ˚C (32 ˚F)	
Space Heating	**Oil-fired boiler with hydronic baseboard heater** Type: Boiler with 86% efficiency and 98 MBH output capacity	**Oil-fired boiler with hydronic baseboard heater** Type: Boiler is 70,000 BTU high-efficiency	**Electric baseboard heaters** Type: 500-W baseboard placed under small windows of living room, entry and bathroom. 1,000-W baseboard placed in the remaining windows of living room, dining room and bedrooms. 300-W baseboard placed in laundry room		**Natural gas boiler with radiant baseboard** Type: Boiler has a maximum output of 141,000 BTU/h with 96% efficiency	
Domestic Hot Water	**Oil-fired boiler with tank** Type: Boiler with 86% efficiency and 98 MBH output capacity. Hot Water Tank with 151-L (40-US-gallon) capacity. Water holding tank with 1,500-L (400-US-gallon) capacity	**Electric hot water heater** Type: 150-L (40-gallon) capacity	**Solar thermal collector and electric water heater with tank** Type: 3.0-m² (32-ft²) solar thermal collector mounted at a 60-degree slope on south porch roof as primary source. Preheat tank with 320-L (85-US-gallon) capacity. Electric hot water heater with 150-L (40-US-gallon) capacity and 0.9 efficiency as backup source	**Electric hot water heater** Type: 150-L (40-gallon) capacity and 0.9 efficiency	**Solar collector and boiler with tank** Type: 4 flat-plate solar collectors mounted on 75-degree angled south-facing roof to preheat water, and auxiliary water heating from boiler. Water tank has 450-L (120-US-gallon) storage	
Solar System	N/A	N/A	**80-m² PV array** on 45-degree sloped roof facing south **3.0-m² (32-ft²) solar thermal collector** mounted at a 60-degree slope on south porch roof		Each unit has **8 224-W photo-voltaic modules** on 75-degree angled roof facing south **4 flat-plate solar collectors** mounted on the 75-degree angled south-facing roof	

11

Energy Performance	296 kWh/m² Consumes about 43% less energy than MNECH	168.31 kWh/m² Consumes about 54% less energy than MNECH	121.77 kWh/m² Consumes about 68% less energy than MNECH	145.43 kWh/m² Consumes about 67% less energy than MNECH	225 kWh/m² Consumes about 49% less energy than MNECH

Figure 2-2 Arviat Northern Sustainable House (CMHC, 2014a)

The Northern Sustainable House in Arviat is a single-story house with three bedrooms and an open-concept area that serves the function of living room, dining room and kitchen. This project is developed by the Nunavut Housing Corporation (NHC) with support from Canada Mortgage and Housing Corporation (CMHC).

During the house design, many features were included based on the local culture and lifestyle. The open-concept space is to provide sufficient area for a large gathering. The sewing room serves for soaking and sewing animal skins. A large storage room holds supplies between sealifts. And two entrances are oriented differently according to the local weather condition: one is for summer and the other is for winter.

The challenge for housing in Arviat is the cold weather, limited construction season (as summer is short), high cost of material and shipment, and need to hire the labor from outside because of a shortage of local labor. The significant wind load and snowdrift also affect the house design.

To achieve the energy savings target, the following features were included. The envelope is airtight and highly insulated. The nominal thermal resistance is RSI 8.0 for exterior walls, RSI 11.6 for ceiling and RSI 9.1 for floor. Advanced framing is used in envelope construction to reduce thermal bridging and minimize the amount of required framing material, thus lowering the cost. Especially in the exterior double wall, the thermal bridges are minimized by the staggered studs of the interior and exterior frame. Special attention is required to ensure the continuity of the air and vapor barrier;

when applying the barriers throughout the building envelope, the lap joints are all double sealed with acoustic caulking and Tuck tape. A blower-door test is carried out to check the airtightness.

Many of the windows are placed on the south side and the house is oriented to optimize the passive solar gain and natural light. Triple-glazed, argon-filled, fiberglass-framed windows are used to minimize heat loss.

An efficient house footprint was designed to minimize the floor area and heated volume. When the floor plan was designed, the piping length was reduced by clustering the kitchen, bathroom and laundry space, consequently reducing use of material, water and hot-water energy.

Energy-efficient equipment, appliances and lighting are specified. The house space and DHW are heated by an ENERGYSTAR oil-fired boiler with 86% efficiency. The required fresh air is heated by an efficient HRV with its sensible heat recovery efficiency of 62.5% at 0 ˚C and 55% at -25 ˚C. To avoid an excessive defrost time, the HRV system uses a preheat coil.

For the future installation of PV panels and a solar water-heating system, a shed-type roof is used to provide extra vertical area on the south façade.

Figure 2-3 Dawson Northern Sustainable House E/2 (CMHC, 2014b)

The Northern Sustainable House E/2 in Dawson is a single-story house with three bedrooms and an open-concept area that serves the function of living room, dining room and kitchen. This project

was built by Han Construction of the Tr'onderk Hwech'in First Nation in cooperation with the Yukon Housing Corporation (YHC) with support from CMHC.

During the house design, the local community identified several features based on the preferences of Tr'onderk Hwech'in Han residents. The house has one story and is built close to the ground to meet their desire to live on the land. The large open area of the living room, dining room and kitchen provides sufficient space for large gatherings and offers enough rooms for occupants to place furniture based on their needs. Additionally, the open kitchen with large pantry and movable island can allow several people to cook at the same time for special events. The porch on the east side of the house can be used as outdoor living or storage or can be converted to a bedroom with a bathroom or to an extra living room. The laundry room is separated from the living space by a door to keep the noise from washers and dryers from disturbing the occupants. Furthermore, the house provides flexibility for occupants with limited mobility. The interior has adequate turning areas for a wheelchair, and the heights of all electric outlets and switches have been modified to be reachable from a wheelchair. Moreover, wheelchair-accessible ramps could be added with simple modifications.

The main feature to lower energy consumption is a highly insulated building envelope with high airtightness. The thermal resistance of the E/2 NSH building is RSI 7.8 for floor, RSI 7.2 for double-stud walls and RSI 10.6 for the roof. To provide a continuous air and vapor barrier, the barrier is installed between the interior and the exterior studs of the wall, and all wiring and plumbing are placed in the interior stud cavity without penetrating the barrier. Advanced framing techniques (AFT) are used to minimize the thermal bridges while reducing framing material usage. The studs are spaced 600 mm (24 in) apart with a single top plate and single lintels over the windows and doors. At the openings, the metal lintel hangers are used in place of the double stud. The roof trusses are aligned with wall studs to achieve better structural performance.

The building is oriented with its longer face toward the south so the large window on that wall can gather solar heat and admit natural light. The windows on the other side has smaller areas to limit heat loss while receiving enough sunlight for the rooms. The installed windows are all triple-glazed with low-E coating.

The truss roof forms a large overhang on all sides that can protect the exterior walls from the rain and improve their durability. The south overhang above the windows projects shading on them during the summer to avoid overheating the rooms with solar heat, while in the winter, when the sun is lower, the sunlight can enter the rooms unimpeded.

Space heating is provided by a high-efficiency oil-fired boiler, which supplies hot water to the radiators located in all rooms and to the water coil in the HRV to preheat the fresh air.

Figure 2-4 Dawson Northern Sustainable House E/9 (CMHC, 2014c)

The Northern Sustainable House E/9 in Dawson is a duplex house with two units named "Solar" and "Flex". This project was also built by Han Construction of the Tr'onderk Hwech'in First Nation in cooperation with YHC with support from CMHC.

The E/9 house is a more advanced project than the E/2, although it has the same basic features to accommodate the local residents' cultural and lifestyle preferences. The main features that differ from E/2 include the use of structural insulated panels (SIPs) to achieve a highly insulated envelope and different systems for space heating and DHW heating.

For space heating, both units use electric baseboard heaters. The E/9 project chose electric baseboard heaters to avoid the control, oversizing and maintenance problems of the hydronic space heating system in the E/2 project. Given that the E/9 house has a very low space heating demand,

the cost of electricity is low. In the electric heating system, various types of electric baseboards are used. In the living room, entry and bathroom, 500-watt baseboard heaters are installed under the small windows. Larger 1,000-watt baseboards are beneath rest windows in the living room, dining room and bedrooms. A 300-watt baseboard is located in the laundry room.

The Solar and Flex units use two different DHW systems. In the Solar unit, two 3.0-m^2 solar thermal collectors mounted at a 60-degree slope on the south-facing roof are the primary DHW heating source. When the house requires more DHW, the backup electric water heater meets the need. In the Flex unit, the DHW is provided by a conventional electric hot water tank. If the Solar house has better energy performance, the Flex house can be converted into a solar house.

Figure 2-5 Inuvik Northern Sustainable House (CMHC, 2014d)

The Northern Sustainable House in Inuvik is a one-story duplex house with an open concept design. This project was developed by the Northwest Territories Housing Corporation (NWTHC) and managed by the Inuvik Housing Authority (IHA) with support from CMHC.

The design features that accommodate the local residents' cultural and lifestyle preferences are the one-story house design, which allows occupants to live close to the ground; a large open area for the living room, dining room and kitchen for large gatherings and various furniture layouts; and an entering vestibule that functions as a storage room and a weather buffer from outdoor conditions.

Due to the layout of the adjacent streets, the house could not face south, and the designed orientation is 35 degrees east of south. This is not the optimal orientation for maximizing solar energy gains, although it still receives reasonable solar heat.

The house has a highly insulated envelope with a nominal value of RSI 8.8 for double-walls, RSI 14.1 for the ceiling and RSI 9.3 for the floor. The double-stud walls were designed to minimize thermal bridges by staggering the interior and exterior studs, and a continuous insulation layer is between them. The air and vapor barrier is located on the warm side between the interior framing studs and the middle insulation layers. On one hand, the location is warm enough to avoid condensation and moisture damage, while on the other hand, it provides sufficient depth for wiring and plumbing with no need to penetrate the air and vapor barrier.

There are two types of windows installed in this house. On the near-south-facing façade, the windows are triple-glazed fiberglass windows, and the larger proportion of windows are placed on this side with roof overhangs to maximize the solar heat gain during the winter while limiting the solar gain entering in the summer. Quadruple-pane fiberglass windows, which have a higher thermal insulation value and lower solar heat gain coefficient, are installed on the near-north side to reduce heat loss while providing sufficient natural light to rooms. All entrance doors are fiberglass insulated.

For space heating, both units are served by a high-efficiency natural gas boiler with radiant baseboards. The boiler is located in the shared mechanical room at the back of the house with an individual entrance from outside. This design is to shield occupants from the noise and disturbance of maintenance.

The DHW is primarily provided by four flat-plate solar collectors on a 75-degree angled south-facing roof with extra heat provided by the boiler. Additionally, this house has 16 solar photovoltaic modules with a capacity of 224 W on the 75-degree angled south roof to generate electricity for the two units.

2.2.2 Energy Efficient Housing in Whitehorse, Yukon

Figure 2-6 Whitehorse Energy-Optimized House (RDH Building Engineering)

The Energy-Optimized House in Whitehorse (RDH Building Engineering) is a two-story building with an attached garage that represents typical new construction in Whitehorse. The project is supported by NRCan, CanmetENERGY and Yukon Territory. This house project aims to determine the most cost-effective and energy-efficient house configuration by modifying the combination of components, assemblies and mechanical equipment in the optimization. More than 20,000 cases were simulated and evaluated using ESP-r and GenOpt optimization software, and the optimal case has lower operating costs than the baseline and the highest energy savings rate (Figure 2-7). Detailed information about the baseline house and the optimal house are listed in Table 2-2.
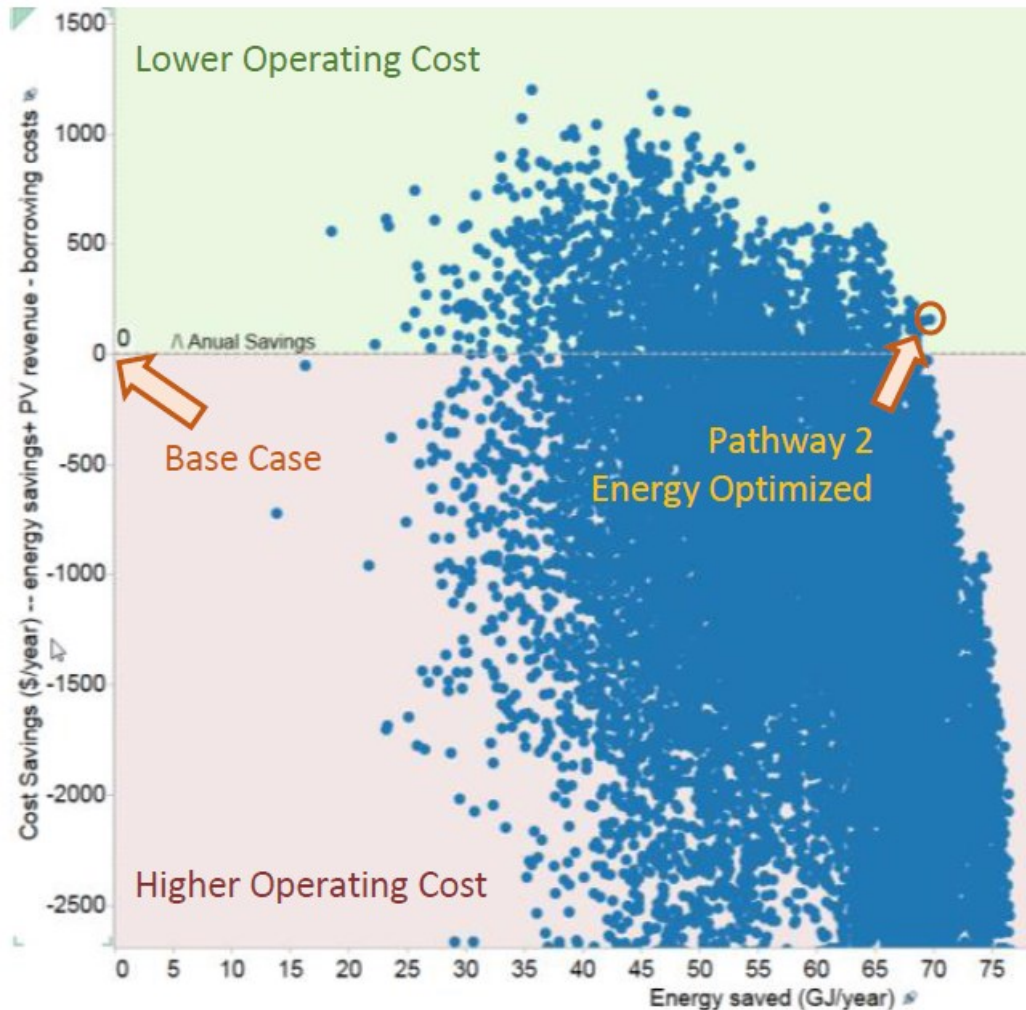
Figure 2-7 The optimization simulation results for the Whitehorse Energy-Optimized House (RDH Building Engineering)

The optimized house has a highly insulated envelope with RSI 10.2 for exterior walls, RSI 19.4 for the ceiling and RSI 6.7 for the floor. The windows triple-pane, argon-filled, low-E hard-coat, vinyl-frame windows with a USI value of 0.694. Furthermore, the house has a high level of airtightness with a 0.5 ACH rate.

Many new houses in Whitehorse use electricity rather than oil for heating according to the new green-building standard. In this house, the primary heating source is the cold climate air source heat pump (CCASHP), and the wood stove is a backup system. The CCASHP can work with the outdoor temperature down to -35 ˚C with the same efficiency as an electric baseboard heater, and when outdoor temperature is above -3 ˚C, the CCASHP efficiency is greatly increased and provides significant advantages over an electric baseboard heater. The wood stove heater is used

as a secondary heat source when the CCASHP has very low efficiency because of extreme cold (-10 ˚C to -40 ˚C).

Table 2-2 Energy-Optimized House compared with the base case (RDH Building Engineering)

Category	Base Case	Energy-Optimized
Basement Slab	Concrete slab with 5-mm (2-in) XPS insulation, RSI-1.76 (R-10)	Concrete slab with 5-mm (2 in) XPS insulation, RSI-1.76 (R-10)
Foundation/Basement Wall	2 x 6 permanent wood foundation with RSI-3.5 (R-20) fiberglass batt	2 x 6 permanent wood foundation with fiberglass batt and 75 mm (3 in) of exterior EPS, RSI-4.9 (R-28)
Casement Windows	Clear, triple-glazed, USI-1.77 (U-0.31), SHGC[1] 0.68	Triple-pane, hard-coat with two low-E coatings, USI-0.694 (U-0.122), SHGC 0.40
Attic	Standard truss with 350 mm (14 in) blown-in cellulose insulation, RSI-8.8 (R-50)	530-mm (21-in) raised-heel trusses with 760 mm (30 in) blown-in cellulose, RSI-19.4 (R-110)
Exposed Floor	2 x 12 joists with 200-mm (8-in) fiberglass batts in floor joist cavities, RSI-4.9 (R-28)	2 x 12 joists with 150-mm (6-in) fiberglass batts in joist cavities and 130 mm (5 in) of mineral wool exterior to the sheathing, RSI-6.7 (R-38)
Air Tightness	1.5 ACH	0.5 ACH
Domestic Hot Water	Electric water heater	Electric heat pump water heater
Heating	Oil 85% AFUE[2] (ducted forced air)	Cold Climate Air Source Heat Pump
Above Grade Wall	2 x 6 wood stud @ 610 mm (24 in) o.c. with fiberglass batts and 65-mm (2.5-in) fiberglass batts interior, RSI-4.9 (R-28)	2X6 Wood stud @ 610 mm (24 in) o.c. with fiberglass batts and 260 mm (10 in) of mineral wool exterior to the sheathing, RSI-10.2 (R-58)
Heat Recovery Ventilation	Yes (70% SRE[3] @ 0 ˚C, 60% SRE @-25 ˚C)	Yes (70% SRE @ 0 ˚C, 60% SRE @-25 ˚C)
Drain Water Heat Recovery	No	Yes
Upgrade Cost (Payments on Principle and Interest)	$0	**$40,260**
Energy Saved and Generated	0 GJ/year	**71 GJ/year**
Energuide Rating System (ERS)	77	**89**
Yearly Operating Cost Savings (Savings on Energy Bills – Payments on Principle and Interest)/Year	$0	**$51**

The DHW is provided by an air source heat pump (ASHP) water heater located in a semi-conditioned indoor room, which the warm ambient conditions would make it more efficient. The HRV is used to preheat the inlet fresh air and a drain water heat recovery system is installed to recover the heat in the drainage water from hot showers.

---

[1] SHGC: solar heat gain coefficient
[2] AFUE: annual fuel utilization efficiency
[3] SRE: sensible recovery efficiency

2.2.3 Research Work for Northern Housing

With the growing concern for having high-performance residential buildings in northern Canada, some research studies have been carried out in recent years to improve building performance.

Thirunavukarasu (2016) analyzed the energy performance of homes in Northwest Territories (NWT) built before and after the adoption of the EnerGuid for Housing (EGH) 80 by-law by data mining information on 1,744 homes in NWT from the EGH database and through interviews with homeowners and builders. A parametric study was carried out to investigate the effect of passive-design parameters, especially parameters such as thermal mass, window-wall ratio (WWR) and active solar systems that have not been included in the existing standards or codes. Based on the parametric study and all relevant standards, guidelines and criteria, a protocol for low-energy homes in northern Canada was developed with the scope including air leakage; moisture management; energy performance; IAQ; heating, ventilation, and air conditioning (HVAC) system selection; schedule and cost; and compatibility of materials.

Kayello (2018) studied the heat, air and moisture performance of SIPs and attic under Arctic climates through laboratory testing and simulations. In the SIP system, the joints formed by the meeting of two envelope elements performed better than those joints formed by the meeting of three envelope elements, and overall the joints can be improved to be less dependent on the tape seal. Results for attic hygrothermal performance indicated the unvented attic has limited capacity to dry out through vapor diffusion if the air leakage rate cannot be minimized. A ventilation rate of at least 1 ACH can be effective in preventing mold growth in a ventilated attic. Furthermore, a BIPV/T system was applied with an attic ventilation system. It was found that adding a BIPV/T system to either a naturally ventilated attic or a mechanically ventilated attic improved the attic's hygrothermal performance. With natural ventilation, the thermal energy from the BIPV/T system could not be fully used, whereas with mechanical ventilation both the thermal energy and the electrical energy from the BIPV/T system were used.

Beattie (2017) evaluated the performance of air to air heat/energy exchangers in Arctic housing, especially the use of vapor-permeable cores and alternating recirculation defrost cycles to manage core frosting. The rate of core frosting was dependent on the inlet supply air temperature and core

frosting decreased the mass flow rate of the exhaust air stream. By comparing the reduction in the exhaust air mass flow rate, the author determined that the vapor-permeable heat exchanger core delayed the onset of core frosting. Recirculation defrost effectively managed frost formation at inlet air temperatures down to -35 ˚C, while it reduced the ventilation rate of fresh air. The use of two heat/energy exchangers with altering recirculation defrost was proposed to manage the core frosting while providing a constant inlet fresh air rate.

2.2.4 Summary

All the northern projects have an envelope thermal resistance value much higher than that required by the national building code and local standards. Additionally, these northern houses have a high level of airtightness to reduce auxiliary heating demand. The house orientation, window area and overhang are the features adopted in the design to maximize the utilization of passive solar heat. The house type and floor layout are designed to accommodate the local residents' preferences based on culture and lifestyle. Detailed construction techniques have been suggested to implement these design features.

When the energy demand of a house is lowered by selecting these passive design parameters, less energy is consumed to maintain comfortable interior conditions, as the mechanical systems for space heating and DHW are more efficient. In northern Canada, the availability of energy sources is a constraint in choosing a heating system. Traditionally, oil is used, while natural gas is more economical but not readily available in most of the northern regions. Electricity is segmentally priced, with its price becoming extremely high after a certain level of consumption is reached. Taking Yellowknife as an example, after a home exceeds 600 kWh within a month, the electricity price is increased from 29.81 ₵/kWh o 68.37 ₵/kWh (NWT Rate Schedule, 2019). Thus, the cost for electricity is acceptable only if the house has a low energy demand. Typically, a project may choose an efficient oil-fired boiler for space heating and DHW, while an electric baseboard heater or an ASHP may be a choice for these newly designed low-energy northern houses.

An active solar system is also implemented in some of the northern projects. The solar thermal collector is designed as a primary heat source for DHW and is mounted on an optimally sloped

south-facing roof. When the solar collector cannot meet the requirements, backup system, boiler or electric water heater is used to provide the needed extra heating. Photovoltaic panels are also installed to generate electricity to offset the house's electricity usage.

The NSH project achieved its low energy target, however, the design process did not include optimization. It is thus difficult to demonstrate that the parameter combinations used are the optimal combinations. The optimal values for window, thermal mass, shading control schedules or ventilation rate control schedules should be included in future studies to maximize the utilization of solar energy during the heating season while preventing overheating during the summer. With consideration of passive solar strategies, the optimal combination of all design parameters may differ. The NSH projects in Dawson and Inuvik demonstrated the benefit of using PV panels to generate electricity on-site. As the BIPV/T system can generate both electricity and thermal energy, the thermal energy from a BIPV/T system would lower a house's heating energy demand or increase the mechanical system's efficiency.

2.3 Optimization Algorithm

It is not a straightforward task to design an energy-efficient building with many conflicting parameters that influence its energy performance. Optimization is typically used to obtain the optimal set of design parameters with better energy performance (Kheiri, 2018). During the optimization, an optimization tool needs to be selected as the optimization algorithm platform to group, evaluate and select the studied parameters, and output the optimal sets of parameters based on the objectives set in the algorithm. As the building performance is required for the evaluation, a building performance assessment model is needed to simulate the building energy performance.

The general building optimization procedure is shown in Figure 2-8. When starting an optimization, an initial building model must be set up, which can be either an existing building or a newly designed building. Based on the objectives of the optimization and building features, the studied variables and objective functions are selected. Then, a proper building performance assessment tool, in which the studied variables served as inputs, and the outputs for objective functions are generated sequentially, is used to set up the initial building model. Following this, an optimization

algorithm is implemented in an optimization engine. The optimization algorithm evaluates the building performance based on the defined objective functions. If the stopping criteria are met, then the optimal results have been acquired. If not, the program modifies the variables and the assessment tool again simulates the building model with the replaced variable values. This cycle is repeated until the stopping criteria are met.
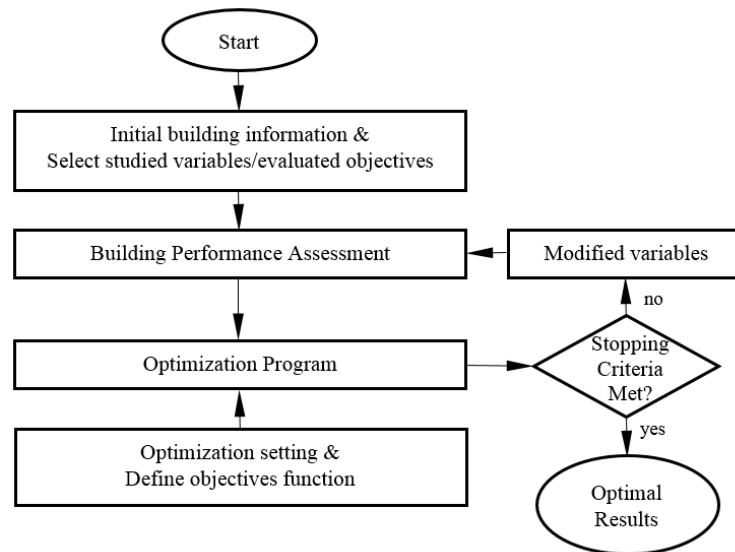
Figure 2-8 The general procedure for building optimization

In recent years, many reviews have focused on building optimization. Machairas et al. (2014) reviewed the methods and tools used in building design optimization and explored the selection basis, abilities and performance issues, as well as the characteristics of their future versions. Nguyen et al. (2014) reviewed simulation-based methods applied to building performance analysis and clarified the advancement, challenges and obstacles in building design optimization. Huang et Niu (2016) reviewed the history, current status and future potential for optimal building envelope design based on simulation performance by comparing and discussing the popular optimization algorithms and collecting and summarizing target objectives, the limitations of the research and potential breakthroughs. Shi et al. (2016) reviewed the optimization of energy-efficient building design from the perspective of architects based on 116 core studies. Through analysis and classification, the review supported the opinion that optimization is a promising technique in designing better-performing buildings. Kheiri (2018) reviewed the different optimization methods applied in energy-efficient building geometry and envelope design; categorized all algorithms, optimization tools, and building energy assessment tools; and summarized the trends in their usage.

This review section focuses on recent studies to provide an overview of the commonly used building performance simulation software, algorithms and optimization tools. The studied parameters and objectives are also summarized.

2.3.1 Algorithm in Optimization

The optimization algorithm is a crucial part of the optimization process shown in Figure 2-8. Optimization tools serve as engines to implement the algorithms, and the building performance assessment tools are required for the building performance values for each case that is queried by the algorithm. Hence, choosing a suitable algorithm for a certain building optimization problem is important. This section focuses on the algorithm that has been commonly used in building optimization. Optimization, generally, involves finding the minimum or, inversely, the maximum value of the objective function/s with various variables.

$$Minimize\ [f_1(\vec{x}), f_2(\vec{x}), \dots, f_m(\vec{x})] \tag{2-1}$$
$$Subject\ to: g_i(\vec{x}) \leq 0, i = 1, 2, \dots, n, \tag{2-2}$$

where $\vec{x}$ is the vector of the studied variables, and m is the number of the objective function. When m equals 1, the optimization has a single objective, and when m is greater than 1, the optimization is termed a multi-objective optimization. The number of constraints, referred to as n, depends on the requirements of the problem (Kheiri, 2018).

The main categories of optimization algorithms introduced in this section are these:

● calculus-based algorithms,

● derivative-free algorithms,

● meta-heuristic algorithms and

● hybrid algorithms.

2.3.1.1 Calculus-Based Algorithms

These methods using mathematical expressions or gradients to search for the optimal objective value and the values of the related variables are divided into the indirect method and the direct method. For the indirect method of the calculus-based algorithm, the results are obtained by setting the gradient of the objective function equal to zero. For the direct method, the optimal value is found by moving in a direction based on the local gradient (Kheiri, 2018; Goldberg, 1989).

Jedrzejuk and Marks (2002a; 2002b) carried out a multicriteria optimization with an explicit mathematical model with three individual objectives: optimization of outer walls of buildings, optimization of the shape of blocks of flats and optimization of heat source utilization. The optimization problems are solved using the analytic-numerical method applied in CAMOS computer system.

The restriction in these methods is that the problems must have an explicit mathematical expression or must permit derivatives (Chantrelle et al., 2011).

2.3.1.2 Derivative-Free Algorithms

A well-known category introduced under the derivative-free algorithm is the direct search method, which does not require the explicit use of derivatives (Kheiri, 2018; Machairas et al., 2014). The general description of the direct search method is to first define a basic point and space, and then search the value at another point in the space and compare it with the basic point. If the second point has a better value than the basic point, it replaces the basic point, and the search is repeated. Otherwise, the basic point remains unchanged, and a new point is selected from the space and compared to the basic point. This process continues until the optimal point is found, all the new points have been compared with the basic point, or the final state is reached (Hooke & Jeeves, 1961).

The advantage of the direct search method is that it is normally more robust for noisy functions, for when the derivatives are unavailable, or for when the finite different approximate gradient is unreliable, even though it is not as effective as derivative-based methods (Machairas et al., 2014;

Torczon, 1992). The hill-climbing method and the Hooke–Jeeves pattern search algorithm are the common methods used in direct search.

Bojić et al. (2014) used the Hooke–Jeeves algorithm for determing the optimal insulation thickness for the envelope when considering both embodied energy and energy consumption. They concluded that an optimal thermal insulation thickness could easily improve the energy efficiency of the house. Cvetoković et al. (2014) also used the Hooke–Jeeves algorithm for determing the optimal insulation thickness for walls, floor and roof considering both embodied energy and energy consumption. The optimization was repeated under different scenarios – namely, with different heating panel locations, wall heating, floor heating, ceiling heating and floor-ceiling heating – and it was found that the wall requires the greatest thickness of insulation while the floor requires the least. It was also determined that the required insulation thickness for certain types of envelopes is greatest when the heating panel is located in that part of the envelope.

The limitations of direct search are that the required objective function has to be continuous, or at most it only has small discontinuities, and that it might become trapped in a local minimum (Machairas et al., 2014; Nguyen et al., 2014). Give the limitations, the optimization objective mostly should be simple and involve fewer variables.

2.3.1.3 Meta-Heuristic Algorithms

The meta-heuristic algorithm is an optimization technique that can find the global optimum (Kheiri, 2018). Evolutionary optimization techniques, such as genetic algorithm (GA), and swarm intelligence, such as particle swarm optimization (PSO) and the ant colony algorithm, are the typical meta-heuristic algorithms (Nguyen et al., 2014).

The genetic algorithm is one of the popular evolutionary algorithm (EAs) (Holland, 1992), which are inspired by natural selection and the survival of the fittest principle of Darwin (Elbeltagi et al., 2005). Generally, a GA encodes the studied character of the house into a chromosome, and randomly generates the first generation as parents. During the evaluation, the algorithm keeps the best-performing individual to the next generation as elitism, and breeding the parents with higher performance by crossover to form the next generation called children. A small degree of mutation

is included to avoid becoming trapped in a local minimum. The iteration process of using the next generation to replace the previous one converges to the optimal solution (Kheiri, 2018). The advantages of GA, as population-based algorithms, are that they can efficiently handle the discontinuities of non-linear problems and problems with many local minima (Machairas et al., 2014). Pernodet et al. (2009) used a GA to optimize the choices for building refurbishment by considering the envelope thermal resistance, the window ratio, the airtightness and the artificial lighting strategies.

Several variations of GA exist geared to certain requirements.

Hamdy et al. (2009) provided two optimization approaches: the preparation process and genetic algorithm (PR-GA) and the genetic algorithm with refined process (GA-RF). Substituting for generating the first generation randomly in a GA, the trusted initial generation is prepared in PR-GA to reduce the number of trials so that the GA focuses on specified areas of the solution space. The GA-RF refines the optimal solution after a GA and improves its solution. In this study, the thermal resistance of the envelope and windows and heat recovery efficiency were included and optimized.

The multi-objective genetic algorithm (MOGA) is used to deal with problems that have two objectives and generate the Pareto front. Shi (2011) did a study on optimized insulation thickness for six different orientations of walls using the MOGA with two objectives of life-cycle cost and life-cycle environmental impact.

The non-dominated sorting genetic algorithm (NSGA-II) is a variation of the MOGA that includes the non-domination concept in reproducing the children in each iteration. It has been widely used in building energy optimization (Kheiri, 2018). Gossard et al (2013) implemented the NSGA-II in designing a residential house in France considering energy consumption and summer comfort to optimize the combination of thermal conductivity and specific heat for walls and roof.

Particle swarm optimization is inspired by a simplified social model in bird flocking, fishing schooling and, particularly, swarming theory. Particle swarm optimization involves both local and global optimum processes, as it considers both individual intelligence and the communication

between individuals (Kheiri, 2018). Carlucci et al. (2013) applied PSO to optimize a residential house in the Mediterranean climate toward net-zero.

Particle swarm optimization is a relatively recent heuristic search method compared with GA (Hassan et al., 2005). Some comparisons have been made between PSO and GA, and various conclusions have been drawn, yet it is difficult to determine which algorithm is better. Elbeltagi et al. (2005) compared five evolutionary-based optimization algorithms and found that PSO performs better than other algorithms, including GA, in terms of success rate and solution quality. Wetter and Wright (2004) studied building optimization algorithms based on cost function evaluation, and a simple GA came closer to the minimum than PSO with comparable numbers of simulation runs. Bichiou and Krarti (2011) developed a comprehensive energy simulation environment to select optimal building envelope features and mechanical systems. The algorithm comparison in their study found that GA required less computational time than PSO or sequential search.

2.3.1.4 Hybrid Algorithms

The hybrid algorithm is a combination of both global optimum finding methods and local optimum finding methods. Among the algorithms introduced, the Hooke–Jeeves algorithm is a local optimum method that has better performance in finding the better solution in the neighborhood of the present point, although it can easily be trapped in a local minimum and miss the global optimum. A GA algorithm is classified as a global optimum method with the ability to search the entire space and find the global minimum. Thus, a typical procedure in a hybrid algorithm is to use a global search method to find the near-optimal point in the entire searching area and then to use a local search method to refine these global optimal points by neighborhood searching. (Kheiri, 2018; Machairas et al., 2014)

In GenOpt, a hybrid algorithm of coupling PSO and Hooke–Jeeves algorithm is a hybrid algorithm. Futrell et al. (2015) implemented PSO + Hooke–Jeeves to optimize a classroom considering both daylighting and thermal performance.

Even though the hybrid algorithm of PSO + Hooke–Jeeves has a lower cost than simple GA, it requires more simulation runs. If the user is willing to accept a slight decrease in accuracy for the

benefit of fewer simulations, simple GA would be a good choice (Wetter et Wright, 2004). However, the performance of Hooke–Jeeves is restricted by the discontinuities of the objective functions.

2.3.1.5 Trends in Algorithms Usage

There are various selections for the searching algorithm in building optimization problems. Depending on the specific objectives, the changed variables, the availability of derivatives of objective functions, and algorithm performance, different optimization studies have used different algorithms (Nguyen et al., 2014).
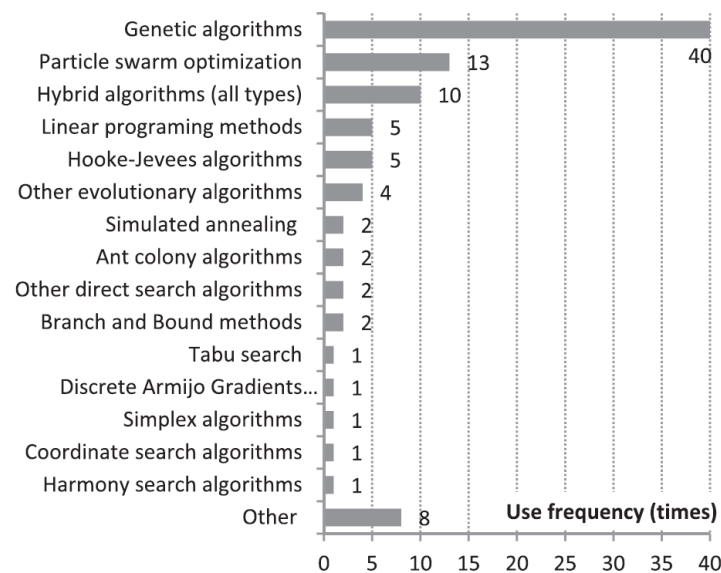
Figure 2-9 Algorithm usage frequency (Nguyen et al., 2014)

Nguyen at al. (2014) summarized the usage frequency of different algorithms from more than 200 building optimization studies. They found GA is far more popular than any other algorithm and among the top algorithms, most are related to the population-based algorithm, such as GA, PSO, hybrid algorithms and EA. (Figure 2-9)

Kheiri (2018) traced changing trends in the use of the four most-used optimization algorithms based on the reference literature. Figure 2-10 illustrates that the use of GA has increased significantly in recent years, as has the use of PSO, whereas calculus-based optimization and direct search methods have a widely spread distribution with a lower frequency.
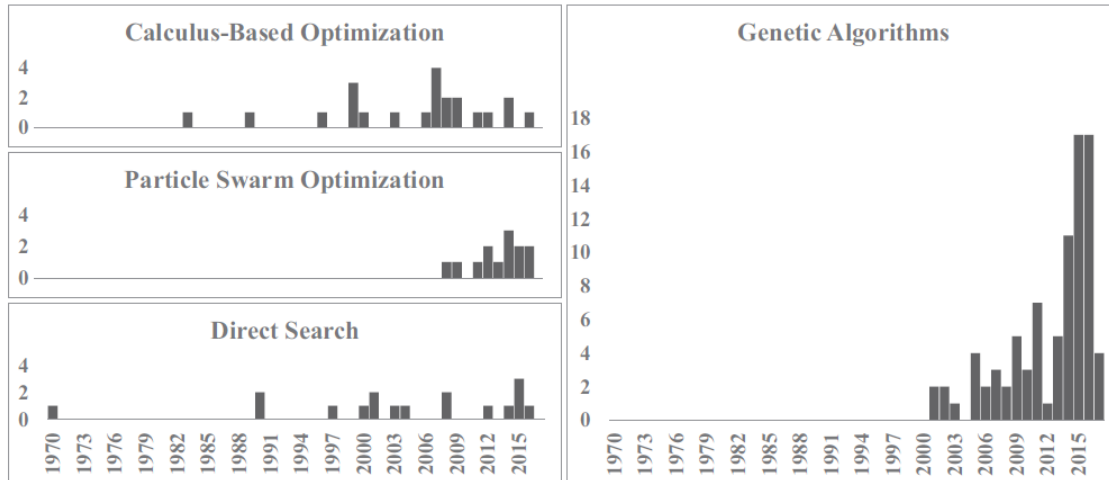
Figure 2-10 Histograms of the four most-used optimization algorithms (Kheiri, 2018)

2.3.2 Building Performance Assessment

As shown in Figure 2-8, the building performance assessment is one of the key steps in optimization, which needs to simulate the building performance, mainly the energy performance, for a designed and optimized building (Kheiri, 2018). The simulation results are calculated and evaluated following the defined objectives until the optimal result is found.

There are three main types of models that are used to estimate building energy performance:

● simplified analytical models,

● detailed building models and

● building performance surrogate models.

2.3.2.1 Simplified Analytical Models

Building performance simplified analytical models can be applied when focusing on a specific problem, and these models are based on thermodynamics and heat transfer principles (Kheiri, 2018; Machairas et al., 2014). The advantages of these models are their ease of use in finding the optimal value with specific optimization algorithms or brute force techniques in searching the entire solution space. The results can be instantaneously extracted and used as inputs in a specific detailed

analysis (Machairas et al., 2014). Castro-Lacouture et al. (2009) used a mixed integrated model for material selection to maximize LEED credits with design and budget as the constraints.

Describing problems mathematically, however, is not an easy task, which limits the application of analytical models in solving simple problems. They are more common in optimizing building control operations (Machairas et al., 2014). Accuracy also needs to be attended to when using these models, since the generalization in simplified methods may not include all the detailed configurations in the model set-up (Kheiri, 2018).

2.3.2.2 Detailed Building Models

Detailed building models can provide accurate results and cover almost all building physics phenomena and processes (Kheiri, 2018; Machairas et al., 2014). Nowadays, the common building simulation software packages used for detailed building performance simulation include EnergyPlus, Trnsys, IDA-ICE (IDA Indoor Climate and Energy), DOE-2 and others. The input and output functions are relatively well-conceived, as most of these energy simulation engines have been developed over decades (Shi et al., 2016). Different building simulation tools have their own applications and limitations, and they should be selected based on program requirements. Harish et al. (2016) summarized the applications and limitations of most building energy simulation programs.

As the detailed building simulation tools require a great deal of information about the designed building, many building details must be collected before setting up these models, and special expertise and validation are needed to ensure the model provides reliable results. Moreover, the computational time of the detailed simulation is typically high, a factor that needs to be considered in optimization (Kheiri, 2018).

2.3.2.3 Building Performance Surrogate Models

Building performance surrogate models, or meta-models, are statistical models, which collect all the results of different cases based on a building simulation model to generate a database and using

these data statistically to train and test the surrogate or meta-model. In other words, the models are created through a machine learning approach, using methods such as artificial neural networks (ANN), genetic programming, Bayesian networks or support vector machines (SVM), all of which are considered surrogate models (Machairas et al., 2014). The surrogate models perform well in solving demanding building design problems that have numerous design parameters, many local minima and a vast search space (Machairas et al., 2014).

Magnier and Hagnighat (2010) carried out the optimization of a two-story house. An ANN was trained and validated as a meta-model by using a validated model in Trnsys. When the ANN was able to evaluate building performance fast enough without sacrificing accuracy or simplifying the problem, the NSGA-II was run using the ANN.

Although this method could generate immediate results faster than using a detailed building performance simulation, the reliability largely depends on the database used for training and testing (Kheiri, 2018). The statistical results for training the models require a detailed building simulation model to run for repeated evaluations until a high model accuracy is reached, which may require the number of the evaluations to equal or exceed the number required in using optimization algorithms coupled with building simulation software (Machairas et al., 2014). In addition, it is essential to have expert knowledge of artificial intelligence when using these models. These are the main reasons that surrogate models are not popular in solving building design problems (Machairas et al., 2014). One of the alternatives when facing these disadvantages is to couple the surrogate models with analytical expressions (Kheiri, 2018).

2.3.2.4 Trends in Building Assessment Tools Usage

Kheiri (2018) reviewed optimization studies based on two criteria: building shape and envelope as studied parameters and minimizing building energy consumption and/or demand as defined objectives. Among the tools reviewed, EnergyPlus was the most frequently used building energy performance assessment tool, followed by calculus-based optimization, Trnsys, Daysim, and so on (Figure 2-11 (a)).

(a)

(b)

(c)
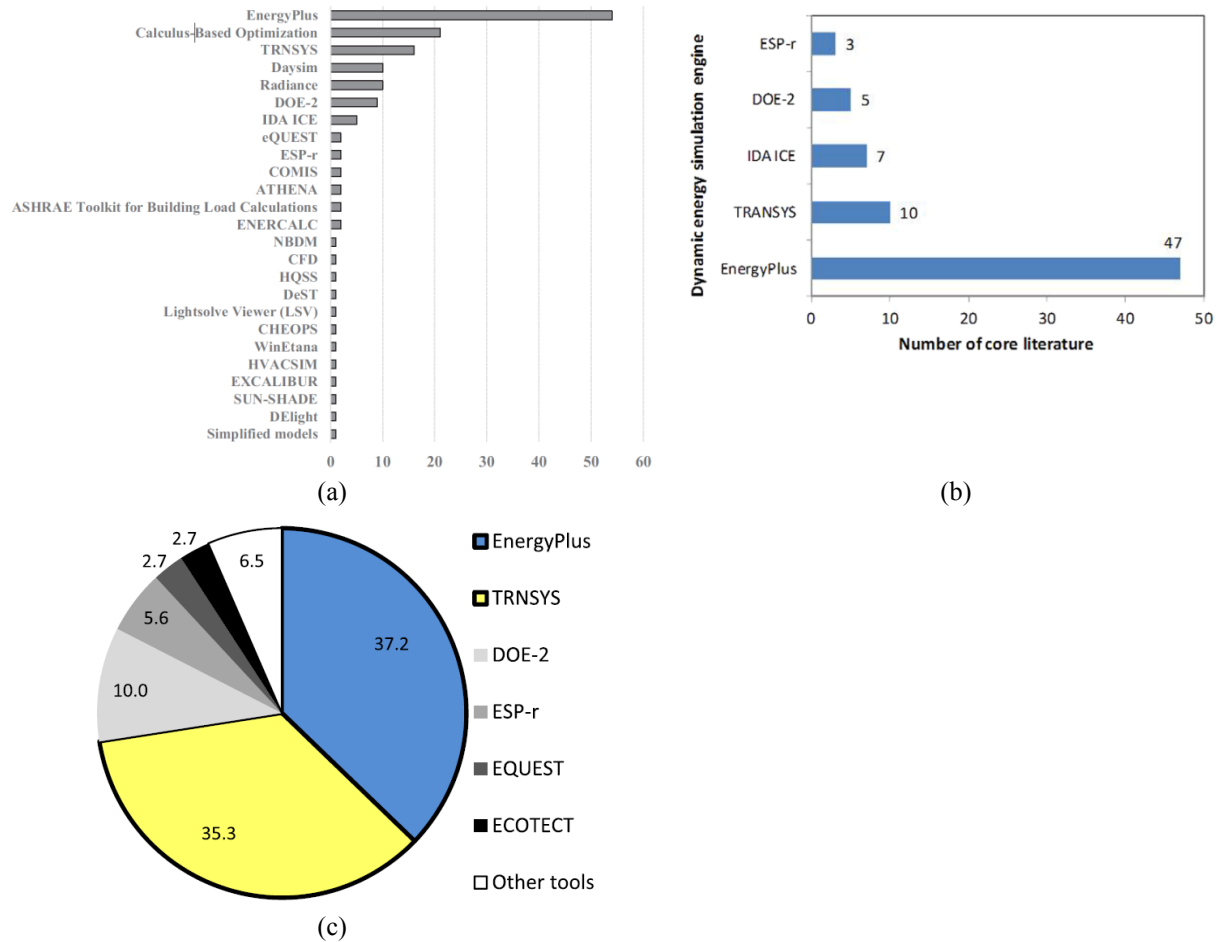
Figure 2-11 Usage trends for building assessment tools (Kheiri, 2018; Shi et al., 2016; Nguyen et al., 2014)

Shi et al. (2016) chose 116 core studies to review. Studies had to present a complete building optimization case and focus on building energy consumption or related objectives, such as CO_2 emission or life cycle cost. They also had to include at least one architectural feature as a variable, such as building shape or envelope. The study found that EnergyPlus was the most commonly used building energy simulation engine, accounting for 47 papers out of 116, or over 40% of the core literature. Trnsys, IDA ICE and DOE-2 were other widely used energy simulation engines after EnergyPlus (Figure 2-11 (b)). Nguyen et al. (2014) showed that the utilization of EnergyPlus and Trnsys as building simulation programs accounted for more than 70% of studies, followed by DOE-2 and ESP-r (Figure 2-11 (c)). These three reviews reached similar conclusions – that among building energy performance assessment tools, EnergyPlus is the most used program, followed by Trnsys and then by DOE-2, IDA ICE, ESP-r and eQuest. They may rank differently in each review, yet they all remain as the top tools.

2.3.3 Optimization Tools

An optimization tool, as a platform, is necessary to execute the algorithm and complete the computation. The building optimization tools can be divided into three main categories:

● custom programmed algorithms,

● general optimization packages and

● special optimization tools for building design.

2.3.3.1 Custom Programmed Algorithms

If a building optimization requires a specialized modification to the algorithm, a custom programmed algorithm is an option for this situation, as the algorithms implemented in many developed optimization tools are not accessible to users (Kheiri, 2018).

Junghans and Darde (2015) optimized a building by minimizing its life-cycle cost using algorithms programmed in C++, including GA, simulated annealing optimization (SA) and GA combined with SA. Xu et al. (2016) built a Java-based application to transfer and process data among the tools, libraries and databases to optimize a building using different variations of NSGA-II.

Flexibility is the main advantage of custom programming, while the disadvantage is also clear: it requires advanced programming skills, and it cannot generate detailed reporting on optimization implementation, which leads to difficulty in reaching a safe conclusion (Machairas et al., 2014).

2.3.3.2 General Optimization Packages

The general optimization packages are referred to the optimization tools that could be linked with various building performance assessment tools and other performance optimization tasks, such as modeFRONTIER, Matlab and GenOpt. The advantages of these general optimization platforms are that they offer a variety of optimization algorithms and user-friendly interfaces to establish the workflow. They also offer strong post-processing capabilities that allow users to view, analyze and compare optimization results based on building program requirements.

Shi (2011) carried out the optimization to minimize the space condition load of an office by coupling EnergyPlus with modeFRONTIER. As EP-Launch cannot be integrated into modeFRONTIER, a RunEPlus batch file was used to run EnergyPlus using several customized codes. Yu et al. (2015) used Matlab with EnergyPlus to implement NSGA-II to optimize a building. GenOpt is an optimization tool widely used with EnergyPlus or Trnsys for building optimization (Asadi et al., 2014; Carlucci et al., 2015; Futrell et al., 2015).

The drawback of using a general optimization package is that it requires users to do some coding, usually not much, to integrate them with a building energy simulation program (Shi et al., 2016).

2.3.3.3 Special Optimization Tools for Building Design

Special optimization tools are different from general optimization packages, in that the special tools only work with specific algorithms and/or specific building assessment software. MOBO and jEPlus + EA are some examples in this category.

jEPlus + EA was developed solely for carrying out energy-efficient building design optimization, and it only can be combined with EnergyPlus (Shi et al., 2016). Schwartz et al. (2016) presented a study using jEPlus coupled with EnergyPlus to minimize a building life-cycle cost and carbon footprint by optimizing the insulation thickness and WWR.

Under this category, the special optimization tools can be easily connected to certain building energy simulation software, but they do not provide as many optimization algorithms as general optimization tools (Shi et al., 2016).

2.3.3.4 Trends in Optimization Tools Usage

Figure 2-12 (a) taken from Shi et al. (2016), shows that GenOpt and Matlab are the most frequently used tools and were used in approximately 40% of the 116 core published studies. The customized techniques account for about 22%.

(a)

(b)
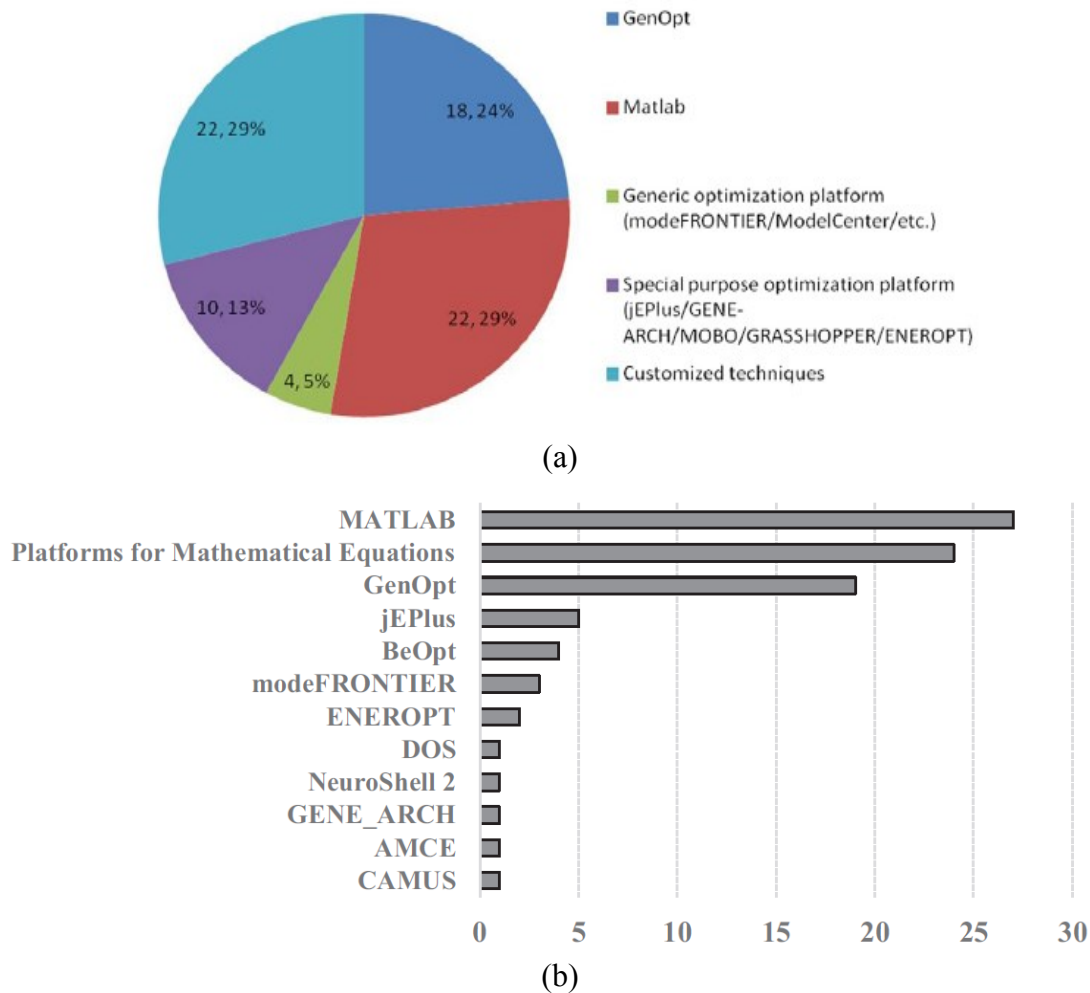
Figure 2-12 Usage trends for optimization tools (Shi et al., 2016; Kheiri, 2018)

Figure 2-12 (b) from Kheiri (2018) shows a similar distribution in usage frequency, with Matlab, GenOpt and platforms specifically developed for building optimization at the top followed by jEPlus, BeOpet, modeFRONTIER, and so on. Matlab is widely used software for solving numerical problems in many disciplines. It can be coupled with different building energy simulation tools by using the Matlab scripting language, and the optimization toolbox provides a variety of optimization methods. These advantages make Matlab more convenient for applying to building optimization problems compared with other optimization tools (Kheiri, 2018). Moreover, other Matlab functions can be included in the optimization process to calculate or improve the final output data for either data presentation or data analysis (Huang et Niu, 2016).

GenOpt is a generic program developed by the Lawrence Berkeley National Laboratory. It can be coupled with any text-based input and output building simulation tools, such as EnergyPlus, Trnsys,

38

IDA-ICE or DOE-2. The flexibility and practicality of GenOpt enable it to carry out a self-defined optimization algorithm based on Java (Kheiri, 2018; Huang et Niu, 2016). However, the limitation of GenOpt is that its library does not contain any GA or multi-objective algorithms (Wetter, 2016), and a Java genetic algorithm package is needed to use the NSGA-II in an optimization (Carlucci et al., 2015).

2.3.4 Studied Parameters

The building design parameters considered in optimization papers vary, including in the number of parameters involved, the study range for each parameter and whether the parameters change discretely or continuously within their range. To evaluate the whole building performance, the resistance of the envelope is the key parameter in the optimization. Most research has separated the envelope into exterior walls, roof and floors. To change the thermal resistance of an envelope, some researchers modified the structure type or the insulation type (Chantrelle et al., 2011), some changed only the thickness of insulation layers (Ascione et al., 2015), and some provided various cases that combined different insulation materials of different thickness (Asadi et al., 2012).

Window type is the second most frequently considered parameter in building optimization, either by varying the U-value of window (Junghans et Darde, 2015) or by changing the types (Azari et al., 2016). Some studies also consider the solar heat gain coefficient (Futrell et al., 2015) or visible transmittance (Carlucci et al., 2015) of the windows. There are some variables whose performance is coupled with window type. Window-wall ratio (Ascione et al., 2016) is typically considered in optimization together with the window type, as the window has lower thermal resistance than the opaque envelope while it also could bring solar heat into the room. The other parameters that couple with window type related to solar heat and natural light include shading strategies (Yang et al., 2017), overhang dimensions (Chen et Yang, 2017), thermal mass (Tuhus-Dubrow et Kraeti, 2010) and artificial lighting control (Pernodet et al., 2009).

Some studies have modified the HVAC system type (Kerdan et al., 2016), HRV type (Hamdy et al., 2016) and heating and cooling system set-point (Ascione et al., 2017) in the optimization

process. The building energy consumption can be lowered when the mechanical system runs optimally.

Building shape and orientation are also included in some studies (Tuhus-Dubrow et Kraeti, 2010), however, it is often difficult to optimize the building orientation and shape, given the constraints of the street or block layout when designing a real building.

Airtightness is another important parameter influencing house energy performance: a well-designed house with a higher insulation level may also have high energy consumption if it has a poor level of airtightness. Different levels of airtightness have been studied in building optimization by Chen and Yang (2017) and Junghans and Darde (2015).

For solar active systems, some studies included a PV system (Hamdy et al., 2016) or a solar collector (Asadi et al., 2014).

2.3.5 Objective Functions

The objective in optimization varies from study to study. The most commonly used objective functions are life-cycle cost, energy consumption with thermal comfort, and initial construction cost with operation cost.

Some researchers have specifically focused on lighting control; Carlucci et al., (2015) used thermal comfort and visual comfort as objectives. In some studies, total energy consumption has been separated into heating consumption and cooling consumption, and both heating and cooling consumption were minimized in the optimization instead of only the total energy consumption being minimized (Ascione et al., 2016). In another case, energy consumption was separated into heating, cooling and lighting energy consumption, and the three were considered as separate objectives in the optimization (Delgarm et al., 2016). Shi (2011) used life-cycle cost and life-cycle environmental impact as objectives.

$$Life-cycle\ Cost \\ = Initial\ Cost + Operaation\ Cost + (Maintanance\ Cost + Replacement\ Cost)_{optional} \quad (2\text{-}3)$$

$$Energy\ Consumption \\ = Energy_{heating} + Energy_{cooling} + Energy_{lighting} + Energy_{appliance} + Energy_{domstic\ hot\ water} \quad (2\text{-}4)$$

$$= \frac{\textit{Discomfort Hour using Average Predicted Mean Vote}}{\textit{Occupied Hours}} \qquad (2\text{-}5)$$

2.3.6 Summary

The review shows that there are various choices in implementing the main optimization components – namely, optimization algorithms, optimization tools and building energy performance tools.

For the optimization algorithms, in general different algorithm methods perform differently in searching the optimum results in various cases with certain objectives (Kheiri, 2018). Still, each algorithm has its limitations in application. The calculus-based algorithm requires a detailed mathematical expression of the objective and permits derivatives. The direct search method introduced in the derivative-free algorithm category is very powerful in finding good solutions (Machairas et al, 2014). It does not require an explicit derivative objective function, but it can be easily trapped into local minima and does not deal well with discontinuous objective functions. The evolutionary algorithm under meta-heuristic algorithms is used as a global search and can easily handle objective functions with many local minima, whereas GA can occasionally fail to reach optimal results if the number of simulations is small (Wetter et Wright, 2004). Hybrid algorithms coupling global search methods with local search methods can have better performance, although they require more computation time, and the local search method is not ideal for discrete variables (Machairas et al, 2014). If the user is willing to accept a slight decrease in accuracy for the benefit of fewer simulations, simple GA can also be a good choice (Wetter et Wright, 2004).

Recently, the GA has become the most popular algorithm used in building optimization, not only because it has good performance in global searching but also because it has numerous variations, such as MOGA and NSGA-II, and it can be hybridized with other preprocess or postprocess algorithms to refine the optimal process and results.

Choosing the appropriate building performance assessment tool depends on the building optimization requirements. The simplified analytical models can save time with a fairly rapid calculation speed, although it requires extra effort to set up the model using simplified analytical equations following thermodynamics and heat transfer equations. In addition, the accuracy of these

models compared to realistically detailed houses is not guaranteed. Rather than a complex energy evaluation, a simplified model is more suitable for optimizing control systems. Building performance surrogate models must be trained with a large database. If the surrogate model only used for one optimization, the number of building evaluations may be higher than the number of simulation runs when optimization algorithms are coupled with building simulation software. The better option for simulating the building is to use detailed building models. Detailed information for setting up a house model in the software is available if there is a prototype building. There are many sophisticated building energy simulation software packages available for setting up detailed building models. When applications, limitations and open source status are considered, EnergyPlus emerges as open-source software for simulating building and energy performance without serious limitations.

Different optimization tools are used to implement the selected optimization algorithm. Custom programmed algorithms require expert programming knowledge, but they have the flexibility to solve specific optimization objectives. If the optimization is without specific requirements, the already programmed algorithms packed in general or special optimization tools can be used with very little time needed for adjusting algorithm inputs. Under general and special optimization tools, different tools have different limitations. Special optimization tools can only be linked to specific building assessment software and/or can only provide specific algorithms. The general optimization packages can provide more flexibility and options but require some customer-programmed code to be linked to building assessment software.

GenOpt and Matlab as general optimization packages are widely used in building optimization. As GenOpt has a more limited algorithm than Matlab, especially as GenOpt does not provide MOGA, it is inconvenient to integrate a Java-based new algorithm into GenOpt. Even though Matlab also requires some self-programmed code to connect the toolbox with simulation software, it still requires less time than that needed to code an entire algorithm in Java.

2.4 BIPV/T System

The BIPV/T system can serve the function of building envelope either on a roof or on a façade, and it can produce thermal and electrical energy by collecting solar energy. An active BIPV/T air system may contribute to achieving a net-zero energy house when the energy consumption is mainly from the heating requirement. To further utilize the thermal energy from the BIPV/T air-based system, it can be integrated with other energy systems in the building (Yang, 2015).

After the optimization to identify the optimal combination of passive design parameters to lower energy demand, this study will focus on a BIPV/T system to utilize solar energy to lower the house energy demand or increase system efficiency. This review of the BIPV/T application is to provide a general understanding of the benefits it provides and of its optimal use of heat and electricity. Based on this, further integration of a BIPV/T system in a residential house is carried out in this thesis.

A BIPV/T system can be coupled with HRV. The main purpose is to shorten the defrost time in the heat-exchanging core. As new houses become more airtight, the minimum fresh air required is set according to IAQ. In a cold climate zone, this amount of fresh air will bring in a large heating load to the building during winter, thus using heat recovery to preheat the inlet air from the exhaust air will lower the heating demand. However, the main problem for HRV is the frost formation due to the extremely low temperature of inlet air, which could cool down the exhaust air below its dew point, after which the vapor will condense and freeze. The use of a BIPV/T system to preheat the HRV inlet air could address this issue. Toffanin et al. (2019) showed that in Iqaluit (NT, Canada), a BIPV/T system on the south façade with an air speed of 5 m/s could reduce the defrost time of HRV by 13%.

The ASHP is one of the most energy-efficient pieces of equipment, with a higher efficiency than a furnace or an electric baseboard heater. The challenge of installing an ASHP in an extremely cold region is that it has a cut-off outdoor temperature (e.g. -15 ˚C) below which it will stop working (Asaee et al., 2017). The ASHP will have a relatively low COP when the ambient temperature is low. The use of a BIPV/T system to heat the air temperature around an ASHP's outdoor unit – namely the evaporator – can extend ASHP working hours and raise the COP, offering energy savings. Tardif et al. (2017) showed that when combining a BIPV/T system with

an ASHP, the total energy saving in heating was 41% compared to the base case. Li et al. (2015) showed that when combined with a BIPV/T system, the COP of an ASHP could be increased from 3.72 to 4.6.

Another simple method for using the thermal energy from a BIPV/T system is to directly introduce the heated air into the conditioned space during the winter whenever it could contribute to reducing the heating demand. Shahsavar and Rajabi (2018) studied a BIPV/T system used to preheat inlet air in ventilation and determined that the system could reduce the energy required for heating ventilation air by 32.52%.

A summary of some recent studies of BIPV/T systems coupled with building energy systems and their conclusions is given in Table 2-3. The table is sorted by energy system, as many studies may include several scenarios of a BIPV/T system connected to different systems, and the reference paper may be repeated under some categories.

Table 2-3 Summary of BIPV/T systems integrated with mechanical systems

BIPV/T coupled system	Reference	Location	Configuration/Conclusion
Heat Recovery Ventilation	Tardif et al. 2017	Montreal (Canada)	• An area of 12.75 m^2 BIPV/T was used to supply 20 kg/(h·m^2) fresh air. The HRV would extract air from BIPV/T at a rate of 0.07 kg/s with a 50-W fan when space heating was required and solar radiation was above 50 W/m^2. • The total net mechanical energy savings were up to 16%, mostly due to the electricity produced by PV panels, while the total energy saving in heating was 1% compared to the base case.
	Toffanin et al. 2019	Iqaluit (Canada)	• BIPV/T system was installed on south façade and south roof with different slope, with the airspeed from 0.5 m/s to 2.5 m/s. • An airspeed of 0.5 m/s achieved the highest frost control time. Under an airspeed of 0.5 m/s, the BIPV/T on south façade generated more energy during the winter and reduced the defrost cycle of HR by 13%. Achieved 32.34% saving on heating oil.
	Kim et al. 2016	N/A	• An area of 6.4 m^2 PV/T was on a 30-degree sloped south-facing roof with an airflow rate of 250 CMH to an HRV. • PVT system with an HRV could save 10% heating energy, and had an overall efficiency rate of 38% based on its thermal and electrical performance level during the heating season.
Air-source Heat Pump	Tardif et al. 2017	Montreal (Canada)	• An area of 27.9 m^2 BIPV/T was used to supply up to 60 kg/(h·m2) warmed air to an ASHP with a 280-W fan when the ASHP was working and solar radiation was above 50 W/m^2. The air from BIPV/T only met 30% of the air flow rate required by the ASHP. • The total net mechanical energy savings were up to 62%, and the total energy saving in heating was 41% compared to the base case.

	Asaee et al. 2017	All provinces in Canada	• BIPV/T was applied on the south or nearly south-facing roof. • With BIPV/T systems, the energy consumption in Canadian house stock would be reduced 227 PJ per year, equivalent to 18% annual energy saving; would remove 10.85 MJ of GHG emission, equivalent to 17% removal of GHF emission.
	Li et al. 2015	Shenyang (China)	• BIPV/T was installed on a vertical façade with an area of 240 m², and inlet airflow rate from 2-6 m/s. • When the outdoor temperature was -5 ˚C, the thermal efficiency of the PV/T could reach 21%. When the inlet air flow rate was at 2-4 m/s, COP increased from 3.72 to 4.6.
	Hailu et al. 2015	Anchorage (USA)	• BIPV/T was installed on the south façade with an area of 22 m², and inlet air flow rate was 1 m/s; a two-stage variable capacity ASHP was involved. • The COP improved significantly when average ambient temperature was above 10 ˚C, and improved when the average ambient temperature was above -3 ˚C, and an improvement was observed when the average ambient temperature was below -10 ˚C. The maximum COP when ASHP with BIPV/T was 5.31 on Feb. 23rd, and the COP at base case was 4.2.
Direct introduce circulate air into condition zone	Ahmed-Dahmane et al. 2018	Ain Benian (Algeria)	• BIPV/T was installed on an eight-story office building southern exterior wall. Each floor has two PV/T air collectors, each with an area of 9.849 m², with an airflow rate of 0.45 m³/s. • BIPV/T system could cover a significant amount of useful thermal energy during the winter.
	Shahsavar and Rajabi 2018	Kermanshah (Iran)	• BIPV/T with an area of 10 m² mounted on a 34-degree sloped roof, with air mass flow rate of 2 kg/s. • BIPV/T system could provide 32.52% of the required heating load for ventilation air on an average basis.

2.5 Chapter Summary

The reviews focus on four components. The codes and standards for Canada or northern Canada in the first section provide explicit requirements on envelope resistance, airtightness and ventilation rate. While the solar strategies are not involved, neither the passive solar strategies of the thermal mass requirement or window-wall ratio nor the active solar strategies of suggesting the usage of PV panels or solar collectors. The basic requirements present in codes and standards provide a baseline for the further optimization of the house.

In the second section, northern high-performance projects were introduced with details about the involved building features and energy systems to show how these projects are designed to deal with an extremely cold climate and consume less energy while being suitable to the local residents' lifestyle and culture. All the houses in these northern projects have a much higher thermal resistance than the requirements of the local standard, and they incorporate construction techniques

to eliminate thermal bridges and ensure the airtightness. The mechanical systems are equipped with high-efficiency equipment. For a primary heating energy source, it has been suggested to use electricity; however, electricity prices become extremely high after usage exceeds a certain amount. For houses designed with low energy demands, it could be better to use electricity for heating; otherwise, fuel heating should be considered. An HRV system is mandatory in all northern house projects. Some projects installed PV panels or solar collectors to utilize solar energy, which makes a significant contribution to helping the house reach its targeted energy savings. Recent northern housing research have studied the energy performance for each passive design parameter, proposed a protocol for northern housing, simulated and experimented with the performance of SIPs, analyzed the hygrothermal performance of attic space with different types of ventilation and optimized the usage of HRV.

The third section introduced commonly used optimization methods, algorithms, optimization tools and building performance assessment models by reviewing recent building optimization papers. Genetic algorithms provide good performance in global searches without being affected by local minima or discontinuities or by the derivative permit of objective functions. Compared to other global searching algorithms, such as PSO or hybrid algorithms, GA provide similar results with fewer simulation runs. EnergyPlus, a sophisticated open-source software tool, could provide accurate results with detailed building models. All the detail information to model a house in EnergyPlus needs to be collected based on the existing reference house examples. General optimization packages have the ability to link algorithms with building assessment tools. Matlab is widely used in building optimization and offers various optimization algorithms. These all provide support to the optimization set-up in Chapter 3, which uses Matlab to run the MOGA and EnergyPlus for building performance simulation.

The application of air-based BIPV/T systems coupled with different house energy systems introduced in the fourth part provided possible solutions for integrating BIPV/T systems with space heating systems, HRV systems and HP systems to reduce house energy consumption or improve system performance.

High-performance houses in the north require design parameters that far exceed the standards or codes requirements, yet passive solar design principles are absent in the existing standards or codes.

The construction costs in the north are very high for a high-performance house, as all the materials are imported from the south during the short summer period. However, the previous northern housing research studies were focused on improving energy performance without considering the restriction of the added cost. Optimization using a multi-objective algorithm is carried out in Chapter 3 to counterbalance the energy performance and the construction cost of the building. Furthermore, the BIPV/T system integrated with mechanical systems is studied in Chapter 4 to provide some suggestions on active utilization of solar energy in northern Canada.

Chapter 3   Optimization of Passive Design Parameters

Northern Canada has considerable solar radiation, while the standards and codes for the north remain silent on passive solar design strategies. A parametric study was carried out by Thirunavukarasu (2016) to investigate the effect of passive design parameters, especially thermal mass, WWR and active solar systems, all of which use solar energy. According to the parametric study, thermal resistance, thermal mass, window type and area, night shutters and strategies to avoid overheating all brought benefits to lower the annual energy demand. Increased thermal resistance for the envelope can save energy, but the thermal resistance values for walls, ceilings and floors may differ from each other in a high-performance house. The performance of thermal mass is influenced by the amount of solar radiation through the window area. If the incident solar radiation through the window remains at a low level, then the excess thermal mass would absorb significant heat from the room in addition to the solar heat, which can have a negative effect on energy savings. Window area, on one hand, can allow more solar heat gain into a room, but on the other hand, it is not ideal for preventing heat loss, as windows have a low thermal resistance. Under these conditions with parameters have conflicting effects or restricting each other, further optimization study is needed to optimally combine these parameters to get a low energy demand house. The following parameters are included in the optimization in this chapter: thermal resistance for walls, ceiling and floor; thermal mass; strategies to avoid overheating; WWR and window type.

In this chapter, building passive design parameters are modified simultaneously and evaluated to determine the optimal combination through optimization. The reference house, which represents a newly built residential house in the north set up by Thirunavukarasu (2016), is involved in the optimization with two cases. The main case optimizes the house located in Yellowknife, NWT, which is the same location used for the parametric study by Thirunavukarasu (2016), and the second one optimizes the house located in Kuujjuaq, QC, where construction cost is much higher yet has a similar weather condition compared with Yellowknife. The influencing factors in the optimization are analyzed in these cases: namely, the location factors used in construction cost calculations, the energy sources, the presence or absence of a thermal mass and the consideration of additional labor costs used to support labor from the south constructing buildings in the north.

3.1 Reference House Models

The studied reference house represents a newly built single-family house in the city of Yellowknife, NWT, built in compliance with the National Building Code of Canada (NBCC, 2015). The building, shown in Figure 3-1, is a detached single-story house with a total floor area of 130 m² and a ceiling height of 2.5 m. The house faces south with 15 m of its length and 8.67 m of its width. A window with variable area is assumed on the south façade only, and a BIPV/T system is placed on the south-facing roof.
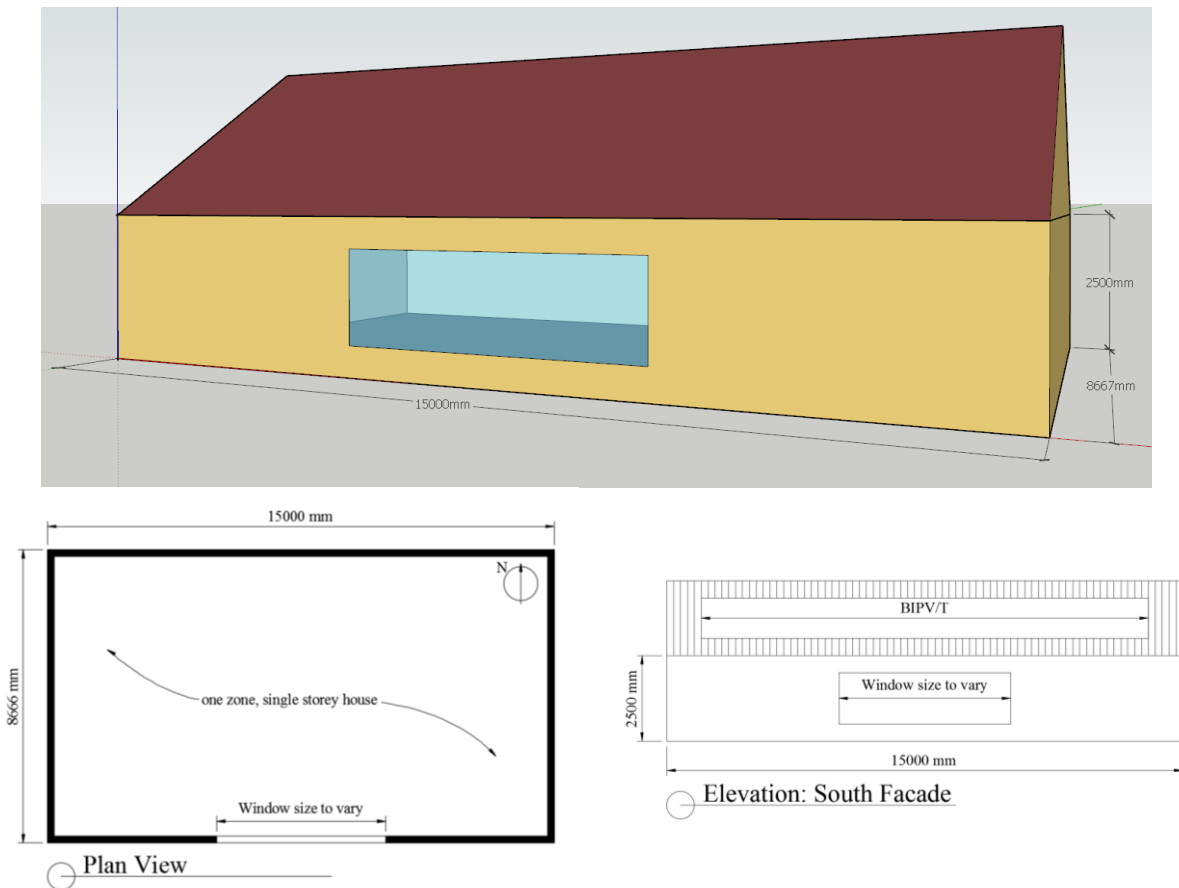
Figure 3-1 Plan view and elevation of the reference house

EnergyPlus was used to model this reference house. This single-family detached house was shaped in SketchUp, and the detail setting is completed in EnergyPlus. All the parameter values for the reference house are listed in Table 3-1. In EnergyPlus, the envelope needs to be structured layer by layer, and the detail information for envelope assemblies and the material properties for each layer are listed in Table 3-2. All the material parameters are cited from the ASHRAE handbook Fundamental (2017). The internal heat gain for the reference house refers to the heat from lighting,

equipment and occupants. In this single-family house, four occupants are assumed, two parents and two children, and they leave the house at 8:00 and come back at 18:00. The heat from occupants is assumed as 62.5 W/person, and the power of lighting and equipment are assumed to be 100 W for each, with an all-day turning on schedule as a simplified assumption. According to IAQ, a minimum ventilation rate is required. A ventilation rate is set as 0.3 ACH, following the mechanical ventilation requirement specified by NBCC (2015). The weather data is the Yellowknife, NWT, weather file downloaded from the EnergyPlus Weather Data website.

The reference house is equipped with an HVAC system called Ideal Loads Air System. This system is an ideal unit that mixes the zone exhaust air and inlet outdoor air and then adds or removes heat and moisture at 100% efficiency to produce the supply airstream at the defined conditions. The energy required to condition the space by the Ideal Loads Air System equal to the house energy demand. The simulation results show that the reference house has an annual energy demand of 132.04 kWh/m^2·a, with a heating demand of 129.50 kWh/m^2·a and a cooling demand of 2.54 kWh/m^2·a (Table 3-1).

Table 3-1 The reference house's detailed information in EnergyPlus

Key design parameters	EnergyPlus
Thermal resistance value for wall	RSI 4.33
Thermal resistance value for ceiling	RSI 5.57 *
Thermal resistance value for floor	RSI 6.06
Thermal mass	6-mm wood tiles on floor and 1 layer of gypsum on walls
Window	Triple-glazed, low-E, argon-filled U 0.907, SHGC 0.477
Window wall ratio (south façade)	20%
Night shutters	None
Shading schedule	None
Ventilation rate	0.3 ACH rate
BIPV/T systems	None
Set-points	26.5 ˚C – cooling set-point 21 ˚C & 18 ˚C – heating set-points
Energy Performance	
Heating demand (kWh/m^2·a)	129.50
Cooling demand (kWh/m^2·a)	2.54
Total energy demand (kWh/m^2·a)	132.04

* The Ceiling RSI is a hand calculation, as EnergyPlus does not output the interior structure's thermal resistance.
* Heating set-point schedule is 21 ˚C for the day, which is the period from 8:00 am to 10:00 pm, and for the night, the setback set-point of 18 ˚C is applied.

Table 3-2 Properties of materials for constructing envelope in EnergyPlus (ASHREA Fundamental, 2017)

	Density [kg/m³]	Conductivity [W/(m·K)]	Resistance [(m²·K/W)]	Specific Heat [kJ/(kg·K)]
Wall				
1. Prefinished structural smart panel siding [a]	460 [1]	-	0.1	1.22
2. Air space [b]	-	-	0.16	-
3. Dupont home wrap Tyvek membrane	-	-	-	-
4. 2 x 6 stud [c] with mineral fiber insulation [d]	615 [2] / 73 [5]	0.15 [3] / 0.035	-	1.63 [4] / 0.8 [6]
5. Mineral fiber insulation [d]	73 [5]	0.035	-	0.8 [6]
6. Polyethylene air and vapor barrier	-	-	-	-
7. 2 x 4 stud [c] with mineral fiber insulation [d]	615 [2] / 73 [5]	0.15 [3] / 0.035	-	1.63 [4] / 0.8 [6]
8. 1/2-in Gypsum board [e]	640	0.16	-	1.15
Ceiling				
1. Mineral fiber insulation [d]	73 [5]	0.035	-	0.8 [6]
2. 2 x 12 stud [c] with mineral fiber insulation [d]	615 [2] / 73 [5]	0.15 [3] / 0.035	-	1.63 [4] / 0.8 [6]
3. Polyethylene air and vapor barrier	-	-	-	-
4. 1/2-in Gypsum board [e]	640	0.16	-	1.15
Floor				
1. 5-cm Concrete [f]	2,240 [7]	1.3 [8]	-	0.80 [9]
2. Polyethylene air and vapor barrier	-	-	-	-
3. SIP – 1/2-in OSB [g]	650	-	0.12	1.88
4. SIP – Expanded polystyrene insulation [h]	20 [10]	0.036 [11]	-	1.5
5. SIP – 1/2-in OSB [g]	650	-	0.12	1.88
Roof				
1. 3/8-in [12] Roofing shingles [i]	920	-	0.078	1.26
2. Self-sealing-membrane type eave	-	-	-	-
3. 1/2-in Plywood [j]	460	-	0.14	1.88
Other Material				
Engineered wood floor tiles [k]	571	-	0.044	2.5

[a] Page. 26.9 Building Board and Siding – Siding – Wood, plywood, lapped 9.5 mm

[b] Page. 26.14 Vertical 13 mm Air Space, Mean Temperature at 10 and Temperature Difference at 5.6 with effective emittance of 0.82

[c] Page. 26.12 Woods – Softwoods – Southern pine

[d] Page. 26.8 Insulating Material – Blanket and batt – Mineral wool, felted

[e] Page. 26.9 Building Board and Siding – Board – Gypsum or Plaster board

[f] Page. 26.11 Masonry Material – Concretes – Sand and gravel or stone aggregate concretes (concrete with >50% quartz or quartzite sand have conductivities in the higher end of the range)

[g] Page. 26.9 Building Board and Siding – Board – Oriented strand board (OSB), 12.7 mm

[h] Page. 26.8 Insulating Material – Board and slabs – Expanded polystyrene, molded beads

[i] Page. 26.10 Roofing – Asphalt shingles

[j] Page. 26.9 Building Board and Siding – Board – Plywood (Douglas fir), 12.7 mm

[k] The density and specific heat of engineered wood taken from Thirunavukarasu (2016), and the resistance value is from "http://www.radiantprofessionalsalliance.org/Pages/FloorCoveringR-ValueChart.aspx" 1/4-in Engineered wood. The R-value is R-0.25 and converted to RSI is RSI-0.044

[1] The siding density value is referred to the Building Board and Siding – Board-Plywood (Douglas fir), 12.7 mm on page 26.9

[2] The wood stud density value is half of the given value. Density = (570 + 660)/2 = 615

[3] The wood stud conductivity value is half of the given value. Conductivity = (0.14 + 0.16)/2 = 0.15

[4] The wood stud specific heat value is referred to the most of the wood specific heat in the list is 1.63 kJ/(kg·K), and the value is related to moisture content (MC), which here is noted as 12% MC

[5] The mineral insulation density value is half of the given value. Density = (16 + 130)/2 = 73

[6] The mineral insulation specific heat value is referred to other mineral material, Mineral fiberboard-wet felted, in the same list

[7] The concrete density value is the closest one to the value in the parametric study provided by Thirunavukarasu (2016); the density in his parametric study is 2,200 kg/m³

[8] The concrete conductivity value use the lowest value of the given values; accordingly, the specific heat value also is the lowest value of the given values

[9] The concrete specific heat value is the lowest value of the given values because it the same value as it in the parametric study provided by Thirunavukarasu (2016); the specific heat in his parametric study is 800 J/(kg·C)

[10] The expanded polystyrene insulation density value is half of the given value. Density = (16 + 24)/2 = 20

[11] The expanded polystyrene insulation conductivity value is half of the given value. Conductivity = (0.035 + 0.037)/2 = 0.036

[12] The roof shingle thickness value refers to the description in the website article (https://www.hunker.com/13401243/how-thick-should-a-roof-be) "Standard asphalt shingles add very little thickness to the roof because a standard three-tab shingle is about 3/16-inch thick. When installed, however, the shingles overlap, doubling the thickness." Thickness=2 * (3/16 in) = 3/8 in = 0.0095 m

3.2 Optimization Methodology

The optimal combination of all the passive design parameters is constrained not only by those parameters that have a conflict influence on energy demand but also by construction costs. If the add-on cost of construction for a higher performance house cannot be offset by the energy savings, then the combination of design parameters will not bring a benefit to the house owners. Initial construction cost and the annual operational cost are the two objectives in evaluating the optimal combination of passive design parameters. A multi-objective optimization considering the initial construction cost and life-cycle energy cost is carried out.

3.2.1 Multi-objective Genetic Algorithm (MOGA)

A MOGA is a GA with more than one objective to minimize or maximize. Generally, under building optimization, a GA encodes the studied characteristics of the house into a chromosome and randomly generates the first generation as parents by coupling the variables with different values within boundaries or following constraints. The first generation is calculated or simulated based on the objective functions, and each result is output for evaluation. During the evaluation, the algorithm keeps the best-performing individuals to the next generation as elitisms and breeds the high-performance individuals by crossover to form the next generation, which called children, and a small degree of mutation is in place to avoid trapping values in local minima. The iterative process of using the next generation to replace the previous one will converge to the optimal

solution, and the iteration will stop and output the final results when the stopping criteria are reached (Kheiri, 2018).

3.2.2 Optimization Procedure

The optimization study couples EnergyPlus and Matlab to adjust all the major passive design parameters at the same time and output the optimal combinations of parameters that would lead to a house with lower energy demand.
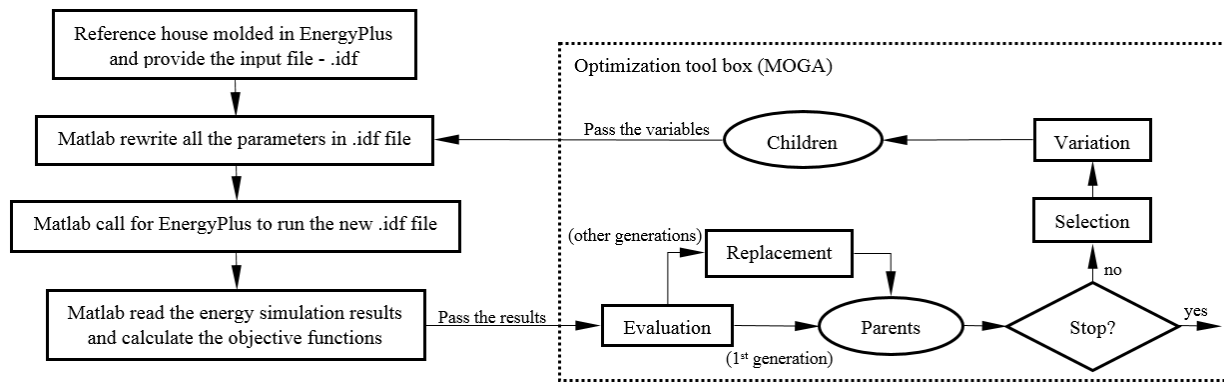
Figure 3-2 Optimization procedure

The optimization procedure (Figure 3-2) can be broken into three parts. The first is EnergyPlus, which simulates energy performance for all the cases the Matlab code passes to it. The second part is a programmed Matlab code that rewrites the values of the parameters in the EnergyPlus input file (.idf file) using the value generated in the optimization toolbox and calls for EnergyPlus to simulate the energy performance. Then the simulated energy results are extracted and sent back to the toolbox for evaluation. The third part is the optimization toolbox with an algorithm chosen to generate the groups of inputs, evaluate the send back results and then output the final optimal results. The inherent optimization toolbox in Matlab could provide functions and algorithms in finding the parameters that minimize or maximize the objectives. The MOGA is the algorithm applied in the optimization toolbox. The toolbox randomly selects the value for the studied parameters, which are listed in Table 3-3 and described in the following section, to form the initial groups of parameters, also referred to as the generation called "Parents". These groups of values are passed to the EnergyPlus input file by the Matlab code. After the Matlab code call for EnergyPlus to simulate energy performance for all groups and send back the results, the algorithm

in the toolbox evaluates those results. If the stopping criteria are met, the best performance results are output. If the stopping criteria are not met, the algorithm selects the high-performing cases and varies the parameters by crossover and mutation to form a new generation called "Children". The cycle is repeated until the stopping criteria are met and the optimal results are output.

3.3 Case Study 1: Yellowknife

The primary case study in optimization is performed for Yellowknife, NWT. In the optimization, the studied parameters are provided with varying values in groups as inputs. The involved parameters and their ranges, the optimization objective functions, and the MOGA settings are introduced. The optimal house over a 25-year life cycle is provided and analyzed. Life-cycle years and the location factor in construction cost calculation, which may influence the final optimal results, are studied.

3.3.1 Studied Parameters and Their Ranges

The parameters investigated include the thermal resistance for walls, ceiling and floor; thermal mass on the floor and the interior walls; and WWR, as shown in Table 3-3. The thermal resistance for the envelope is varied by adjusting the insulation thickness. The cross-section of walls, ceiling and floor are shown in Figure 3-3. The WWR is varied by changing the width and height of the window on the south façade, and the WWR is calculated according to the window area after the simulation. Window type is kept as the triple-glazed, low-E coating, argon-filled window, which has the best performance among all window types shown in the parametric study done by Thirunavukarasu (2016). Also, the strategies to avoid overheating are applied, which are shading, blocking 90% of solar radiation, and increased ventilation rate, from 0.3 ACH to 2 ACH if cooling is required.

The ranges for each parameter are referenced from the following codes and standards: National Building Code of Canada (2015), National Energy Code of Canada (2017), ASHRAE 90.2 (2018) and 60.2 (2016), R-2000 standards (2012) and Good Building Practice for Northern Facilities

(2011). The lowest boundary of thermal resistance for the envelope is the maximum value listed in the codes and standards. For thermal mass, none of the codes and standards provide a clear requirement for thermal mass. The range of thermal mass is determined based on experience and the literature. The window type and the minimum ventilation rate are also in compliance with codes and standards. All codes and standards requirements for each parameter are summarized in Appendix A.

Table 3-3 Studied passive parameters and the range used in optimization

Parameters	Unit	Studied range	Description
Thermal resistance for walls	$m^2 \cdot K/W$	[5.6 20]	Modified the thickness of insulation
Thermal resistance for ceiling	$m^2 \cdot K/W$	[8.75 21)	Modified the thickness of insulation
Thermal resistance for floor	$m^2 \cdot K/W$	[7 20]	Modified the thickness of insulation in SIPs
Thermal mass on the floor	m	[0.05 0.2]	Modified the thickness of concrete
Thermal mass on the walls	layers	[1 3]	Modified the number of gypsum board layers
WWR	%	(0 90]	Modified the window width and height
Window type	---	Triple glazed	---
Shading	---	Block 90% of solar radiation if cooling is required	---
Ventilation rate	ACH	0.3 or 2 if cooling is required	---

In EnergyPlus, the thermal resistance of the envelope is calculated based on the thickness and conductivity of each layer of material. The thermal resistance of the envelope in EnergyPlus can be adjusted by changing the thickness of the insulation layer. The range of insulation thickness is shown in Table 3-4. The window dimensions are defined in EnergyPlus by using the coordinates at the four corners, and the window area is varied by changing the width and height in the coordinates. The width and height of the window are listed in Table 3-4 corresponding to the range of WWR studied.

Table 3-4 The modified variable values and boundaries in the multi-objective genetic algorithm

Description	Variable	Range
Wall – the thickness of insulation in between the double studs	X_1	0.0095-0.5 m
Ceiling – the thickness of extra insulation other than the insulation in 2 x 12 stud cavity	X_2	0.0762-0.5 m
Floor – the thickness of insulation in SIPs	X_3	0.2381-0.5 m
Window width	X_4	0.2-14.8 m
Window height	X_5	0.2-2.3 m
Floor – the thickness of concrete	X_6	0.05-0.2 m
Wall – the number of layers of gypsum board	X_7	1-5

(Exterior)
- Smart panel siding
- 13 mm (1/2 in) Airspace
- Dupont home wrap
- 38x140 mm @ 400 mm o.c. (2x6 in. @ 16 in. o.c.) Wood stud
  with mineral wool batt insulation in the cavity
- (varied thickness) Rigid fiberglass insulation
- Polyethylene air and vapor barrier
- 38x89 mm @ 400 mm o.c. (2x4 in. @ 16 in. o.c.) Wood stud
  with mineral wool batt insulation in the cavity
- (varied layers) Gypsum board, 1 layer is 13 mm (1/2 in.)
(Interior)

(a) Exterior walls

(Exterior)
- Roof shingles
- Self-sealing-membrane
- 13 mm (1/2 in) Plywood
- 6/12 Roof Truss
  39x300 mm @ 400 mm o.c. (2x12 in. @ 16 in. o.c.) Wood stud
  with blown-in fiberglass insulation in the cavity
- (varied thickness) Blown-in fiberglass insulation
- Polyethylene air and vapor barrier
- 13 mm (1/2 in.) Gypsum board
(Interior)

(b) Ceiling

(Interior)
- (varied thickness) Concrete
- Polyethylene air and vapor barrier
- 13 mm (1/2 in) OSB
- (varied thickness) Expanded polystyrene insulation
- 13 mm (1/2 in.) OSB
(Exterior)

(c) Floor

Figure 3-3 Cross-sections of the envelope

3.3.2 Objective Functions

The objective functions for optimization are the construction cost and operation cost.

$$Construction\ Cost = Location\ Factor\ \times\ US\ Average\ Cost \qquad (3\text{-}1)$$

$$Annual\ Operation\ Cost\ = Local\ Electricity\ Price\ \times Energy\ Consumption \qquad (3\text{-}2)$$

The construction cost is calculated based on RSMeans Residential Cost Data (2017) according to the construction detail set up in the EnergyPlus house model. The detailed calculation of the construction cost and the price for each material are listed in Appendix B. As RSMeans provides the US average price, a location factor is used to covert the US average cost in US dollars to the local price in local currency. For Yellowknife, the location factor provided by RSMeans is 1.13, and this converted the house construction cost to the Yellowknife local price in Canadian dollars.

The operation cost is based on the energy price from Northwest Territories Power Corporation (NWT Rate Schedule, 2019) and the energy consumption output from EnergyPlus. During the optimization, the house is equipped with an HVAC system called Ideal Loads Air System. This system is an ideal unit that mixes the zone exhaust air and inlet outdoor air and then adds or removes heat and moisture at 100% efficiency to produce the supply airstream at the defined conditions. The energy required to condition the space by the Ideal Loads Air System is the house energy demand. The purpose of optimization is to counterbalance the initial construction cost and the house energy demand. To have a further means of evaluating initial construction cost against energy demand, a simple assumption was made to convert the energy demand to an annual operation cost, which assumed the house is conditioned by an electrical system with a COP of 1. The energy demand output from EnergyPlus is equal to the energy consumption, and an electric price was selected based on the local power corporation.

3.3.3 MOGA Settings

The MOGA settings are provided in the optimization toolbox options (Figure 3-4). Default settings are used for most of the parameters, as listed in Table 3-5. The population size is 200 individuals, and the maximum generation is 100 with a crossover faction of 0.8 and a mutation fraction of 0.2.

Table 3-5 MOGA settings in Matlab toolbox

Population type	Population size	Selection	Crossover	Mutation	Generation
Double vector	200	Tournament	Intermedia Fraction: 0.8	Adaptive feasible Fraction: 0.2	<100

As defined in the Matlab optimization toolbox quick reference, the setting functions are described below:

Tournament: selects each parent by choosing individuals at random, the number of which you can specify by Tournament size, and then choosing the best individual out of that set to be a parent;

Intermedia: Intermediate creates children by a random weighted average of the parents. Intermediate crossover is controlled by a single parameter Ratio; and

Adaptive feasible: randomly generates directions that are adaptive with respect to the last successful or unsuccessful generation. A step length is chosen along each direction so that linear constraints and bounds are satisfied.
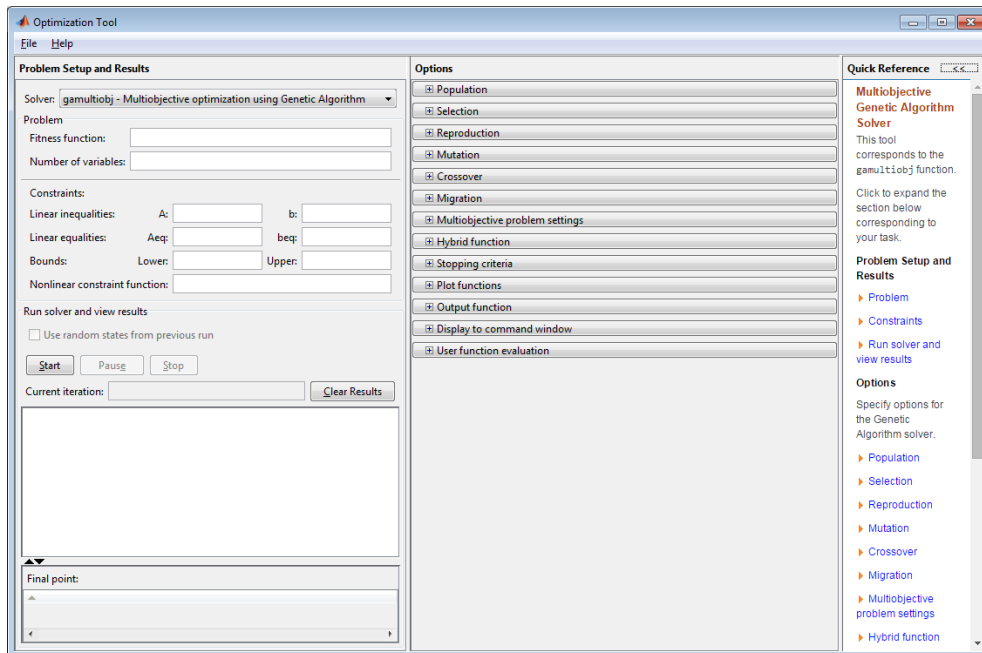
Figure 3-4 Optimization toolbox in Matlab

3.3.4 Optimization Results

Figure 3-5 shows the optimization results for all cases. The cases on the Pareto front are the optimal cases based on initial construction cost and annual operation cost. As expected, a house with a higher construction cost has better performance in energy efficiency and thus has a lower operation cost.
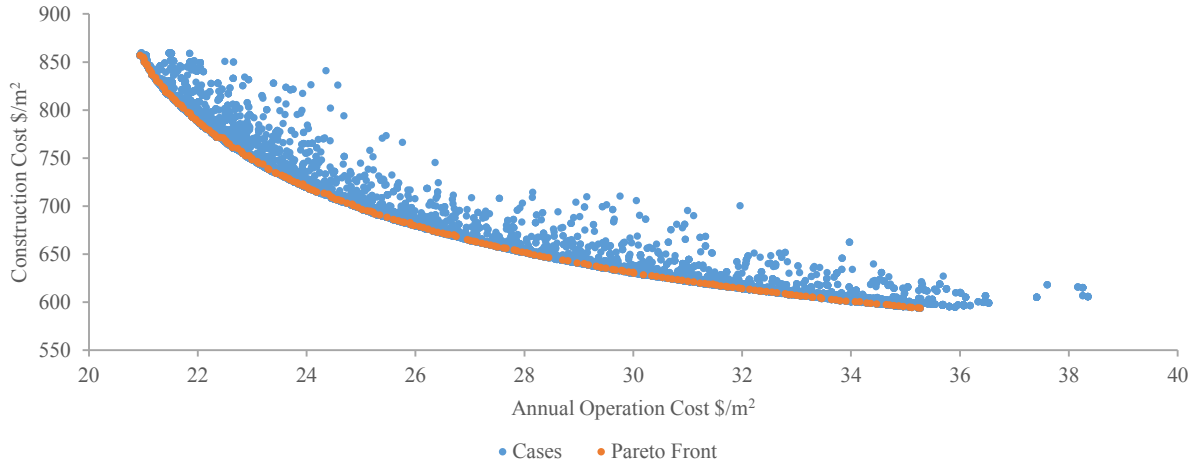
Figure 3-5 Optimization results

To get the optimized house, a life-cycle cost analysis over a 25-year period, which includes the initial construction cost and the total operation cost, is carried out. The optimized house is the case with the minimum life cycle cost. All the operation costs in future years are converted back to the present value by using the interest rate (discount rate) of 3.5% and keeping the energy price as constant (RDH Building Engineering). The electricity price for Yellowknife is 29.81 ₵/kWh (NWT Rate Schedule, 2019).

$$Total\ Life - cycle\ Cost = Construction\ cost + Total\ operation\ Cost \qquad (3\text{-}3)$$

$$Total\ Operation\ Cost = \sum_{i=0}^{years} (Local\ Electricity\ Price \times Energy\ Consumption) \quad (3\text{-}4)$$

$$Present\ Cost = \frac{Cost\ in\ year\ i}{(1 + discount\ rate)^i} \qquad (3\text{-}5)$$

Table 3-6 shows that the optimized house could decrease the energy demand from 132.04 kWh/m²·a down to 71.29 kWh/m²·a, which saves about 46% of energy demand compared with the reference house. The energy saving is mainly achieved from heating demand. With higher

thermal resistance of the building envelope to reduce heat loss, a larger window area to increase the solar heat gain, and the thermal mass to store the solar energy during the daytime and release the heat during the night, the optimized house requires less heating to maintain the indoor air temperature at the set-points.

Table 3-6 Optimal passive design parameters of the optimized house with a 25-year life cycle

Parameters	Unit	Reference Value	Optimal value
Thermal resistance for walls	m²·K/W	4.26	9.17
Thermal resistance for ceiling	m²·K/W	5.57	20.34
Thermal resistance for floor	m²·K/W	6	11.36
Thermal mass on the floor	m	0.006 – wood tile	0.055 – concrete
Thermal mass on the walls	layers	1 – Gypsum	1 – Gypsum
WWR	%	20	47
Window/floor ratio	%	5.8	13.7
Window type	---	Triple glazed	Triple glazed
Shading	---	None	Block 90% solar radiation if cooling is required
Ventilation rate	ACH	0.3	0.3 or change to 2 if cooling is required
Annual Energy demand	kWh/m²·a	132.04	71.29
Annual Heating demand	kWh/m²·a	129.50	67.68
Annual Cooling demand	kWh/m²·a	2.54	3.61
Construction cost	$	81,438.79	89,941.51
	$/m²	626.45	691.86
HDD (2008-2018) (CWS, 2019)	-	7,964	

(a) without avoid overheating strategies   (b) with avoid overheating strategies
Figure 3-6 Indoor temperature without HVAC system and outdoor temperature

During the cooling season, however, the high thermal resistance of envelope and the large window area of the optimized house may result in overheating in the house, and the house would require higher cooling energy. The shading schedule and ventilation rate control are the strategies applied
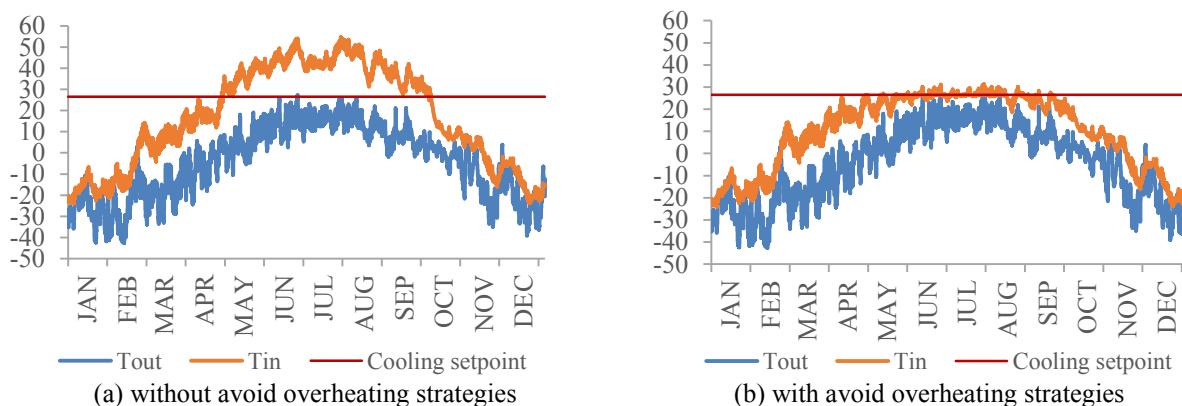
60

to avoid overheating. As shown in Figure 3-6, the indoor air temperature without the HVAC system exceeds the overheating threshold if there are no overheating control strategies applied. With the strategies to avoid overheating applied to the optimized house, the overheating is almost eliminated, which leads to a cooling demand for the optimized house slightly higher than that for the reference house.

For the envelope parameters shown in Table 3-6, all the thermal resistance for walls, ceiling and floor are increased. The required increase of thermal resistance for ceiling is the highest, about 4 times the reference value, and the increase of thermal resistance for walls and floor is about 2 times the reference value. This is because the blown-in fiberglass insulation for the ceiling has the lowest price among all insulations – that is, 4.6 $/m^2 for ceiling blown-in fiberglass insulation at 0.1 m thick and 30.3 $/m^2 for wall rigid fiberglass insulation at 0.1 m thick – and this leads to the optimal solution favoring adding insulation to the ceiling based on economics. For the thermal mass, no extra layer of gypsum board is required to be added to interior walls. The optimal solution is to have a layer of 5.5-cm concrete on the floor. The optimal WWR of the optimized house is 47%, which is lower than the optimal WWR of 70% with strategies to avoid overheating implemented in the parametric study done by Thirunavukarasu (2016). This is because the reference house in the parametric study has lower thermal resistances for the building envelope, and a larger window area is required to obtain more solar heat gain. The other constraint in enlarging the WWR up to 60% in this optimization is the higher price of a triple-glazed window.

Other life-cycle periods of 20 years, 30 years and 50 years are also evaluated. Because the window has a shorter service life, normally 20 to 30 years (True Professional Inc), the construction cost of the house includes the cost of window replacement when the life-cycle period is greater than 30 years. As shown in Table 3-7, the optimal values over a 20-year life-cycle period have a lower thermal resistance for the envelope and lower WWR. The energy demand is increased by 3.8 kWh/m^2·a compared to the optimal results with a 25-year life cycle, and the construction cost is decreased by $2,441. Basically, a house with lower energy demand would benefit the house owner over a longer period. The optimal results over a 30-year life cycle shown in Table 3-7, however, are the same as the optimal results over a 25-year life cycle. This is because the Pareto front is formed by discrete solutions rather than a continuous line, thus the optimal results under different life cycle periods do not change continuously. The energy demand of the optimized house with a

50-year life cycle is lower than the optimized house with a 25-year life cycle. The optimal values with a 50-year life cycle have a higher thermal resistance for the envelope; in particular, the thermal resistances for walls and floors are increased compared to the optimal values for a 25-year life cycle. This is because the thermal resistance of the ceiling has almost reached its highest boundary of 21 $m^2 \cdot K/W$ (accordingly the maximum thickness of modified insulation is 0.5 m), and the optimized house with a 50-year life cycle needs to increase the thermal resistance for walls and floor to achieve the overall thermal resistance required by the envelope. For a life cycle of 50 years, the window is replaced once, which doubles the expense for the window. The optimized house with a 50-year life cycle tends to have a smaller window area compared with the optimized house with a 25-year life cycle.

Table 3-7 Optimal passive design parameters of the optimized house under different life cycle periods

Parameters	Unit	Optimal value over 20 years	Optimal value over 25 years	Optimal value over 30 years	Optimal value over 50 years
Thermal resistance for walls	$m^2 \cdot K/W$	8.93	9.17	9.17	10.64
Thermal resistance for ceiling	$m^2 \cdot K/W$	17.82	20.34	20.34	20.36
Thermal resistance for floor	$m^2 \cdot K/W$	10.10	11.36	11.36	13.16
Thermal mass on the floor	m	0.056 – concrete	0.055 – concrete	0.055 – concrete	0.062 – concrete
Thermal mass on the walls	layers	1 – Gypsum	1 – Gypsum	1 – Gypsum	1 – Gypsum
WWR	%	43	47	47	39
Window/floor ratio	%	12.5	13.7	13.7	11.1
Window type	---	Triple glazed			
Shading	---	Block 90% solar radiation if cooling is required			
Ventilation rate	ACH	0.3 or change to 2 if cooling is required			
Annual Energy demand	$kWh/m^2 \cdot a$	75.08	71.29	71.29	68.11
Annual Heating demand	$kWh/m^2 \cdot a$	72.09	67.68	67.68	65.38
Annual Cooling demand	$kWh/m^2 \cdot a$	2.99	3.61	3.61	2.72
Construction cost	$	87,500.59	89,941.51	89,941.51	95,828.05
	$/m^2$	673.08	691.86	691.86	737.14
HDD (2008-2018) (CWS, 2019)	-	7,964			

In general, the optimal case over a longer life cycle period turns out to have a higher initial construction cost and lower annual operation cost. A zoomed-in Pareto front in Figure 3-7 shows the selected optimal cases under different life-cycle periods. Comparing the optimal case over a 15-year life cycle and the optimal case over a 50-year life cycle, the annual operation cost is changed from 27.5 $/m^2$ to 24.3 $/m^2$, and the initial construction cost is increased from 658 $/m^2$

to 714 $/m². As the Pareto front is discrete, some optimal cases under adjacent life-cycle years are the same. The optimal cases under the 25-year life cycle and 30-year life cycle are the same, and the four optimal cases under the 35-year, 40-year, 45-year and 50-year life cycles are the same.
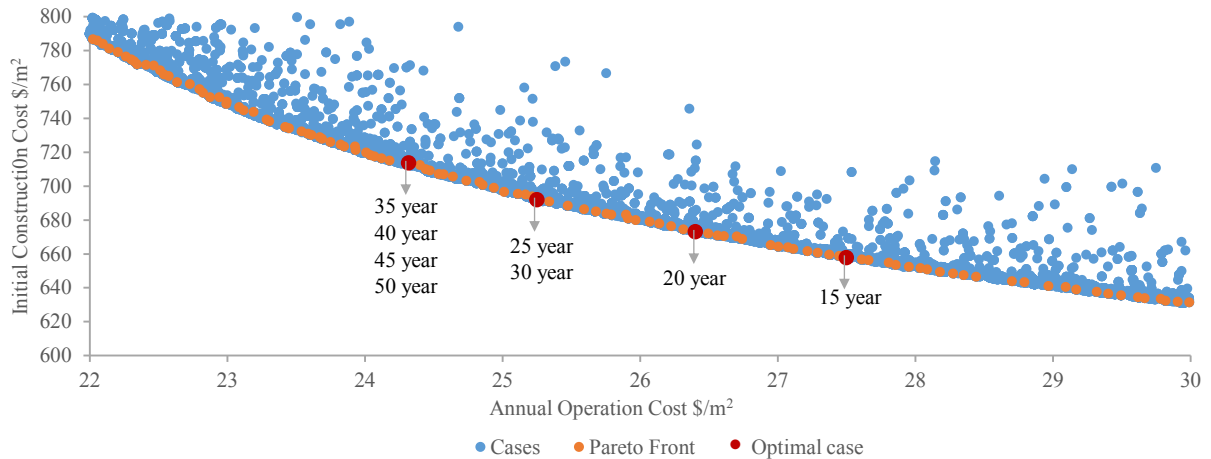
Figure 3-7 Zoomed-in Pareto front with optimal cases under different life cycle periods

Figure 3-8 shows all the cases on the Pareto front evaluated under different life-cycle periods, with the horizontal axis showing the initial construction cost and the vertical axis showing the benefits to the house owner, including the add-on to construction cost and the operation cost saving compared to the reference house under the same life-cycle years. The cases below the dashed line have lower life-cycle costs than the reference house.
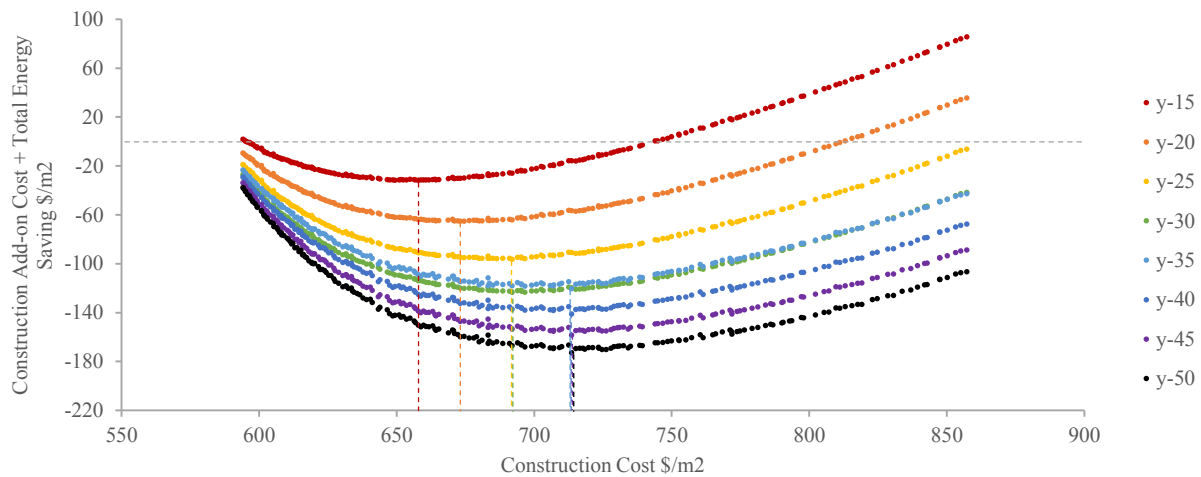
Figure 3-8 The Pareto front cases evaluated under different life-cycle periods

With a longer life cycle, the optimal house provides more benefits in cost savings. The lowest point of each curve represents the optimal case for each corresponding life-cycle period, which are

63

shown as the optimal cases in Figure 3-7. Under a shorter life cycle period, not every case on the Pareto front could bring benefits to the house owner. For example, over a 15-year life cycle, the cases on the Pareto front with an initial construction cost higher than 744 $/m^2 will not provide any savings for the house owner, and over a 20-year life cycle, the cases with an initial construction cost over 813 $/m^2 cannot save money for the house owner.

3.3.5 Influence of Construction Cost

With the same thermal performance house, the construction may differ from case to case for two reasons. First is the material unit price. To achieve the same thermal resistance, many types of materials could be chosen, especially the insulation type. As Table. B-1 in Appendix B shows, the cost of blown-in fiberglass insulation for the ceiling, 0.59 $/ft^2 for 5 in thick, is much lower than that for the rigid fiberglass insulation for walls, 1.04 $/ft^2 for 1 in thick. If rigid insulation is also chosen for the ceiling, it would cost more to maintain the same thermal resistance of the ceiling. The same situation may happen with other materials, as for some there are many alternative choices.

The second reason is the location factor. The cost data reference usually does not provide detailed cost for each location, as there are numerous places in the country. Instead it usually provides the average cost for the country or for some big cities, and it uses a location factor to convert the cost for a given place. Different references may provide different factors. The cost conversion rate between Yellowknife and Montreal is 1.08, as in the RSMeans (2017) reference to the US average, the location factor for Montreal is 1.05 and for Yellowknife is 1.13. In the Canadian Cost Guide (Altus Group, 2017), however, the conversion rate is 1.98 to 2.96, as this source lists a factor of 1.7 for Yellowknife indexed to the greater Toronto area, and a single-family residential house costs 105-200 $/ft^2 (1,130-2,153 $/m^2) in the greater Toronto area and 90-115 $/ft^2 (969-1,238 $/m^2) in Montreal.

Another optimization is done using 1.87 as Yellowknife's new location factor. This new location factor multiplies 1.10 – the factor converting the US average cost to Toronto local price provided in RSMeans (2017) – by 1.7, the factor converting the Toronto cost to Yellowknife local price

presented in the Canadian Cost Guide (2017). The optimization based on different location factors is meant to analyze how high construction cost influences the optimization results.

Table 3-8 shows the optimal results with different location factors. The case with the 1.87 location factors has a lower thermal resistance for each envelope part, less thermal mass and a smaller WWR compared to the case with a location factor of 1.13. In terms of annual energy demand, the case with a 1.87 location factor requires 19% more energy than the case with a location factor of 1.13, and the construction cost is 52% higher. With a higher location factor, the optimal house not only has a higher energy demand but also costs more for the construction.

Table 3-8 Optimal passive design parameters with different city indices for Yellowknife

Parameters	Unit	Reference Value	Optimal value (1.13)	Optimal value (1.87)
Thermal resistance for walls	$m^2 \cdot K/W$	4.26	9.17	7.09
Thermal resistance for ceiling	$m^2 \cdot K/W$	5.57	20.34	14.06
Thermal resistance for floor	$m^2 \cdot K/W$	6	11.36	8.85
Thermal mass on the floor	m	0.006 – wood tile	0.055 – concrete	0.050 – concrete
Thermal mass on the walls	layers	1 – Gypsum	1 – Gypsum	1 – Gypsum
WWR	%	20	47	36
Window/floor ratio	%	5.8	13.7	10.5
Window type	---	Triple glazed	Triple glazed	
Shading	---	None	Block 90% solar radiation if cooling is required	
Ventilation rate	ACH	0.3	0.3 or change to 2 if cooling is required	
Annual Energy demand	$kWh/m^2 \cdot a$	132.04	71.29	84.95
Annual Heating demand	$kWh/m^2 \cdot a$	129.50	67.68	82.84
Annual Cooling demand	$kWh/m^2 \cdot a$	2.54	3.61	2.11
Construction cost	$	81,438.79 (1.13) 134,770.39 (1.87)	89,941.51	136,840.30
	$/m^2$	626.45 (1.13) 1,036.70 (1.87)	691.86	1,052.62
HDD (2008-2018) (CWS, 2019)	-	7,964		

As shown in Figure 3-9, the Pareto front for cases with 1.87 as the location factor has a steeper slope, which means that to reduce the operation cost, a significant incremental construction cost is required. With a higher initial construction cost, the optimized house over a 25-year life cycle tends to have a higher operation cost, in terms of saving construction cost. Over a 25-year life cycle, for the optimal case with a 1.13 location factor, the operation cost is 71.29 $kWh/m^2 \cdot a$, while for the optimal case with a 1.87 location factor, the operation cost is 84.95 $kWh/m^2 \cdot a$, which is higher.
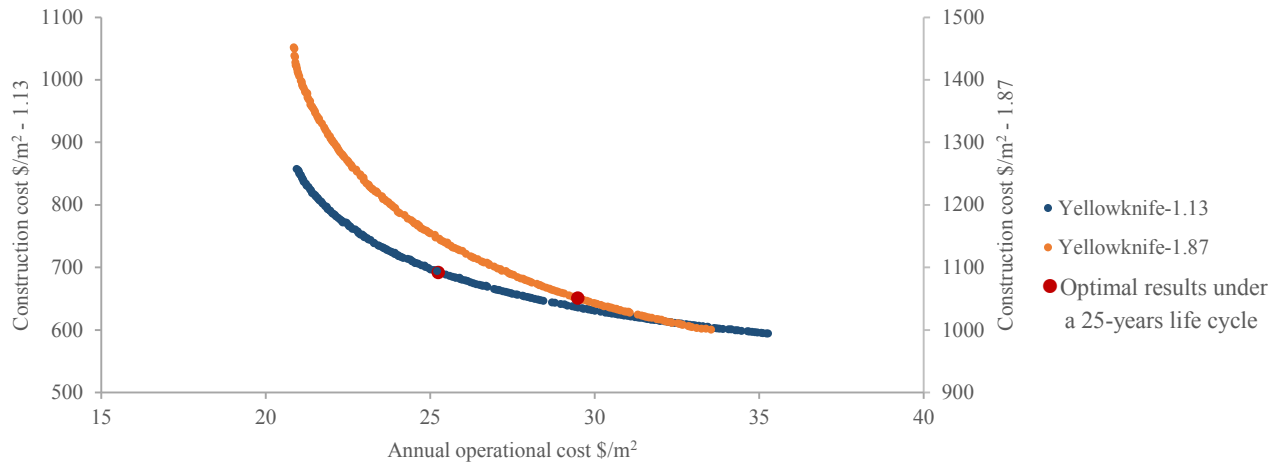
Figure 3-9 Pareto front for the optimization case with different location factors

3.4 Case Study 2: Kuujjuaq

The same reference house is studied for Kuujjuaq, a city located in Northern Quebec, Canada. Compared to Yellowknife, Kuujjuaq is a smaller city with a smaller population and limited transportation to connect with other big cities, which leads to much higher construction costs, as materials need to be transported and laborers are mostly hired from the south. The number of heating degree days in Kuujjuaq is similar to that in Yellowknife, yet with different weather data.

The comparison of weather data between Kuujjuaq and Yellowknife is shown in Figure 3-10. As can be seen from Figure 3-10 (a), which graphs the daily outside air temperatures, Kuujjuaq has a higher air temperature in winter, namely the periods from January to March and November to December. This indicates that the house in Kuujjuaq does not need to be super-insulated to prevent heat loss in winter, and the thermal resistance for the house in Kuujjuaq could be lower than that for the house in Yellowknife when it has similar heating energy performance. During the summer, however, Kuujjuaq is much cooler than Yellowknife. If the house is not well insulated, it may require some heating during the summer, and if the house is sufficiently insulated, with the ventilation and shading controls to avoid overheating, the overheating in the house could be easily removed by the cooler air temperatures in Kuujjuaq during the summer.
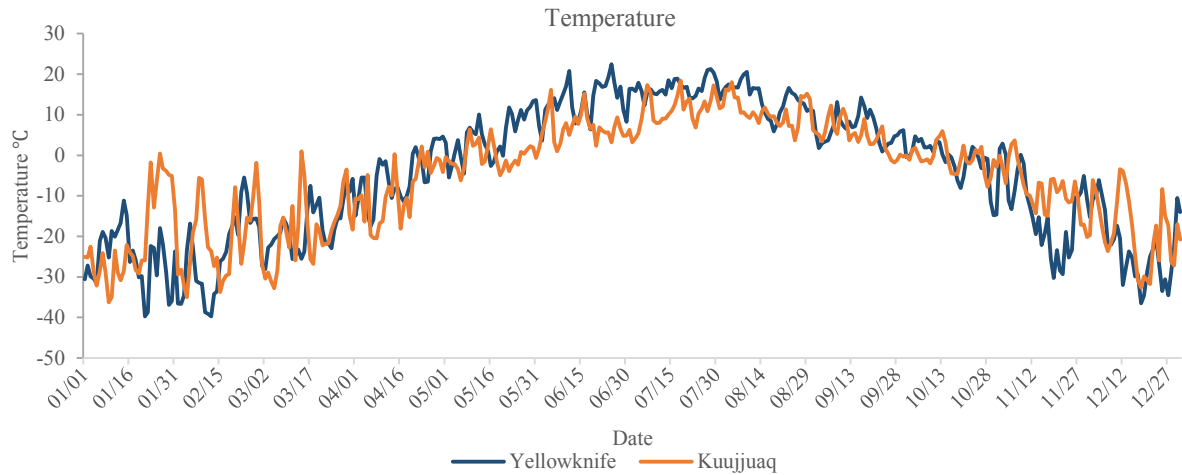
(a) Daily average outdoor air temperature for Yellowknife and Kuujjuaq
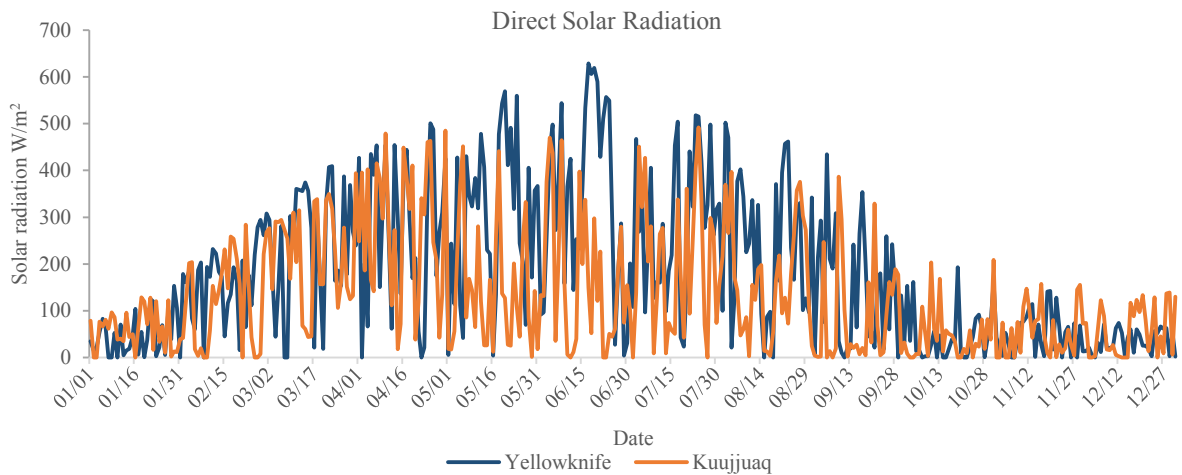
(b) Daily average direct solar radiation for Yellowknife and Kuujjuaq
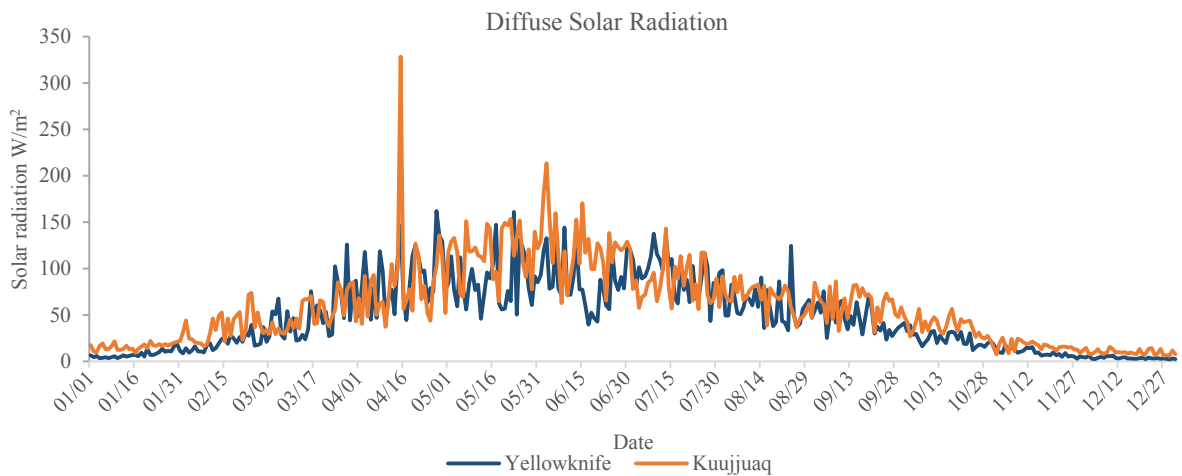
(c) Daily average diffuse solar radiation for Yellowknife and Kuujjuaq

Figure 3-10 Comparison of daily weather data for Yellowknife and Kuujjuaq

In terms of solar radiation, shown in Figure 3-10 (b) and (c), Kuujjuaq has slightly higher solar radiation than Yellowknife. The summary results for solar radiation during the heating periods show that Kuujjuaq does have higher solar radiation than Yellowknife, for the total diffuse and direct solar radiation in winter for Kuujuuaq are 229 kW/m^2 and 436 kW/m^2, respectively, and for Yellowknife are 109 kW/m^2 and 421 kW/m^2, respectively. Thus, increasing the WWR in the house at Kuujjuaq could bring more energy saving benefits from solar heat gain, with the consideration of balancing the extra cost to enlarge the window with energy savings.

The construction calculations for both cases are presented below.

Yellowknife: *Construction cost = 1.13 × US Average Cost*
1.13 is the location factor provided by RSMeans to convert the cost from the US average to Yellowknife.

Kuujjuaq: *Construction cost = 2.4 × 1.10 × US Average Cost + 2,100 $/m^2 × 130 m^2*
1.10 is the location factor provide by RSMeans to convert the cost from the US average to Toronto; 2.4 is the city index provided by Altus Group to convert the cost from Toronto to Kuujjuaq; 2,100 $/m^2 is the approximate estimated cost to hire labor from the south for the construction work; 130 m^2 is the floor area of the house.
*Altus Group only provides the city index for Iqaluit and not the city index for Kuujjuaq. Here it is assumed Kuujjuaq has the same city index as Iqaluit.

The estimated cost to hire labor from the south to work in the north is calculated based on the material construction cost from RSMeans and the actual construction cost in Kuujjuaq presented in Housing in Nunavik (SHQ, 2014), which is approximately 3,520 $/m^2, and the experience construction range in Kuujjuaq of 5,000-7,000 $/m^2. The detailed calculation and description are present in Appendix C. For the optimization in Kuujjuaq, 2,100 $/m^2 additional labor cost is chosen for the calculation.

Table 3-9 presents the optimal results in both Yellowknife and Kuujjuaq over a 25-year life cycle. The energy demand of the optimal house is 71.29 kWh/m^2·a for Yellowknife and 87.64 kWh/m^2·a for Kuujjuaq. The construction cost in Kuujjuaq is about 5.1 times higher than the construction cost in Yellowknife. There are two factors contributing to the much higher construction cost in Kuujjuaq. First, Kuujjuaq has a higher location factor plus the additional cost to hire skilled workers from the south. Second, the electricity price in Kuujjuaq, 6.08 ₵/kWh (Hydro Quebec, 2019), is cheaper than the electricity price in Yellowknife, 29.81 ₵/kWh (NWT Rate Schedule, 2019). Thus the optimal case in Kuujjuaq tends to have a slightly higher energy demand attributed

to a lower thermal resistance for the envelope meant to reduce the construction cost. The WWR and thermal mass are similar to those in Yellowknife.

Table 3-9 Optimal passive design parameters for Yellowknife and Kuujjuaq

Parameters	Unit	Reference Value	Optimal value (YK)	Optimal value (Kuujjuaq)
Thermal resistance for walls	m²·K/W	4.26	9.17	5.95
Thermal resistance for ceiling	m²·K/W	5.57	20.34	11.09
Thermal resistance for floor	m²·K/W	6	11.36	7.58
Thermal mass on the floor	m	0.006 – wood tile	0.055 – concrete	0.055 – concrete
Thermal mass on the walls	layers	1 – Gypsum	1 – Gypsum	1 – Gypsum
WWR	%	20	47	43
Window/floor ratio	%	5.8	13.7	12.5
Window type	---	Triple glazed	Triple glazed	
Shading	---	None	Block 90% solar radiation if cooling is required	
Ventilation rate	ACH	0.3	0.3 or change to 2 if cooling is required	
Annual Energy demand	kWh/m²·a	132.04 (Y) 130.64 (K)	71.29	87.64
Annual Heating demand	kWh/m²·a	129.50 (Y) 130.42 (K)	67.68	87.37
Annual Cooling demand	kWh/m²·a	2.54 (Y) 0.22 (K)	3.61	0.28
Construction cost	$	81,438.79 (Y) 463,264.07 (K)	89,941.51	460,168.00
	$/m²	626.45 (Y) 3,563.57 (K)	691.86	3,539.75
HDD (2008-2018) (CWS, 2019)	-		7,964	8,142

Figure 3-11 (a) shows the Pareto front of the optimization cases in Yellowknife and Kuujjuaq. As stated above, Kuujjuaq has higher construction costs and lower electricity prices than Yellowknife. The Pareto front for the Kuujjuaq case remains in the top-left corner within the high construction cost range and low electricity cost range, while the Pareto front for the Yellowknife case appears at the bottom-right within its changing range in low construction cost and high electricity cost.

For easier comparison, the horizontal axis is changed to energy demand in Figure 3-11 (b), The slope of the Pareto front for the Kuujjuaq case is steeper than for the Yellowknife case. To achieve the same amount of energy savings, the house in Kuujjuaq needs to pay more in initial construction costs to have better energy performance. Furthermore, Kuujjuaq has a low electricity price, but the savings from energy costs can hardly offset the increased amount in construction costs, leading to

the optimal house over a 25-year life cycle being the case with low construction cost and acceptable high energy cost.

(a)

(b)
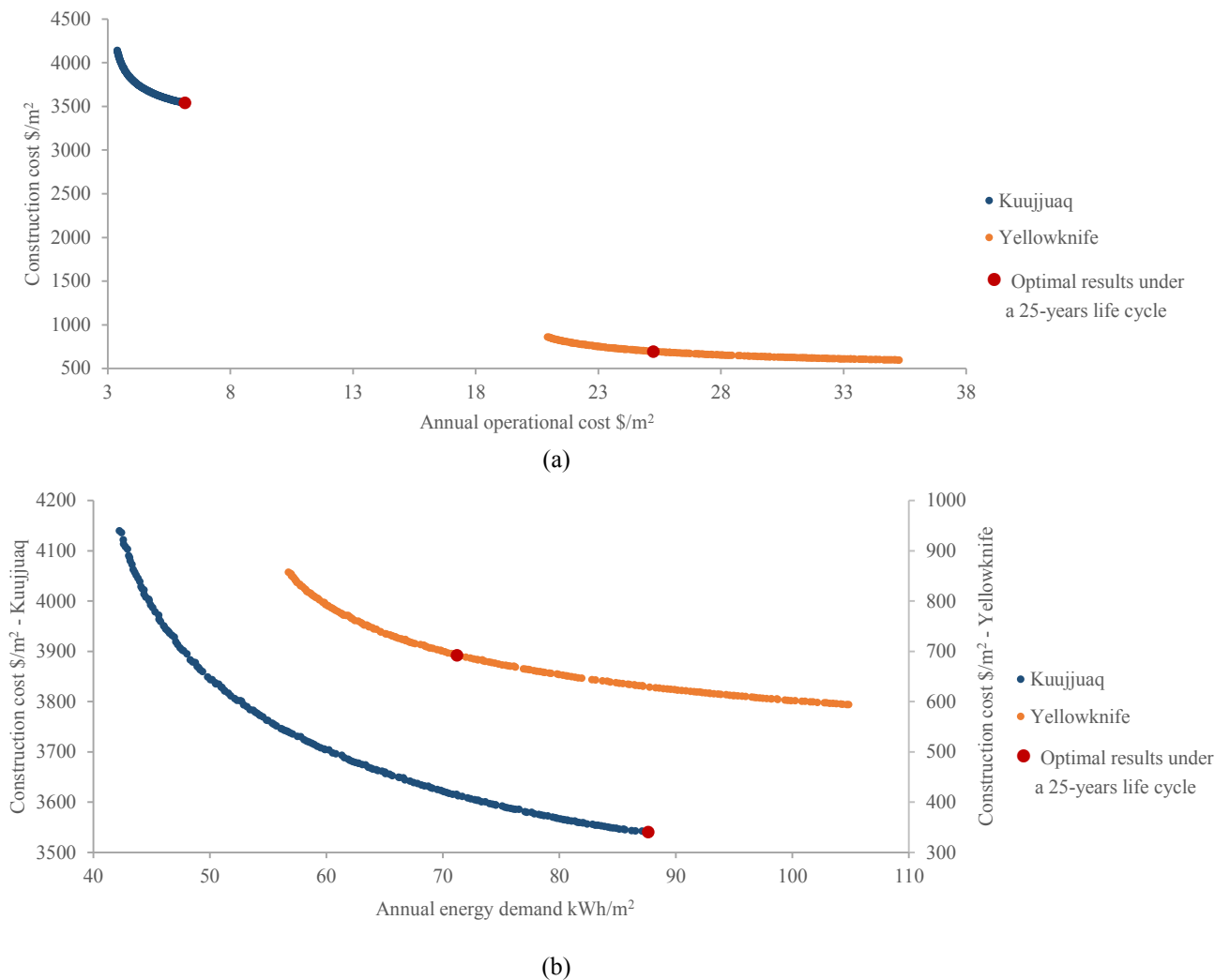
Figure 3-11 Pareto front for the optimization cases in Yellowknife and Kuujjuaq

3.4.1 Influence of the Energy Source

Among the 14 Nunavik Inuit communities, they were still compelled to rely on non-renewable fossil fuels as of 2010 for electricity and house heating (Kativik et Makivik, 2012). "Plan Nunavik" proposes an interconnection with Hydro Quebec's provincial electricity grid to reduce fuel usage with a construction period of 6 to 14 years (Kativik et Makivik, 2012; Karanasions et Parker, 2016). Using fuel as heating source is still common in Kuujjuaq. An optimization case in Kuujjuaq is

repeated with different energy sources, including a case using electricity only and a case using electricity for lighting and equipment and fuel for heating. The energy price in Kuujjuaq is 6.08 ₵/kWh for electricity (Hydro Quebec, 2019) and $2.03/L (equivalent 21.7 ₵/kWh) for fuel (Makivik Corporation. 2018), the efficiency of the fuel heating is 0.8.

Table 3-10 presents the optimal results in Kuujjuaq with different energy sources. The thermal resistance for the envelope remains similar in both cases, while the WWR is much larger in the case with two energy sources than the case using electricity only. This is because with relatively abundant solar radiation in Kuujjuaq, maximizing the utilization of solar energy could reduce the heating energy demand, and the larger WWR in the case with two energy sources reduces its heating demand. The larger WWR is also due to the high energy cost for fuel; the energy cost savings from a larger WWR could easily outweigh the increased construction cost. The energy demand for the case with two energy sources is 79.79 kWh/m^2·a, which is 9.0% lower than the energy demand for the case using electricity only.

Table 3-10 Optimal passive design parameters with different energy sources in Kuujjuaq

Parameters	Unit	Reference Value	Optimal value (ele)	Optimal value (ele+fuel)
Thermal resistance for walls	m^2·K/W	4.26	5.95	6.21
Thermal resistance for ceiling	m^2·K/W	5.57	11.09	11.05
Thermal resistance for floor	m^2·K/W	6	7.58	7.46
Thermal mass on the floor	m	0.006 – wood tile	0.055 – concrete	0.051 – concrete
Thermal mass on the walls	layers	1 – Gypsum	1 – Gypsum	1 – Gypsum
WWR	%	20	43	64
Window/floor ratio	%	5.8	12.5	18.4
Window type	---	Triple glazed	Triple glazed	
Shading	---	None	Block 90% solar radiation if cooling is required	
Ventilation rate	ACH	0.3	0.3 or change to 2 if cooling is required	
Annual Energy demand	kWh/m^2·a	130.64	87.64	79.79
Annual Heating demand	kWh/m^2·a	130.42	87.37	78.86
Annual Cooling demand	kWh/m^2·a	0.22	0.28	0.93
Construction cost	$	463,264.07	460,168.00	463,786.52
	$/m^2	3,563.57	3,539.75	3,567.59
HDD (2008-2018) (CWS, 2019)	-	8,142		

3.4.2 Influence of the Thermal Mass

The optimization case in Kuujjuaq with two energy sources gives a high WWR of 64%, which is a large value for windows in a northern city in Canada. The possible reason why the optimal house in Kuujjuaq has a WWR this large, in addition to Kuujjuaq's sufficient solar radiation, is that thermal mass performance well couples with the WWR, with the thermal mass storing excess solar radiation during the day and releasing heat back to the room at night. To study how the thermal mass impacts the optimal results, the same house, without concrete on the interior side of the floor and a fixed one-layer gypsum board on the interior side of the wall, is optimized in Kuujjuaq.

Table 3-11 Optimal passive design parameters with and without thermal mass in Kuujjuaq

Parameters	Unit	Reference Value	Optimal value (with)	Optimal value (without)
Thermal resistance for walls	$m^2 \cdot K/W$	4.26	5.95	5.75
Thermal resistance for ceiling	$m^2 \cdot K/W$	5.57	11.09	13.08
Thermal resistance for floor	$m^2 \cdot K/W$	6	7.58	7.25
Thermal mass on the floor	m	0.006 – wood tile	0.055 – concrete	N/A
Thermal mass on the walls	layers	1 – Gypsum	1 – Gypsum	1 – Gypsum *
WWR	%	20	43	26
Window/floor ratio	%	5.8	12.5	7.5
Window type	---	Triple glazed	Triple glazed	
Shading	---	None	Block 90% solar radiation if cooling is required	
Ventilation rate	ACH	0.3	0.3 or change to 2 if cooling is required	
Annual Energy demand	$kWh/m^2 \cdot a$	130.64	87.64	96.59
Annual Heating demand	$kWh/m^2 \cdot a$	130.42	87.37	96.42
Annual Cooling demand	$kWh/m^2 \cdot a$	0.22	0.28	0.16
Construction cost	$	463,264.07 (w/) 432,047.28 (w/o)	460,168.00	458,046.60
	$/m^2	3,563.57 (w/) 3,323.44 (w/o)	3,539.75	3,523.44
HDD (2008-2018) (CWS, 2019)	-	8,142		

* Fixed value – not changed during the optimization

Table 3-11 shows the optimal results in Kuujjuaq for both cases – with and without thermal mass. The case without thermal mass has an envelope thermal resistance similar to that of the case with thermal mass, with a slightly lower thermal resistance for the walls and floor and a higher thermal resistance for the ceiling. Without the thermal mass to preserve the solar radiation during the day and release heat at night, the case without thermal mass has a WWR 40% less than the case with

thermal mass. Without fully using solar heat during the winter, the case without thermal mass requires 10% more energy than the case with thermal mass.

Figure 3-12 shows the Pareto front of both cases, and the case without thermal mass has a steeper curve. This is because without the thermal mass to lower the energy demand by utilizing solar heat, another way to lower the house energy demand is to increase the thermal resistance of the envelope, and for the same amount of energy savings, the cost to increase the thermal resistance for the envelope is greater than the cost to increase the interior thermal mass. With the same construction cost, the optimal result from the case with thermal mass has a lower energy operational cost than the optimal result from the case without thermal mass. Furthermore, with a higher initial construction cost, the difference in energy operation cost between the optimal results from the two cases becomes larger. In other words, considering thermal mass in the optimization could save more energy without increasing the construction cost.
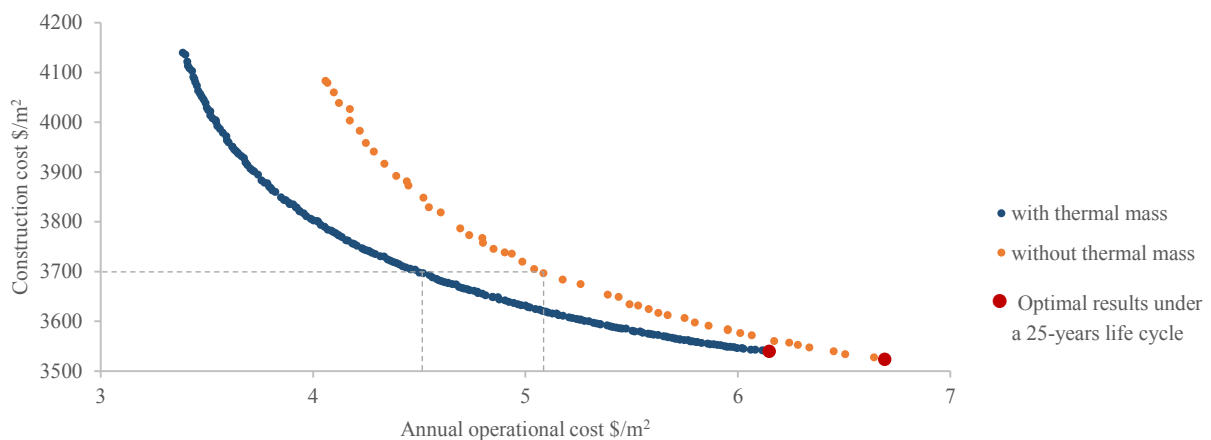
Figure 3-12 Pareto front for the optimization case with and without thermal mass in Kuujjuaq

3.4.3 Influence of the Additional Labor Cost

The additional labor cost indicates that the expense of supporting labor from the south to work in the north is estimated to be in the range of 1,200-2,900 $/m^2 in Kuujjuaq. The median value of 2,100 $/m^2 is chosen for the optimization calculation. For any given project, this additional labor cost may be higher or lower. Two cases – with and without the additional labor cost – are studied to demonstrate how the additional labor cost would impact the results.

Table 3-12 shows the optimal design parameters for both cases – with and without additional labor cost – over a 25-year life cycle. The thermal resistance for the envelope and thermal mass are similar in both cases. The WWR for the case with additional labor cost is 43%, while the WWR for the case without additional labor cost is 29%, which is lower. The case without additional labor cost has an energy demand 9.6% higher and a construction cost 2,122 $/m^2 lower than the case with additional labor cost. This difference in initial construction cost is close to the assumed additional labor cost, 2,100 $/m^2.

Table 3-12 Optimal passive design parameters for Kuujjuaq with and without add-on labor cost

Parameters	Unit	Reference Value	Optimal value (with)	Optimal value (without)
Thermal resistance for walls	m^2·K/W	4.26	5.95	6.02
Thermal resistance for ceiling	m^2·K/W	5.57	11.09	9.67
Thermal resistance for floor	m^2·K/W	6	7.58	7.75
Thermal mass on the floor	m	0.006 – wood tile	0.055 – concrete	0.055 – concrete
Thermal mass on the walls	layers	1 – Gypsum	1 – Gypsum	1 – Gypsum
WWR	%	20	43	29
Window/floor ratio		5.8	12.5	8.4
Window type	---	Triple glazed	Triple glazed	
Shading	---	None	Block 90% solar radiation if cooling is required	
Ventilation rate	ACH	0.3	0.3 or change to 2 if cooling is required	
Anuual Energy demand	kWh/m^2·a	131.44	87.64	96.01
Annual Heating demand	kWh/m^2·a	131.26	87.37	95.94
Anuual Cooling demand	kWh/m^2·a	0.18	0.28	0.06
Construction cost	$	463,264.07 (w/) 190,264.07 (w/o)	460,168.00	184,219.27
	$/m^2	3,563.57 (w/) 1,463.57 (w/o)	3,539.75	1,417.07
HDD (2008-2018) (CWS, 2019)	-	8,142		

Figure 3-13 shows the Pareto front for both cases, and curves overlap each other when the vertical axis scale for the case without additional labor cost is lowered by 2,100 $/m^2 relative to the vertical axis scale for the case with additional labor cost. With or without additional labor cost, the changing trends of the Pareto front are the same.
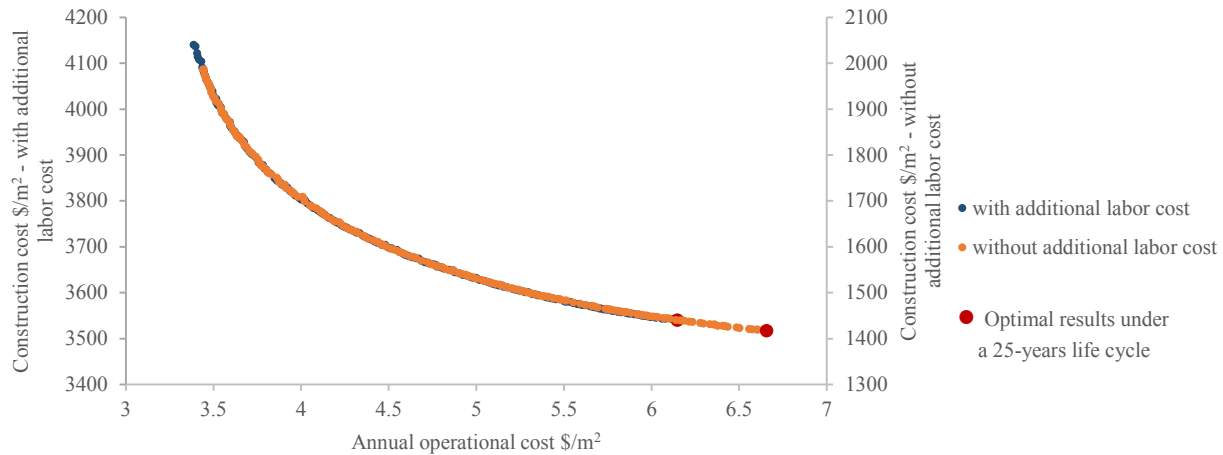
Figure 3-13 Pareto front for the optimization case with and without thermal mass in Kuujjuaq

3.5 Chapter Conclusion

Optimization of passive design parameters for the reference house has been carried out for two locations, Yellowknife and Kuujjuaq. The optimal house over a 25-year life cycle in Yellowknife could save about 46% in energy consumption compared with the reference house, with an incremental construction cost of about 10%. The optimal house in Kuujjuaq, where there are higher construction costs and lower electricity prices, could save about 33% in energy consumption with a similar initial construction cost. In the remote communities of the Canadian north, given the much higher construction cost due to the remoteness and lack of skilled labor, optimized passive design can provide significant energy savings with only a small increase to the initial construction cost.

The influence of location factors, different energy sources, thermal mass and additional labor cost are studied. The location factor influences the local construction cost, and the optimization with a higher location factor, namely with higher construction cost, shows the optimized house with a 25-year life cycle tends to have higher energy demand, 19% higher than for the optimization case with a lower location factor. Different energy sources have different energy prices, which affects the energy operational cost. In Kuujjuaq, electricity is cheaper than fuel, and the optimized house using fuel for heating and electricity for lighting and equipment over a 25-year life cycle tends to have lower energy demand and acceptably higher construction cost compared to the optimization

case using electricity only. Thermal mass in the northern house can make a contribution to energy savings. With the same construction cost, the optimal results for the case with thermal mass always have a lower energy cost than the optimal results for the case without thermal mass. The additional labor cost is the fixed cost in a given project, and the optimization without additional labor cost shows that the fixed cost in a house project does not affect the optimal results.

Chapter 4   Solar Strategy Applied to the Optimized House

4.1 Introduction of BIPV/T Combined System

The BIPV/T system not only generates valuable electricity for on-site usage but also provides heated air to reduce house energy consumption (Chen, 2012). In this chapter, the optimized houses from Chapter 3 are used as the reference house, and the integration of a BIPV/T system with different mechanical systems, including a space heating system, HRV system and HP outdoor unit, are studied with their energy performance presented.

4.1.1 Basic System in the Reference House

The reference house presented in this chapter is the optimized house over a 25-year life cycle for Yellowknife with a mechanical system added.
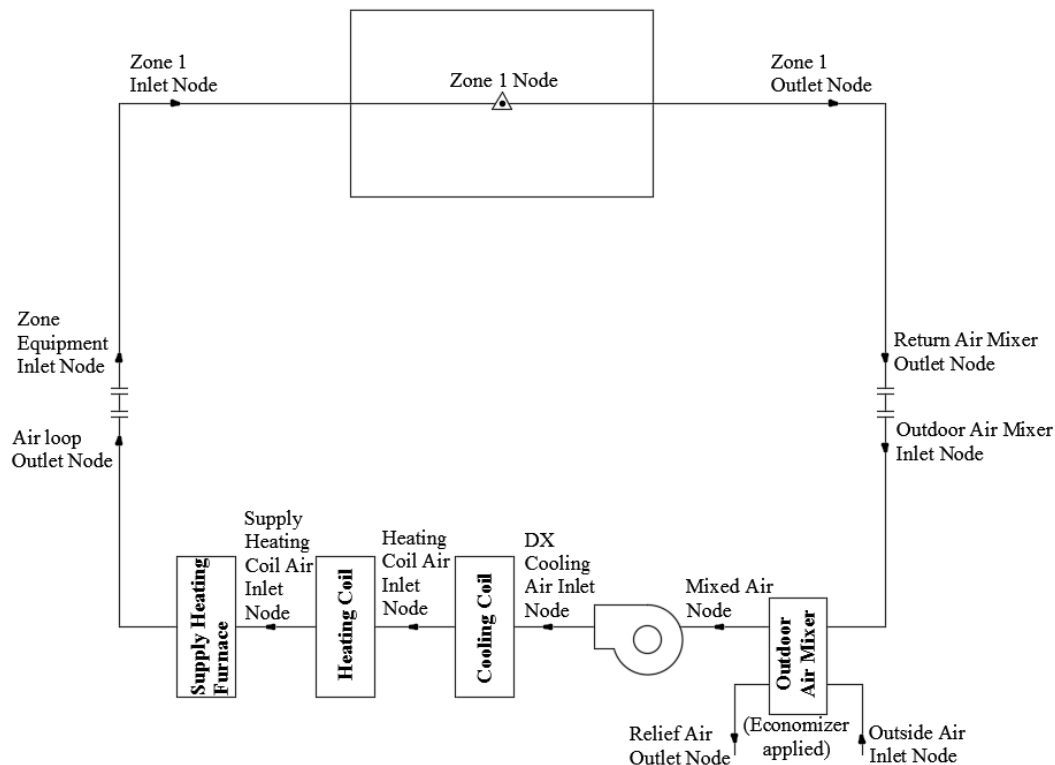

Figure 4-1 Configuration of the basic mechanical system

In the basic mechanical system, the HP is used for cooling and heating, and when HP cannot provide sufficient heat or the HP compressor stops working during very cold outdoor temperatures

(below -15 ˚C), a furnace will work as a supplemental heating source, as illustrated in Figure 4-1. The outdoor air mixer can adjust the amount of fresh air in the air loop.

Table 4-1 HP and furnace settings

	HP for heating	HP for cooling	Furnace
COP/Efficiency	2.75	3	0.8
Capacity	35 kW	32 kW	45 kW

Figure 4-2 shows that the outdoor air temperature at Yellowknife is usually below the cooling set-point, 26.5 ˚C, during the summer, while the indoor air temperature without mechanical cooling or ventilation is much higher, because of the heat preserved well by the highly insulated envelope and the contributions from solar heat gain through windows and internal heat gain from lighting, equipment and occupants. Under this condition, free cooling could be used during the summer to cool down the room temperature without consuming much energy. The setting for the outdoor air mixer could be changed from the minimum fresh air rate of 0.3 ACH (0.027 m^3/s) required by IAQ to increase the fresh air flow rate to 1.7 m^3/s to remove heat from the room during the cooling season when the outdoor air temperature is below 26.5 ˚C, in order to fully use the free cooling.
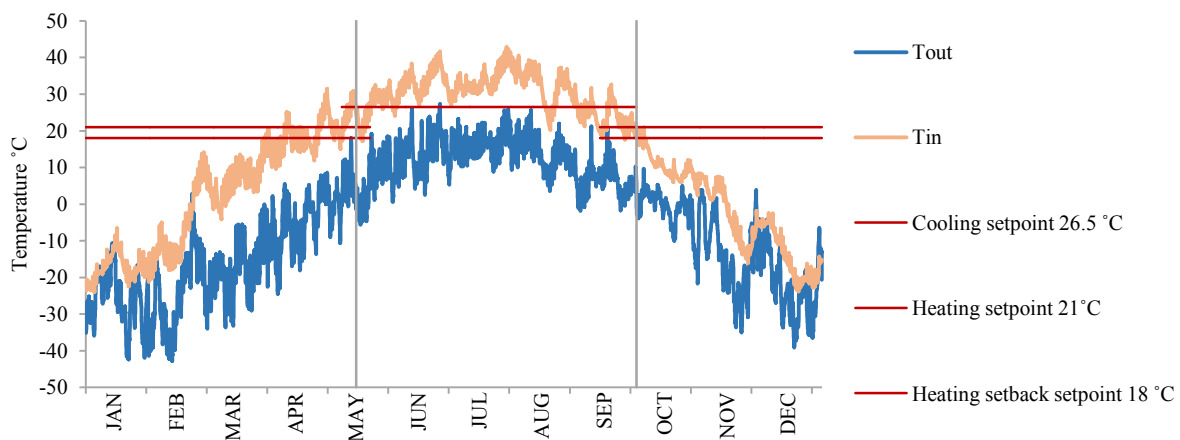
Figure 4-2 Indoor air temperature without HVAC system and outdoor air temperature

Table 4-2 shows that with the application of an economizer, the cooling energy consumption is reduced from 126.43 kWh without free cooling to 5.46 kWh with free cooling over the whole year.

Furthermore, during the wintertime, as seen in Figure 4-2, the outdoor is extremely cold, with temperatures reach -40 ˚C, which represents a large temperature difference from the heating

temperature setpoint of 21 ˚C. A minimum fresh air change rate of 0.3 ACH must be introduced into the room constantly during winter to meet the IAQ requirement specified by ASHRAE 62.2 (2016). This leads to a large energy cost to bring fresh air from a very low temperature up to the required room temperature. An HRV system applied to exchange heat between the exhaust air and the inlet fresh air would bring large energy savings.

Table 4-2 Annual energy consumption with and without economizer and HRV system

Case	Total	HP cooling	HP heating	Furnace heating	Fan
HVAC w/o Economizer	109.92 kWh/m²	126.43 kWh	2,358.29 kWh	8,003.49 kWh	2,048.79 kWh
HVAC w/ Economizer	109.16 kWh/m²	5.46 kWh	2,358.29 kWh	8,003.49 kWh	2,071.12 kWh
HVAC w/ HRV & Economizer	76.19 kWh/m²	5.50 kWh	1,419.31 kWh	4,787.03 kWh	1,940.84 kWh

Table 4-2 shows that with HRV, the total energy consumption is reduced by about 30.2% compared to the mechanical system without HRV but with an economizer. The main source of energy savings with HRV is from the reduction in heating consumption, as HP heating consumes 39.8% less energy and furnace heating about 40.2% less.
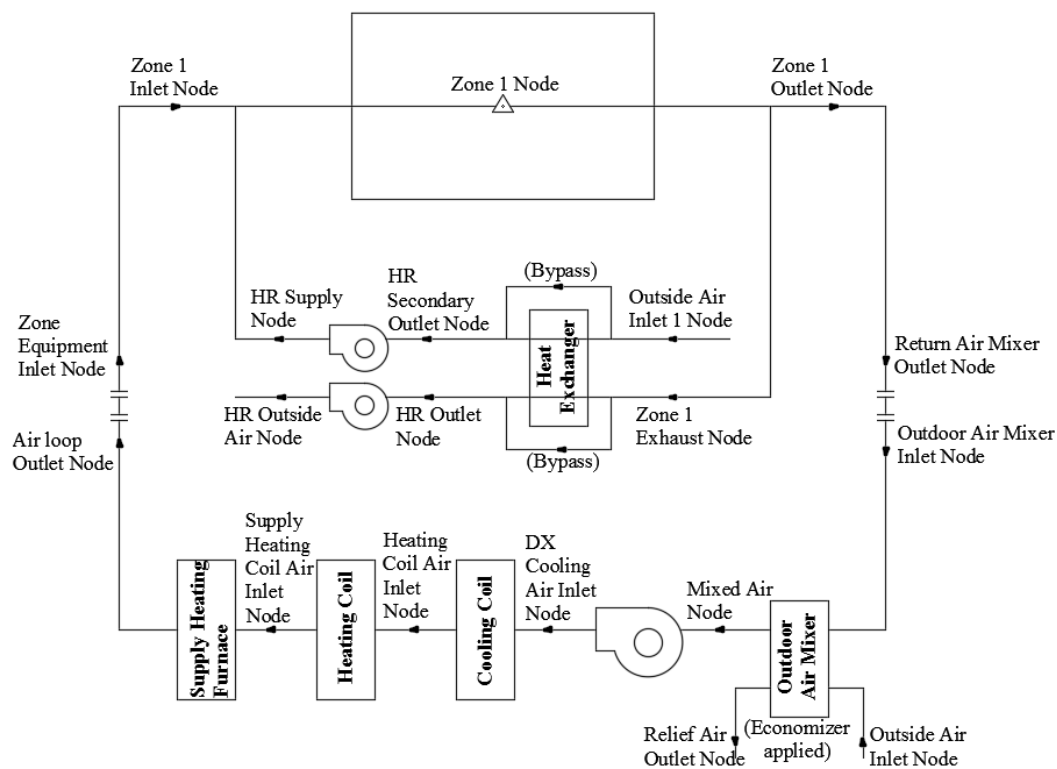
Figure 4-3 Configuration of the HVAC system with HRV and Economizer

Finally, the HVAC system used as reference applied to the reference house is shown in Figure 4-3. HP is used for cooling and heating, with the nominal COP set as 3 for cooling and 2.75 for heating, and when the HP cannot provide sufficient heat or the HP compressor stops working during very cold outdoor temperatures (below -15 ˚C), the furnace works as a supplemental heating source. Additionally, an economizer is used with the outdoor air mixer to fully use the free cooling by increasing the flow rate of outdoor air when the temperature is below 26.5 ˚C during the cooling season; otherwise, no fresh air is introduced through the outdoor air mixer. The fresh air required for the house to maintain proper IAQ is passed through the HRV system: a constant fresh air flow rate at 0.3 ACH exchanges heat with the exhaust air before entering the house.

4.1.2 Configuration of BIPV/T Combined System

Based on the reference house with the HVAC system presented in the previous section, configurations of different combinations integrating the BIPV/T system with the HVAC system are described below.
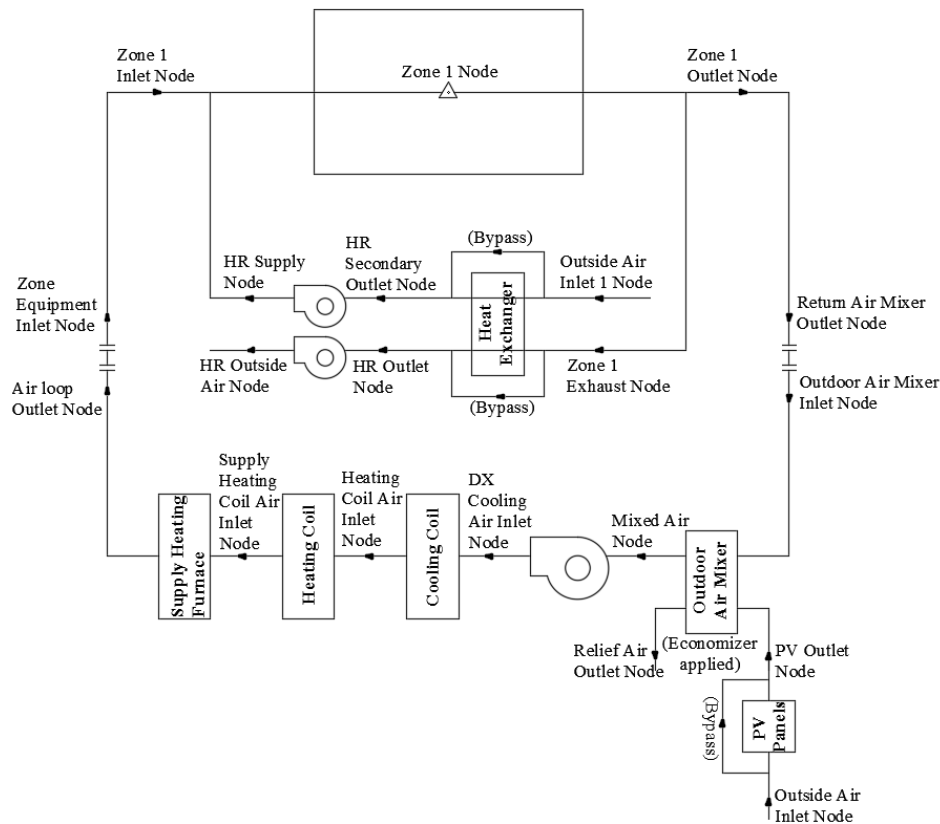
Figure 4-4 Configuration of BIPV/T system combined with space heating

1) BIPV/T system combined with space heating (Case: BIPV/T + SpaceHeating)

The heated air from the BIPV/T system is introduced into the conditioned space when it can make a contribution to decreasing the heating load. Under this configuration (Figure 4-4), a simple BIPV/T model is set up and connected to the HVAC air loop through the outdoor air mixer. The controller for the outdoor air mixer adjusts the airflow rate from the PV section based on the temperature at the mixed air node, as the air from the PV section mixed with the return air could increase the mixed air temperature above the heating set-point (21 ˚C, with 18 ˚C as a setback during the night) but not exceed the cooling set-point (26.5 ˚C).
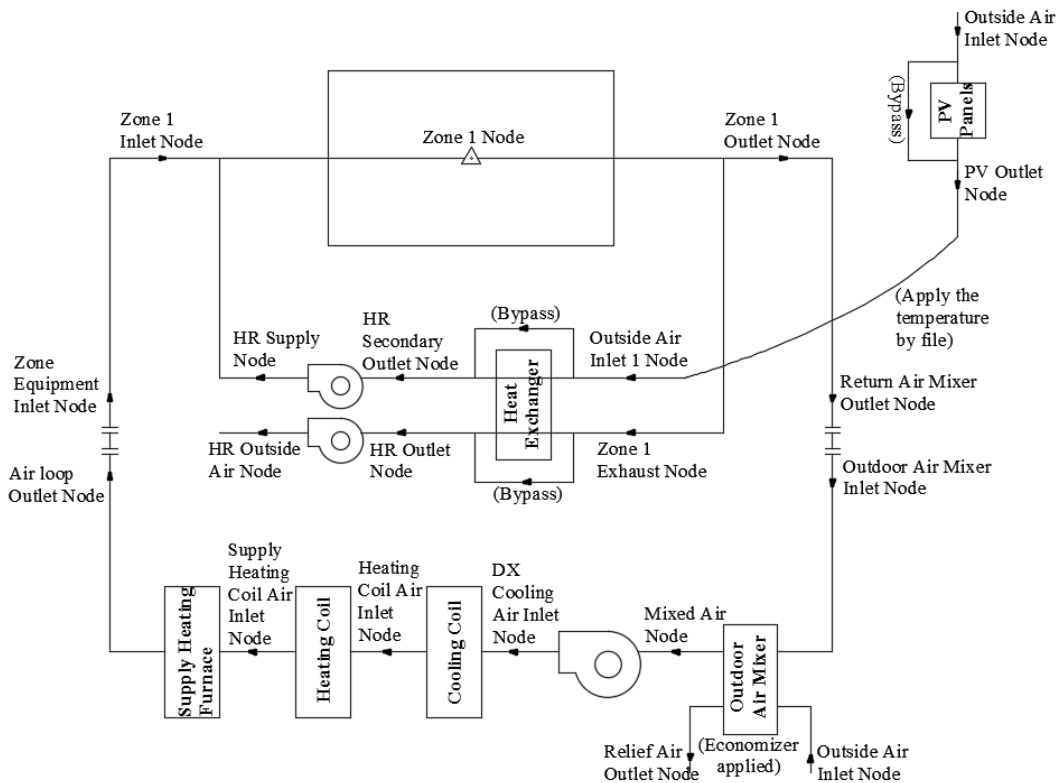
Figure 4-5 Configuration of BIPV/T system combined with HRV

2) BIPV/T system combined with HRV (Case: BIPV/T + HRV)

The thermal energy from the BIPV/T system could be used to preheat the HRV incoming air to reduce its frost risk time, which typically occurs when the HRV inlet air temperature is below -5 ˚C. In this case, the BIPV/T system is modeled by programmed Matlab code using an explicit finite difference method, and the hourly outlet air temperature is applied to the HRV inlet air node during the heating season to model the situation of connecting the BIPV/T system with the HRV

system to preheat the inlet air during winter, as Figure 4-5 illustrates. The control strategy at the HRV inlet during the heating season is to use the air temperature from the BIPV/T system when it is higher than the environment air temperature and otherwise to use the environment air temperature as the inlet air temperature.
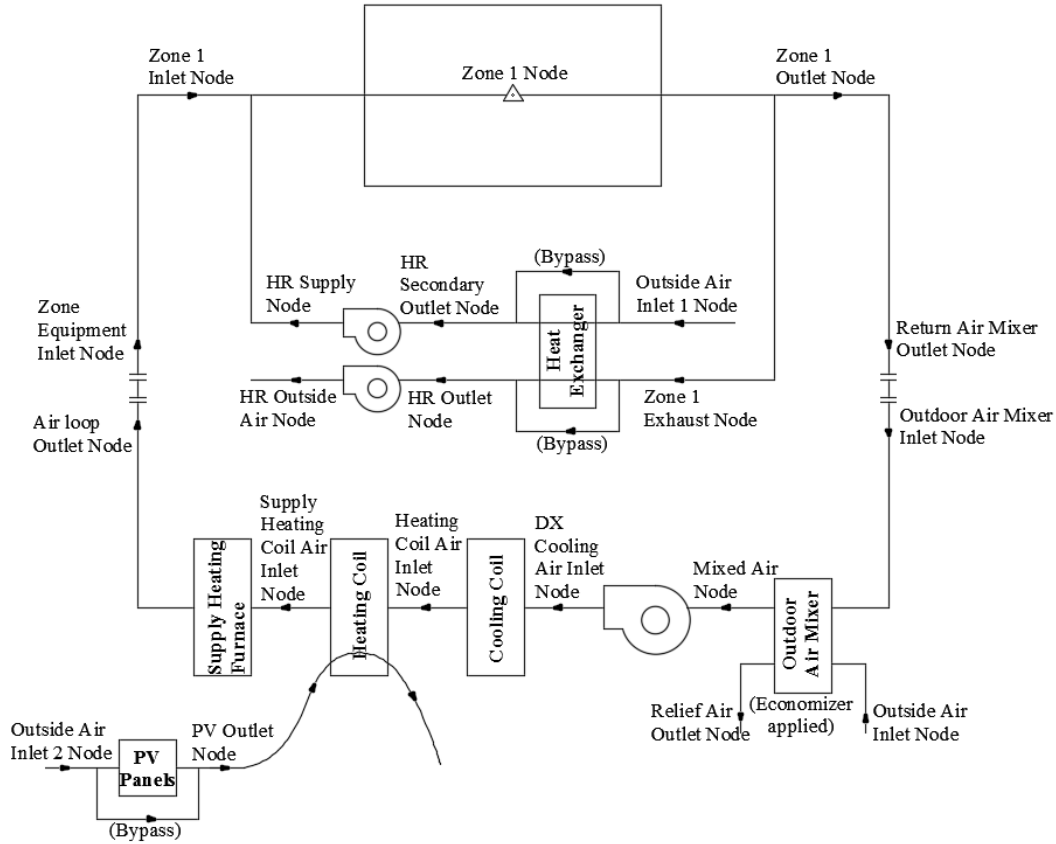
Figure 4-6 Configuration of BIPV/T system combined with HP outdoor unit

3) BIPV/T system combined with HP outdoor unit (Case: BIPV/T + HP)

The thermal energy from the BIPV/T system could also be used to extend the working hours and efficiency of the ASHP under cold conditions by introducing preheated air from the BIPV/T system to the outdoor unit of the HP. In this case, the BIPV/T is also modeled in Matlab code, and the hourly outlet air temperature from the BIPV/T system is applied to the HP evaporator (outdoor unit) inlet air node during the heating season to model the situation of connecting the BIPV/T system with the HP outdoor unit to raise that unit's ambient air temperature during the winter, as Figure 4-6 shows. The control strategy at the HP outdoor unit during the heating season is to use

the air temperature from the BIPV/T system when it is higher than the environment air temperature and otherwise to use the environment air temperature as the inlet air temperature.

4.2 BIPV/T Simulation

EnergyPlus version 8.9.0 is limited in modeling BIPV/T coupling with different system components, providing only a simple BIPV/T model that must connect to the HVAC air loop (EnergyPlus Engineering Reference, 2016). The BIPV/T system is modeled in two ways. For the BIPV/T system with space heating system study case, the BIPV/T is modeled in EnergyPlus with the electricity efficiency and thermal efficiency keep the same as the outputs from the Matlab code. For the HRV and HP study cases, the output air temperature from the BIPV/T system is simulated by Matlab code using a one-dimensional thermal network and a finite difference method, and this temperature profile is applied to the system inlet node.

4.2.1 Simplified BIPV/T Model (EnergyPlus)

Currently, version 8.9.0 of EnergyPlus only has one simple model based on user-defined efficiencies, which calculates the outlet temperature as follows (EnergyPlus Engineering Reference, 2016):

$$Q_{therm} = A_{surf} \cdot f_{activ} \cdot G_T \cdot \eta_{thermal} \tag{4-1}$$

where

Q_{therm} is the thermal energy collected, W;

A_{surf} is the net area of the surface on which the PV/T would be installed, m^2;

f_{activ} is the fraction of surface area with active PV/T collectors;

G_T is the solar radiation on the surface, W/m^2; and

$\eta_{thermal}$ is the thermal conversion efficiency, which is user-defined efficiency.

$$T_{out} = T_{in} + \frac{Q_{therm}}{\dot{m} \cdot c_p} \tag{4-2}$$

where

T_{out} is the temperature of the air leaving the BIPV/T, ˚C;

T_{in} is the temperature of the air entering the BIPV/T, ˚C;

$\dot{m}$ is the entire mass flow of the air through the BIPV/T, kg/s; and

c_p is the specific heat of the air, J/kg·K.

If the BIPV/T model chooses air as the fluid passing under the PV panels, the BIPV/T system is involved in the HVAC air system loop, using the outdoor air as its inlet air. The temperature set-point can be applied to the outlet node of the BIPV/T system to control the bypass damper to ensure that the outlet temperature does not exceed the required temperature.

$$f_{bypass} = \frac{(T_{set,out} - T_{out})}{(T_{in} - T_{out})} \tag{4-3}$$

where

f_{bypass} is the air bypass fraction and

$T_{set,out}$ is the temperature set-point at the BIPV/T outlet, ˚C.

4.2.2 Thermal Network BIPV/T Model (Matlab Code)

A one-dimensional thermal network model, shown in Figure 4-7, could be used as a common representation of BIPV/T to calculate the temperature at each time step using the finite-difference method (Yang, 2015).

The energy balance of the air (Charron et al., 2006) is

$$\mathrm{M} \cdot \mathrm{c}_p \cdot dT_a = \left[h_{c,p}(T_{pv} - T_a) + h_{c,b}(T_{bot} - T_a) \right] \cdot w \cdot dx \tag{4-4}$$
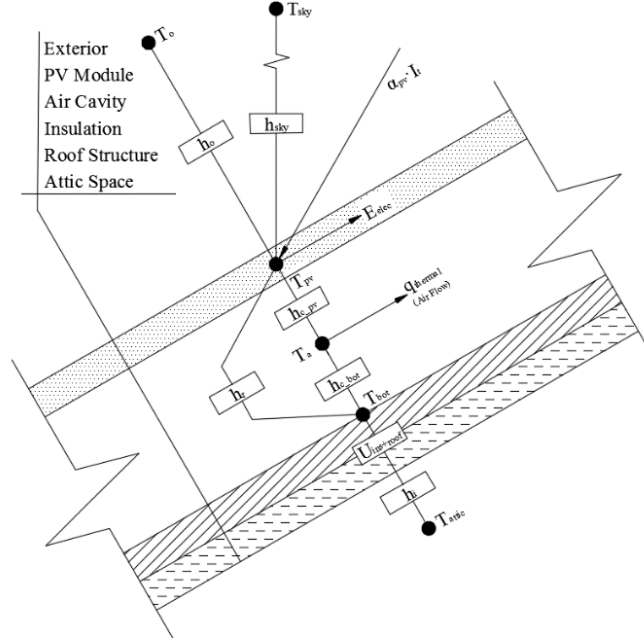
Figure 4-7 BIPV/T thermal network model

The air temperature in the cavity beneath the PV panels is

$$T_a(x) = \frac{h_{c,p} \cdot T_{pv} + h_{c,b} \cdot T_{bot}}{h_{c,p} + h_{c,b}} + \left(T_o - \frac{h_{c,p} \cdot T_{pv} + h_{c,b} \cdot T_{bot}}{h_{c,p} + h_{c,b}}\right) \cdot e^{-\frac{h_{c,p} + h_{c,b}}{a}x} \qquad (4\text{-}5)$$

$$a = \frac{M \cdot c_p \cdot \rho}{w} \qquad (4\text{-}6)$$

where

T_a is the temperature of the air in the BIPV/T cavity, ˚C;

T_{pv} is the temperature of the PV panels, ˚C;

T_{bot} is the temperature of the bottom surface of the BIPV/T cavity, ˚C;

T_o is the outdoor air temperature, ˚C;

x is the distance from the air inlet vent, m;

M is the volume flow rate of the air, m³/s;

$h_{c,p}$ is the convective coefficient between PV panels and the cavity air, W/m²·K;

$h_{c,b}$ is the convective coefficient between the cavity air and the cavity bottom surface, W/m²·K;

c_p is the specific heat of the air, J/kg·K;

ρ is the density of the air, kg/m³; and

w is the width of the BIPV/T cavity, m.

To calculate the air temperature in cavity T_a, the initial temperature of the PV panel T_{pv} and the bottom cavity surface T_{bot} are assumed, and these initial values will be replaced by the new temperatures calculated using the following energy equations. The mean air temperature in the cavity $T_{a(mean)}$ required in the equations is the average value calculated from the cavity air temperature equation (4-5). Then the iteration will repeat until the temperatures of both surfaces, T_{pv} and T_{bot}, match the corresponding temperatures from the previous iteration.

$$T_{pv} = \frac{T_o \cdot h_o \cdot A_{pv} + T_{a(mean)} \cdot h_{c,p} \cdot A_{pv} + T_{bot} \cdot h_r \cdot A_{pv} + I_t \cdot \alpha_{pv} \cdot A_{pv}(1 - \eta_{elec})}{h_o \cdot A_{pv} + h_{c,p} \cdot A_{pv} + h_r \cdot A_{pv}} \qquad (4\text{-}7)$$

$$T_{bot} = \frac{T_{a(mean)} \cdot h_{c,b} \cdot A_{pv} + T_{pv} \cdot h_r \cdot A_{pv} + T_{attic} \cdot \dfrac{1}{R_{ins+roof}} \cdot A_{pv}}{h_{c,b} \cdot A_{pv} + h_r \cdot A_{pv} + \dfrac{1}{R_{ins+roof}} \cdot A_{pv}} \qquad (4\text{-}8)$$

$$\eta_{elec} = 0.15 \left(1 - 0.004 * \left(T_{pv} - 25\right)\right) \qquad (4\text{-}9)$$

where

h_o is the exterior air film coefficient, W/m²·K;

A_{pv} is the area of the PV panels, also referred to as the project area of the bottom/back surface, m²;

$T_{a(mean)}$ is the average temperature of T_a at each section, ˚C;

h_r is the interior air film coefficient of the south roof, where the PV panel is installed, W/m²·K;

I_t is the solar radiation falling on the south roof, W/m²;

α_{pv} is the absorptivity of the PV panels;

η_{elec} is the PV panel electrical efficiency;

T_{attic} is the air temperature in the attic, ˚C; and

$R_{ins+roof}$ is the thermal resistance, including the extra RSI 1 insulation on the bottom surface and the thermal resistance of the roof, m²·K/ W.

The convection coefficient in the BIPV/T cavity is calculated using the Nusselt number. There are two ways to calculate the Nusselt number. One method by Candanedo et al. (2011) uses the average Nusselt number, which is a constant along the channel on both surfaces. The other method uses local Nusselt number correlations (Yang, 2015), which changes along the channel.

$$h_c = \frac{k \cdot Nu}{D_h} \tag{4-10}$$

Average Nusselt number on both surfaces:

$$Nu_{pv} = 0.052 \cdot Re^{0.78} \cdot Pr^{0.4} \quad 250 \leq Re \leq 7,500 \tag{4-11}$$

$$Nu_{bot} = 1.017 \cdot Re^{0.471} \cdot Pr^{0.4} \quad 800 \leq Re \leq 7,100 \tag{4-12}$$

Local Nusselt number on both surfaces:

$$Nu_{pv} = 8.188 \cdot Re^{0.77} \cdot Pr^{3.85} \cdot e^{-\frac{x^{0.2}}{2.8 \cdot D_h}} + 0.061 \cdot Re^{0.77} \cdot Pr^{3.85} \tag{4-13}$$
$$2,300 < Re < 9,500$$

$$Nu_{bot} = 4.02 \cdot Re^{1.09} \cdot Pr^{19.3} \cdot e^{-\frac{x^{0.2}}{14 \cdot D_h}} + 0.005 \cdot Re^{1.09} \cdot Pr^{19.3} \tag{4-14}$$
$$2,300 < Re < 9,500$$

where

k is the thermal conductivity, W/m·K;

h_c is the convective coefficient in the PV cavity, W/m²·K;

Nu is the Nusselt number;

D_h is the hydraulic diameter, m;

Re is the Reynolds number, $\rho V D_h / \mu$; and

Pr is the Prandtl number, ν/α.

The radiation coefficient between the PV panels and the cavity bottom surface (Chen, 2012) is

$$h_r = \frac{4\sigma \cdot T_m^3}{\frac{1}{\varepsilon_{pv}} + \frac{1}{\varepsilon_{bot}} - 1} \tag{4-15}$$

$$T_m = 0.5(T_{pv} + T_{bot}) \tag{4-16}$$

or

$$h_r = \frac{\sigma \cdot \left(T_{pv}^4 - T_{bot}^4\right)}{\left(\frac{1}{\varepsilon_{pv}} + \frac{1}{\varepsilon_{bot}} - 1\right) \cdot \left(T_{pv} - T_{bot}\right)} \tag{4-17}$$

where

h_r is the radiation coefficient between the PV panels and the cavity bottom surface, W/m^2·K;

σ is the Stefan-Boltzmann constant, W/m^2·K^4;

T_m is the mean of the PV temperature and the bottom surface temperature, ˚C;

ε_{pv} is the emissivity of the inside face of the PV panels; and

ε_{bot} is the emissivity of the inside face of the bottom surface.

The exterior air film convection coefficient is a function of the wind speed; the correlations are from the EnergyPlus engineering reference (EnergyPlus Engineering Reference, 2016) and another studied reference (Candanedo et al., 2011):

$$h_o = D + EV_{wind} + FV_{wind}^2 \tag{4-18}$$
$$h_o = 8.55 + 2.56V_{wind} \tag{4-19}$$
$$h_o = 11.9 + 2.2V_{wind} \tag{4-20}$$
$$h_o = 5.7 + 3.8V_{wind} \tag{4-21}$$

where

V_{wind} is the wind speed on the surface and

D, E and F are the material roughness coefficients under the simple combined method.

Table 4-3 Roughness Coefficients D, E and F (EnergyPlus Engineering Reference, 2016)

Roughness Index	D	E	F	Example material
1 (Very Rough)	11.58	5.894	0.0	Stucco
2 (Rough)	12.49	4.065	0.028	Brick
3 (Medium Rough)	10.79	4.192	0.0	Concrete
4 (Medium Smooth)	8.23	4.0	-0.057	Clear pine
5 (Smooth)	10.22	3.1	0.0	Smooth Plaster
6 (Very Smooth)	8.23	3.33	-0.036	Glass

The efficiency of the BIPV/T system is calculated as follows.

Thermal efficiency:
$$\eta_{thermal} = \frac{Q_{therm}}{I_t \cdot \alpha_{pv} \cdot A_{pv}}$$
(4-22)

Electricity efficiency:
$$\eta_{elec} = \frac{E_{elec}}{I_t \cdot \alpha_{pv} \cdot A_{pv}}$$
(4-23)

Total efficiency:
$$\eta_{total} = \frac{Q_{therm} + E_{elec}}{I_t \cdot \alpha_{pv} \cdot A_{pv}}$$
(4-24)

Other necessary parameters are input or calculated as follows:

1) The BIPV/T system dimensions are designed to meet the requirement of cavity air velocity between 0.5 m/s and 2 m/s and with a constraint of the roof dimensions on which the BIPV/T system is placed.

2) The outdoor temperature, wind speed and solar radiation on the surface are from the EnergyPlus weather data file.

3) The thermal resistance of the roof, the attic temperature and the interior and exterior air film coefficients are given by EnergyPlus output variables.

4) The properties of the air are the air properties at 20 ˚C.

5) An extra insulation layer with its thermal resistance of RSI 2 is added between the bottom of the BIPV/T cavity and the roof.

6) The depth of the cavity beneath the PV panel can be adjusted between 5 cm and 10 cm, and the air velocity within the cavity is controlled at between 0.5 m/s and 2 m/s.

4.2.3 BIPV/T Efficiency

The BIPV/T system simulated in Matlab code that the output temperature would be used in the studied BIPV/T cases using the average Nusselt number correlations and the exterior air film coefficient correlations from EnergyPlus. Further discussion of the effects of other correlations or settings on the results are presented in Appendix D. In general, different correlations and settings do result in different BIPV/T outlet air temperatures. However, the differences in the outlet air temperatures between compared cases are mostly less than 1-2 ˚C, which are acceptable and can be considered as negligible temperature differences for a BIPV/T system in a whole residential building simulation.

Table 4-4 shows the BIPV/T key efficiencies under different simulation cases. In the BIPV/T + SpaceHeating case, the BIPV/T input parameters in EnergyPlus are the Matlab calculated values.

Table 4-4 BIPV/T parameters

Case		Area	Electricity efficiency	Thermal efficiency	Airflow rate/velocity
BIPV/T + SpaceHeating	E+	99% of south roof area (72 m^2) 15 arrays	0.153	0.101	Adjusted, Max: 0.4 m^3/s
	Matlab	99% of south roof area (72 m^2) 15 arrays	0.153	0.101	0.4 m^3/s 0.53 m/s
BIPV/T + HRV	Matlab	7% of south roof area (4.8 m^2) 1 array	0.153	0.102	0.027 m^3/s 0.54 m/s
BIPV/T+HP	Matlab	99% of south roof area (72 m^2) 15 arrays	0.155	0.180	1.7 m^3/s 1.13 m/s

4.3 Case Study: Yellowknife

Table 4-5 presents energy consumption results under each BIPV/T integration case for Yellowknife. By integrating the BIPV/T system with the space heating system, the total energy consumption of the house can be reduced by 15.5%, while the heating energy consumption can be reduced by 47% for the HP and 23% for the furnace.

By integrating the BIPV/T system with the HRV system – that is, preheating the inlet air for the HRV system – the frost risk time, when the HR inlet air temperature is below -5 ˚C, is reduced by

about 7.8%. The defrost time[4], which is the time spent in the actual defrost process when the HR is frosted, is reduced by about 8.8% (Table 4-6). The energy saving for this configuration, however, is only 1.4% (Table 4-5).

Table 4-5 Energy consumption of BIPV/T cases in Yellowknife

Case	Total kWh/m^2	Heating-HP kWh	Furnace kWh	Improvement
HVAC	76.19	1,419.31	4,787.03	---
BIPV/T + SpaceHeating	64.37	747.62	3,673.57	15.5%
BIPV/T + HRV	75.11	1,386.65	4,696.52	1.4%
BIPV/T+HP	76.32	1,542.08	4,725.01	-0.2%
* Total consumption includes the consumption of heat pump, furnace, fans, heat recovery ventilator, lighting and appliances.				

As can be seen from Table 4-6, by integrating the BIPV/T system with the HP outdoor unit, the HP working period – the time during which the air temperature at the outdoor unit is above -15 ˚C – is extended by about 128 hours, of which 101 hours are in March or April. The actual working time of the HP in heating mode is increased by about 72 hours.

Table 4-6 HRV frost hours and HP working hours of BIPV/T integration case in Yellowknife

Case	Defrost time (hr)	Frost risk time (hr)	Hours of temperature over -15 ˚C at HP outdoor unit	HP heating hours	Average COP
HVAC	696.64	3,938	6,013	1,650	2.00
BIPV/T + HRV	635.02	3,630	---	---	---
BIPV/T+HP	---	---	6,141	1,722	2.05

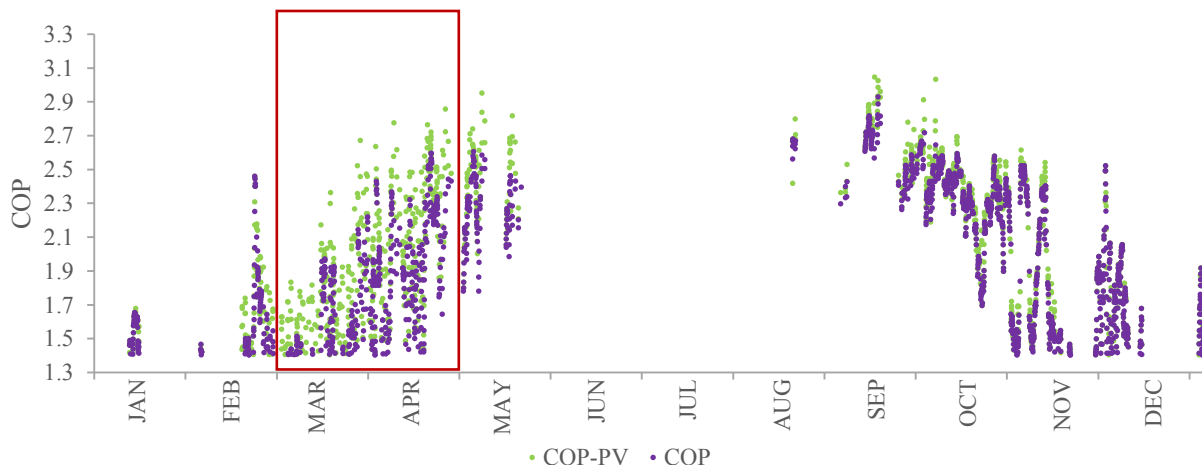Figure 4-8 HP hourly COP for a whole year for the BIPV/T and HP integration cases in Yellowknife

---

[4] The defrost time is the time that the HR is undergoing defrost processes as calculated in the EnergyPlus simulation. This is calculated based on the formula of given initial fraction, temperature fraction and temperature difference of inlet air temperature, and the input threshold temperature of frost.
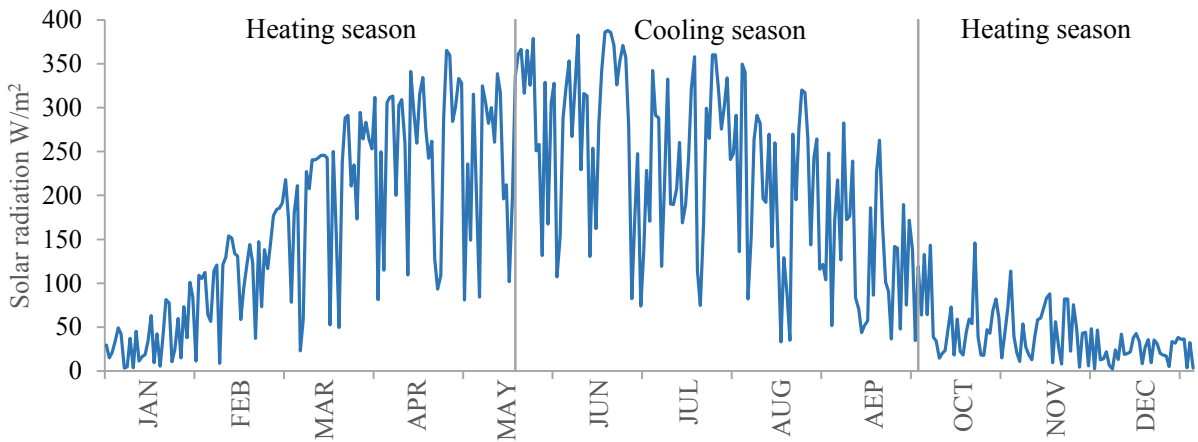
Figure 4-9 Daily solar radiation on the south-facing roof @26.6˚ in Yellowknife

As shown in Figure 4-8, by integrating the BIPV/T system with the HP outdoor unit, the COP of the HP is increased, especially during March and April. This is because solar radiation is more abundant at this time than during the rest of the heating season (Figure 4-9). Overall, the average COP for heating is increased by about 2.5%.

The COP improvement is not very obvious in the yearly average data. The hourly COP improvement is studied, and the maximum increase of COP can be as high as 58%, as shown in Figure 4-10. Figure 4-11 graphs hourly data over several days to provide a clearer view of the relation between the COP and the HP outdoor unit's inlet air temperature.

Figure 4-10 Hourly COP increase for the BIPV/T and HP integration cases in Yellowknife

92
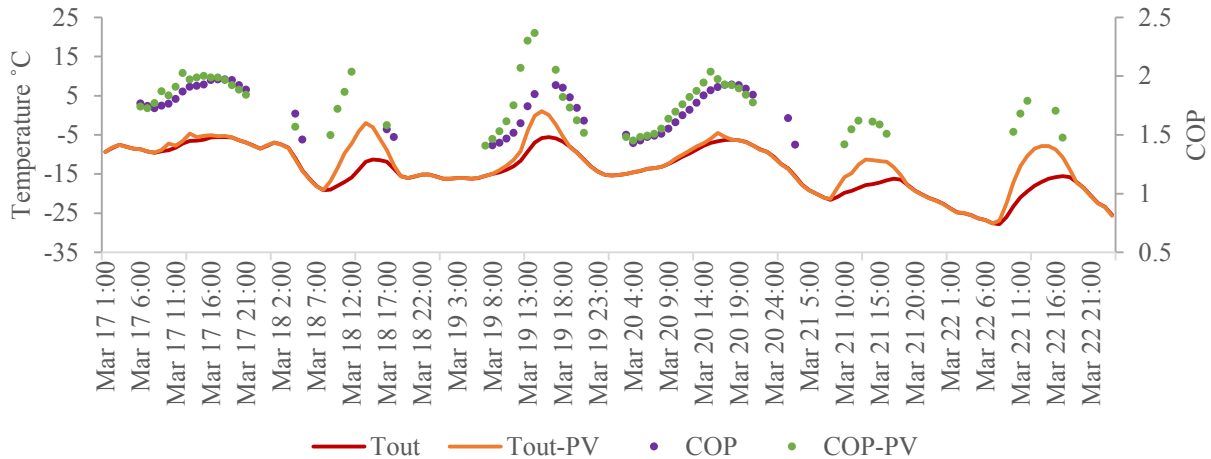
Figure 4-11 Hourly COP and temperature at HP outdoor unit - evaporator

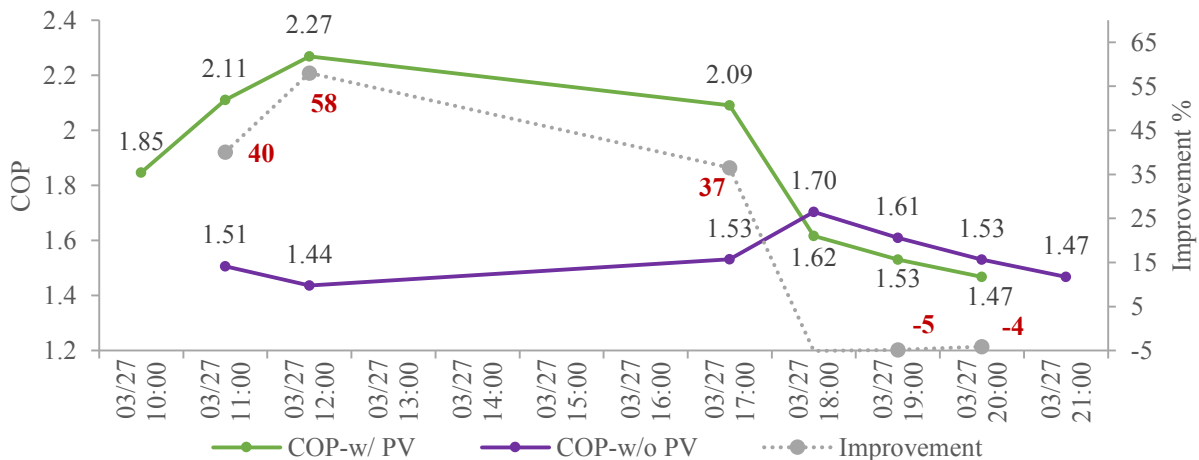In terms of energy consumption, however, the BIPV/T system with HP does not provide any energy-saving benefit, as can be seen from Table 4-5. This is because when switching from furnace to HP as the heating source during the prolonged HP working period, the air flow rate for the HP is lower than that for the furnace, which indicates that the heat transferred by the fan motor into the air loop with the HP is lower than that with the furnace. Therefore, the HP needs to consume more energy to produce the heat to compensate for the fan motor's lower rate. As the optimized house has a low heating demand due to its passive design, the difference caused by the reduced heat from the fan motor becomes significant. Although the HP has a higher efficiency than the furnace, the heat loss from the fan motor offsets the energy savings from higher heating efficiency.
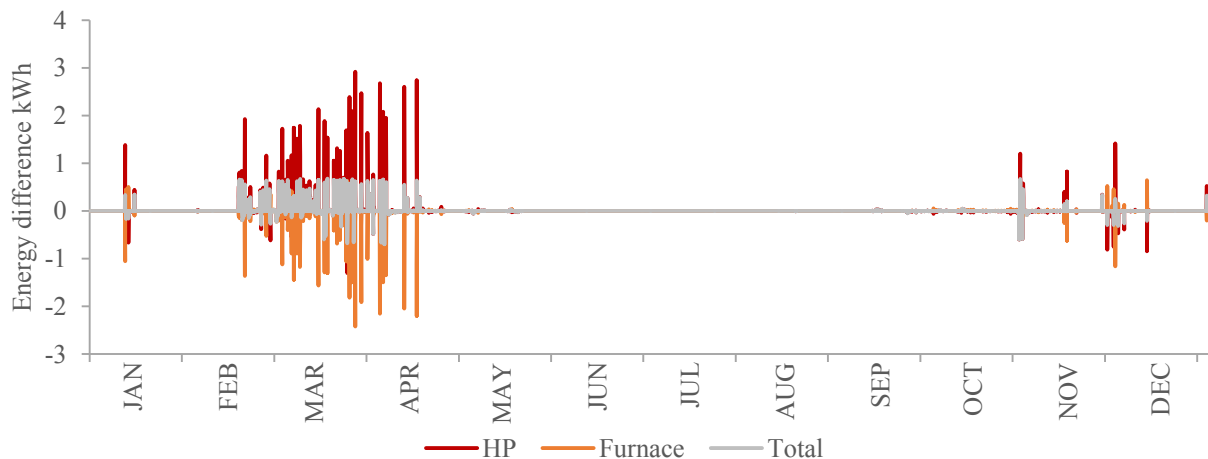

Figure 4-12 Hourly COP and temperature at HP outdoor unit - evaporator

The electricity generated by the BIPV/T system (covering 99% of the south-facing roof area) is estimated in EnergyPlus at 14,892.7 kWh (114.56 kWh/m^2) for a whole year, which can potentially

cover the energy demand of the house in the simulation on an annual basis. To achieve a net-zero house, however, measures need to be provided to address the mismatch between electricity and thermal generation periods and the house energy demand times through the use of an on-site battery, thermal storage, sharing among the community or local area, or interaction with the grid, if available.

4.4 Case Study: Kuujjuaq

The same BIPV/T integration study was performed for the optimized house for Kuujjuaq, and the simulation results are presented in this section. As the monthly weather data shows in Figure 4-13, Kuujjuaq has a cooler summer and a slightly warmer winter than Yellowknife. Comparing the incident solar radiation on the south-facing roof for the two locations, Kuujjuaq has a lower level of solar radiation than Yellowknife during the summer and a slightly higher level during the winter. During the shoulder season, the levels of solar radiation incident on the south-facing roof for Kuujjuaq and Yellowknife are similar.
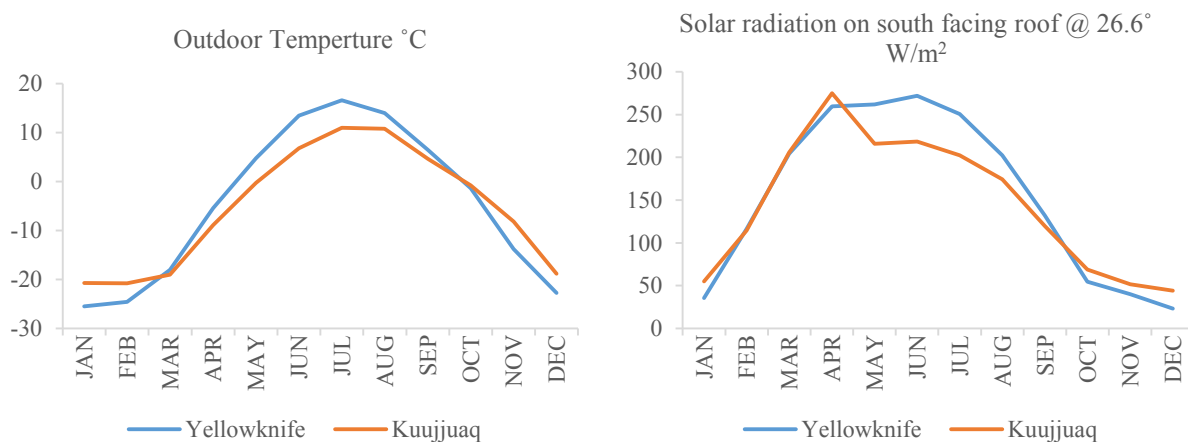
Figure 4-13 Monthly outdoor air temperature and incident solar radiation on south-facing roof @ 26.6˚ for Yellowknife and Kuujjuaq

Table 4-7 displays energy consumption under each BIPV/T integration case for the optimized house in Kuujjuaq. By integrating the BIPV/T system with the space heating system, the total energy consumption of the house can be reduced by 21.3%, which is a greater energy reduction than that seen with the integration of BIPV/T with space heating in Yellowknife. There are two reasons for this greater reduction in energy consumption. First, the optimized house for Kuujjuaq

requires heating for a longer period of time than the optimized house in Yellowknife because Kuujjuaq has a cooler summer, and the Kuujjuaq house is less energy efficient than the Yellowknife house. Second, solar radiation on the south-facing roof during the heating season is similar for the two locations, and the thermal energy produced by the BIPV/T system in Kuujjuaq can meet the heating requirements during the shoulder season and the early winter.

Table 4-7 Energy consumption of BIPV/T cases in Kuujjuaq

Case	Total kWh/m^2	Heating-HP kWh	Furnace kWh	Improvement
HVAC	86.64	2,919.93	4,790.94	---
BIPV/T + SpaceHeating	68.21	1,633.39	3,682.89	21.3%
BIPV/T + HRV	84.63	2,821.73	4,648.97	2.3%
BIPV/T+HP	86.95	3,205.53	4,625.56	-0.4%
* Total consumption includes the consumption of heat pump, furnace, fans, heat recovery ventilator, lighting and appliance.				

By integrating the BIPV/T system with the HRV system – that is, by preheating the inlet air for HRV system – the frost risk time (when the HR inlet air temperature is below -5 ˚C) is reduced by about 9.9%, and the defrost time (when the frosted HR is actually defrosting) is reduced by about 14.0% (Table 4-8). The energy saving for this configuration, however, is only 2.3% (Table 4-7). Kuujjuaq has a slightly warmer winter than Yellowknife, and the HRV frost time in Kuujjuaq is 562 hours, which is less than the 697 hours of HRV frost time in Yellowknife. With similar solar radiation on the south-facing roof and a higher outdoor air temperature during winter in Kuujjuaq, the BIPV/T system is more efficient at heating up the HRV inlet air and reducing its frost time.

Table 4-8 HRV frost hours and HP working hours of BIPV/T integration case in Kuujjuaq

Case	Defrost time (hr)	Frost risk time (hr)	Hours of temperature over -15 ˚C at HP outdoor unit	HP heating hours	Average COP
HVAC	562.23	3,726	6,476	3,512	2.16
BIPV/T + HRV	483.30	3,356	---	---	---
BIPV/T+HP	---	---	6,635	3,633	2.22

As shown in Table 4-8, by integrating the BIPV/T system with the HP outdoor unit in Kuujjuaq, the HP working period (when the air temperature at the HP outdoor unit is above -15 ˚C) is extended by about 159 hours. The actual working time of the HP in heating mode is increased by about 121 hours in the optimized Kuujjuaq house, which is longer than the 72-hour increase for the Yellowknife house. As mentioned above, the similar solar radiation on the south-facing roof

and higher outdoor air temperature during winter in Kuujjuaq allow the BIPV/T system in Kuujjuaq to heat the HP outdoor unit air above -15 °C for a longer period.
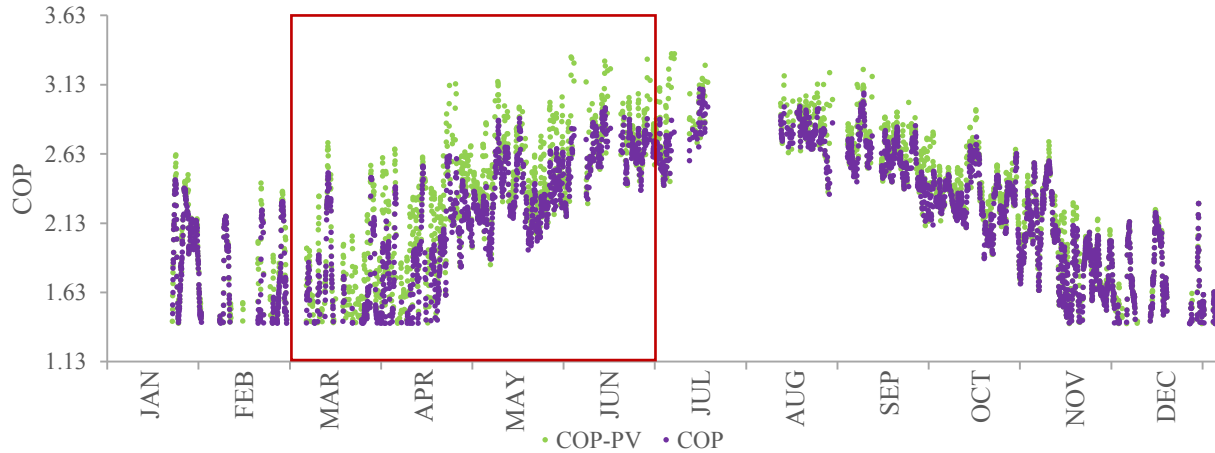
Figure 4-14 HP hourly COP for a whole year for the BIPV/T and HP integration cases in Kuujjuaq

As can be seen from Figure 4-14, integrating the BIPV/T system with the HP outdoor unit increases the HP's COP, especially from March to June. Overall, the average COP for heating is increased by about 2.8%. The COP improvement is not obvious in the yearly average data, but studying the hourly COP improvement reveals that the maximum COP increase can be as high as 53%, as graphed in Figure 4-15.
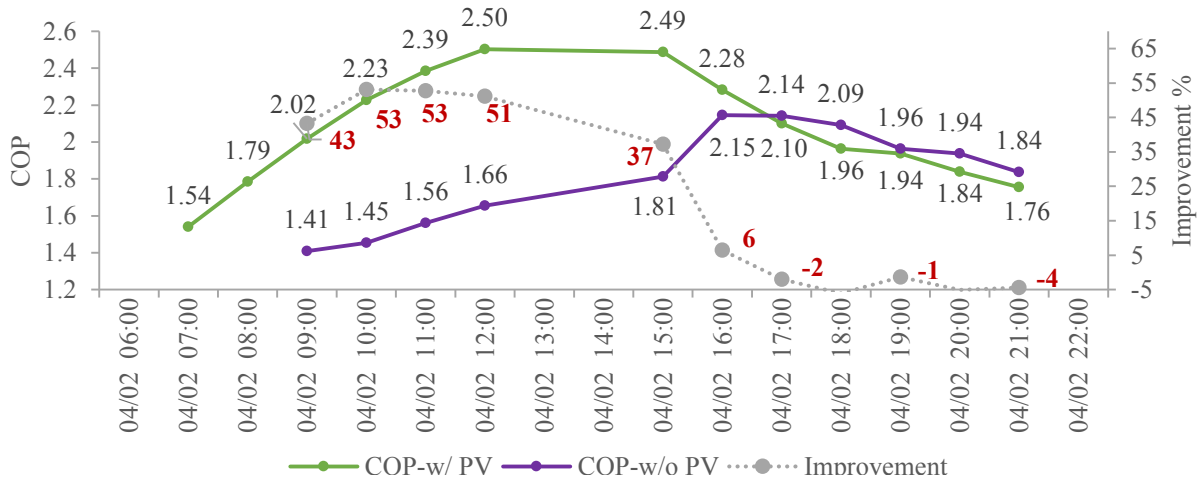

Figure 4-15 Hourly COP increase for the BIPV/T and HP integration cases in Kuujjuaq

The electricity generated by the BIPV/T system (covering 99% of the south-facing roof area) is estimated in EnergyPlus at 14,397.5 kWh (110.75 kWh/m^2) for a whole year, which can potentially cover the energy demands of the house in simulation on an annual basis.

4.5 Case Study: Resolute

Resolute is another northern city, with around 12,000 HDD, for the BIPV/T integration study. The studied house for Resolute is the same as the optimized house for Yellowknife.
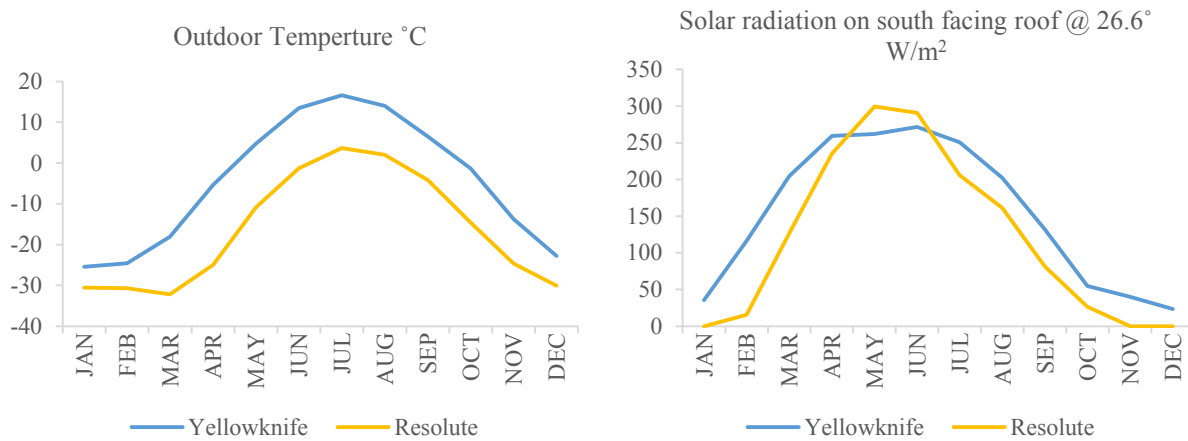
Figure 4-16 Monthly outdoor air temperature and incident solar radiation on south-facing roof @ 26.6˚ for Yellowknife and Resolute

As the monthly weather data shows in Figure 4-16, Resolute has a lower temperature than Yellowknife. As Resolute has a cold summer, the house there may require heating during the summer. Compared with the incident solar radiation on the south-facing roof in Yellowknife, Resolute has a lower level of solar radiation for most of the year except during May and June, when the solar radiation is higher in Resolute than in Yellowknife.

With the same design parameters, the house in Resolute has a heating demand of 129.44 kWh/m^2, which is double the heating demand of the house in Yellowknife (67.68 kWh/m^2). As Resolute has a cold summer, the cooling demand of the house remains at a very low level. Overall, the energy demand of the house in Resolute is 129.53 kWh/m^2, and the energy demand of the house in Yellowknife is 71.29 kWh/m^2 (Table 4-9).

Table 4-10 shows energy consumption under each BIPV/T integration case for the optimized house in Resolute. By integrating the BIPV/T system with the HVAC system, the total energy consumption of the house can be reduced by 15.1%, which saves more energy than that saved by the integration of a BIPV/T system with a space heating system in Yellowknife. This is because

the optimized house in Resolute requires more heating during the summer than the house in Yellowknife, and during this time the heating requirement is at a low level and the BIPV/T system supplies enough thermal energy to meet the need.

Table 4-9 Energy demand and passive design parameters for Yellowknife and Resolute

Parameters	Unit	Optimized House for Yellowknife	Optimized House for Resolute
Thermal resistance for walls	m^2·K/W	9.17	9.17
Thermal resistance for ceiling	m^2·K/W	20.34	20.34
Thermal resistance for floor	m^2·K/W	11.36	11.36
Thermal mass on the floor	m	0.055 – concrete	0.055 – concrete
Thermal mass on the walls	layers	1 – Gypsum	1 – Gypsum
WWR	%	47	47
Window/floor ratio	%	13.7	13.7
Window type	---	Triple glazed	
Shading	---	Block 90% solar radiation if cooling is required	
Ventilation rate	ACH	0.3 or change to 2 if cooling is required	
Annual Energy demand	kWh/m^2·a	71.29	129.53
Annual Heating demand	kWh/m^2·a	67.68	129.44
Annual Cooling demand	kWh/m^2·a	3.61	0.09
HDD (2008-2018)	-	7,964	11,814

* Annual energy demand contains the demand for heating and cooling.

Table 4-10 Energy consumption of BIPV/T cases in Resolute

Case	Total kWh/m^2	Heating-HP kWh	Furnace kWh	Improvement
HVAC	137.91	1,445.07	11,391.08	---
BIPV/T + SpaceHeating	117.15	677.73	9,341.20	15.1%
BIPV/T + HRV	136.30	1,407.31	11,241.71	1.2%
BIPV/T+HP	137.92	1,594.58	11,306.70	-0.01 %

* Total consumption includes the consumption of heat pump, furnace, fans, heat recovery ventilator, lighting and appliances.

By integrating the BIPV/T system with the HRV system – that is, preheating the inlet air for the HRV system – the frost risk time, when the HR inlet air temperature is below -5 ˚C, is reduced by about 6.9%, and the defrost time, when the frosted HR is being defrosted, is reduced by about 7.2% (Table 4-10). The energy saving for this configuration, however, is only 1.2% (Table 4-11). Resolute has a much colder winter than Yellowknife, and the HRV frost time in Resolute is 1,339 hours, which is more than the 697 hours of HRV frost time in Yellowknife. Additionally, during the winter, Resolute has less solar radiation, especially during January, November and December,

when there is no solar radiation in Resolute. During this period, the BIPV/T system in Resolute can hardly heat the HRV inlet air and reduce the frost time.

Table 4-11 HRV frost hours & HP working hours of BIPV/T integration case in Resolute

Case	Defrost time (hr)	Frost risk time (hr)	Hours of temperature over -15°C at HP outdoor unit	HP heating hours	Average COP
HVAC	1,339.31	6,073	4,043	1,875	2.00
BIPV/T + HRV	1,247.31	5,637	---	---	---
BIPV/T+HP	---	---	4,183	1,990	2.05

As shown in Table 4-11, by integrating the BIPV/T system with the HP outdoor unit in Resolute, the HP working period (during which the air temperature at the HP outdoor unit is above -15 ˚C) is extended by about 140 hours. The actual working time of the HP in heating mode is increased by about 115 hours. As shown in Figure 4-17, integrating the BIPV/T system with the HP outdoor unit increases the HP's COP, especially from April to June. As stated above, Resolute has a very cold climate, the HP working period covers the shoulder season and the summer, and during the harsh winter, the required heating is supplied only by the furnace.
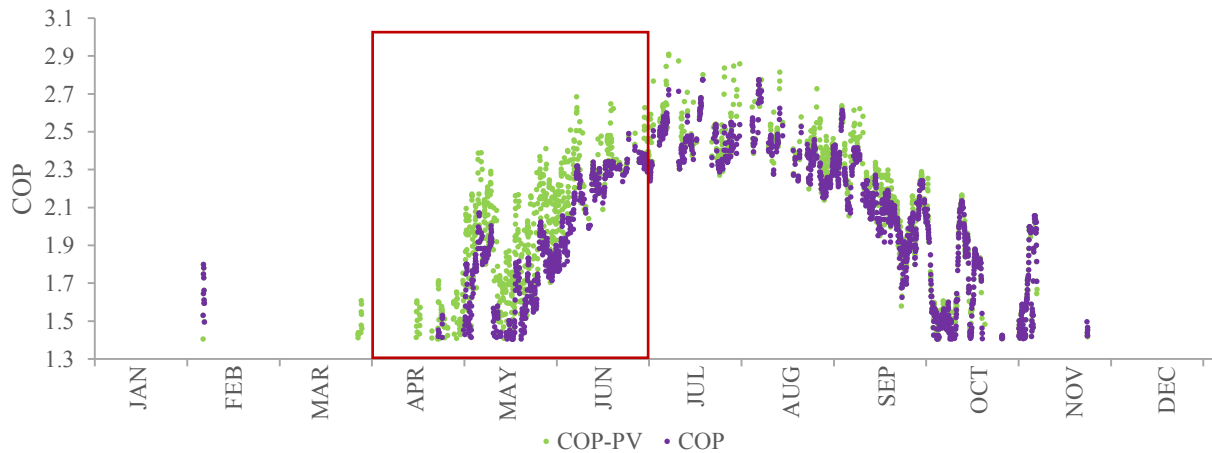
Figure 4-17 HP hourly COP in a whole year for the BIPV/T and HP integration cases in Resolute

The COP improvement, which is about 2.5%, is not obvious in the yearly average data. Studying the hourly COP improvement, however, shows the maximum increase of COP can be as high as 44%, as illustrated in Figure 4-18.

The electricity generated by the BIPV/T system (covering 99% of the south-facing roof area) is estimated in EnergyPlus at 12,249.4 kWh (94.23 kWh/m^2) for a whole year. This can only partially cover the energy demand of the house in simulation on an annual basis.
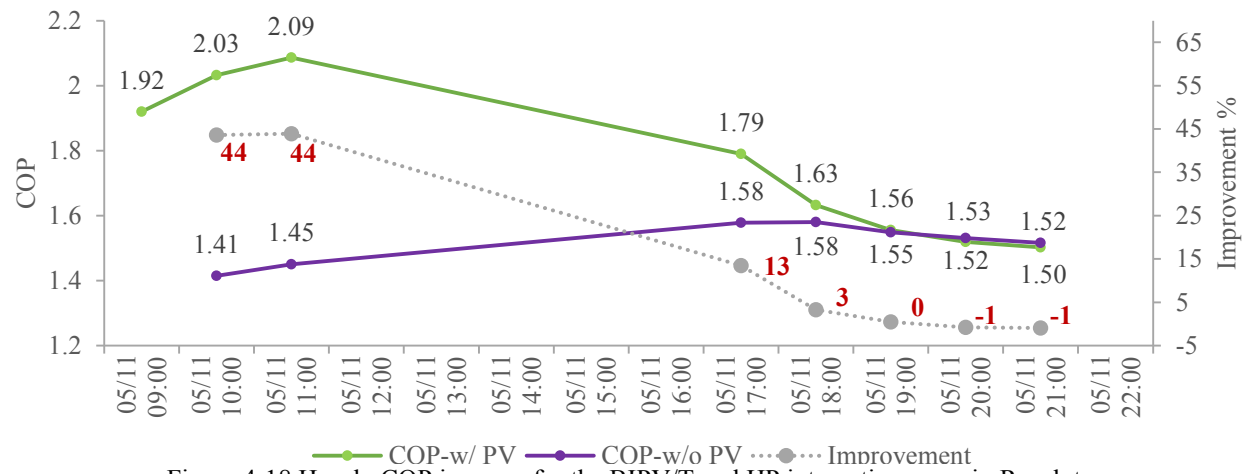
Figure 4-18 Hourly COP increase for the BIPV/T and HP integration cases in Resolute

Chapter 5   Conclusion

Houses in the north of Canada face many challenges: the harsh weather, higher costs, a vast area with a sparse population and lack of skilled laborers. Building an affordable house with better energy performance in the north requires considering all influencing parameters as a group and striking a balance among them to get optimal results. This thesis presents an optimization for a residential house in the north of Canada, and the results are summarized below.

(1) The main optimization was done for Yellowknife considering passive parameters together and simulating the optimal results by using a multi-objective genetic algorithm. The optimal house over a 25-year life cycle could save about 46% in energy consumption compared with the reference house with an increase in construction cost of about 10%. The optimization was repeated for Kuujjuaq, which has higher construction costs and lower electricity prices. Under these conditions, the optimal house in Kuujjuaq could save about 33% energy consumption with the construction cost remaining the same. In the north of Canada, where construction costs are higher because of fewer connections with the big cities of the south, an optimal set of parameters could bring significant energy savings by slightly increasing the initial construction cost. Several factors that would influence the optimization results are analyzed – namely, the location factor, energy source, thermal mass and additional labor cost. Different projects in the same city may have varied construction costs, and a study of how the construction cost affects the optimal results finds that, with a higher construction cost, the optimal house tends to be less energy saving than one with a lower construction cost. The multiple energy source case in Kuujjuaq shows that the optimal house that uses both electricity and fuel has a lower energy demand than the optimal house that uses only electricity. This is because the fuel price in Kuujjuaq is higher than the electricity price, which leads to considerable energy savings from a house with better energy performance. This comparison case also proved that, with a higher energy price, the optimal house tends to be a house with lower energy demand yet an acceptably higher construction cost. Thermal mass in the northern house can make a contribution to energy saving. The optimal results for optimizing the same house with thermal mass could reduce energy use by 9% compared to the house without thermal mass. Moreover, to achieve the high performance from thermal mass, the WWR is almost doubled. The fixed costs in the project, such as the additional labor cost in Kuujjuaq, do not affect the optimal results.

101

(2) With the low energy demand optimized house, a BIPV/T system was applied to further decrease energy consumption. The BIPV/T system on the south-facing roof was integrated with the space heating, HR and HP systems separately. For Yellowknife, the results show that a BIPV/T system with space heating, which introduces the BIPV/T-warmed air directly into the room, reduced energy consumption 15.5%; a BIPV/T system with an HR system, which uses thermal energy from PV panels to heat the inlet fresh air, lowered energy consumption about 1.4%; and a BIPV/T system with an HP system provided almost no energy saving benefit. Moreover, a BIPV/T system with an HR system lowered the heat exchanger defrost time by 8.80%, and a BIPV/T system with an HP system, which introduces the warmed air from PV panels to the HP outdoor unit, extended the HP working time by 128 hours and increased the COP by 2.5% over one year. For Kuujjuaq, a place with cooler summers, slightly warmer winters and similar solar radiation levels during the heating season, the results show that the energy savings brought by a BIPV/T system are greater than those seen with the cases in Yellowknife. For Kuujjuaq, a BIPV/T system with space heating reduced energy consumption by 21.3%, a BIPV/T system with an HR system reduced the heat exchanger defrost time by 14.0%, and a BIPV/T system with an HP system extended the HP's working time by 159 hours over one year and increased its COP about 2.8%. The same house that was optimized for Yellowknife was optimized for Resolute for the BIPV/T integration study. The energy performance improvement from a BIPV/T system in Resolute, with its harsh climate and reduced solar radiation, is similar to what is seen for the cases in Yellowknife, although the total energy consumption is much higher than in Yellowknife.

Reference

Ahmed-Dahmane, M., Malek, A., & Zitoun, T. (2018). Design and analysis of a BIPV/T system with two applications controlled by an air handling unit. *Energy conversion and management*, *175*, 49-66.

Altus Group, (2017), Canadian Cost Guide. Retrieve from: https://www.altusgroup.com/wp-content/uploads/2017/05/altusgroup_costguide2017_web.pdf

Asadi, E., Da Silva, M. G., Antunes, C. H., & Dias, L. (2012). Multi-objective optimization for building retrofit strategies: A model and an application. *Energy and Buildings*, *44*, 81-87.

Asadi, E., Da Silva, M. G., Antunes, C. H., Dias, L., & Glicksman, L. (2014). Multi-objective optimization for building retrofit: A model using genetic algorithm and artificial neural network and an application. *Energy and Buildings*, *81*, 444-456.

Asaee, S. R., Nikoofard, S., Ugursal, V. I., & Beausoleil-Morrison, I. (2017). Techno-economic assessment of photovoltaic (PV) and building integrated photovoltaic/thermal (BIPV/T) system retrofits in the Canadian housing stock. *Energy and Buildings*, *152*, 667-679.

Ascione, F., Bianco, N., De Stasio, C., Mauro, G. M., & Vanoli, G. P. (2015). A new methodology for cost-optimal analysis by means of the multi-objective optimization of building energy performance. *Energy and Buildings*, *88*, 78-90.

Ascione, F., De Masi, R. F., de Rossi, F., Ruggiero, S., & Vanoli, G. P. (2016). Optimization of building envelope design for nZEBs in Mediterranean climate: Performance analysis of residential case study. *Applied energy*, *183*, 938-957.

Ascione, F., Bianco, N., De Stasio, C., Mauro, G. M., & Vanoli, G. P. (2017). CASA, cost-optimal analysis by multi-objective optimisation and artificial neural networks: A new framework

for the robust assessment of cost-optimal energy retrofit, feasible for any building. *Energy and Buildings*, *146*, 200-219.

ASHRAE Standard Committee. (2016). ANSI/ASHRAE/IES Standard 62.2 Ventilation and Acceptable Indoor Air Quality in Low-Rise Residential Building.

ASHRAE Standard Committee. (2018). ANSI/ASHRAE/IES Standard 90.2 Energy-Efficient Design of Low-Rise Residential Building. Retrieved from: https://ashrae.iwrapper.com /ViewOnline/Standard_90.2-2018

Azari, R., Garshasbi, S., Amini, P., Rashed-Ali, H., & Mohammadi, Y. (2016). Multi-objective optimization of building envelope design for life cycle environmental performance. *Energy and Buildings*, *126*, 524-534.

Beattie, C. J. (2017). Experimental study of air-to-air heat/energy exchangers for use in Arctic housing (Master thesis, Concordia University).

Bichiou, Y., & Krarti, M. (2011). Optimization of envelope and HVAC systems selection for residential buildings. Energy and Buildings, 43(12), 3373-3382.e

Bojić, M., Miletić, M., & Bojić, L. (2014). Optimization of thermal insulation to achieve energy savings in low energy house (refurbishment). *Energy conversion and management*, *84*, 681-690.

Bre, F., Silva, A. S., Ghisi, E., & Fachinotti, V. D. (2016). Residential building design optimisation using sensitivity analysis and genetic algorithm. *Energy and Buildings*, *133*, 853-866.

Bristow, M., & Gill, V. (2011). Northern Assets: Transportation Infrastructure in Remote Communities.

Canada inflation rate. Retrieve from: https://tradingeconomics.com/canada/inflation-cpi. June 10th 2019

Canada Mortgage and Housing Corporation. (2009). The Northern Sustainable House: An Innovative Design Process

Canada Mortgage and Housing Corporation. (2014a). Northern Housing Project Profile: The Arviat Northern Sustainable House

Canada Mortgage and Housing Corporation. (2014b). Northern Housing Project Profile: The Dawson E/2 Northern Sustainable House

Canada Mortgage and Housing Corporation. (2014c). Northern Housing Project Profile: The Dawson E/9 Northern Sustainable House

Canada Mortgage and Housing Corporation. (2014d). Northern Housing Project Profile: The Inuvik Northern Sustainable House

Canada Weather Stats, Heating Degree Days. Retrieve from: https://www.weathersatts.ca. June 28th 2019

Canadian Commission on Building and Fire Code, (2015), National Building Code of Canada

Canadian Commission on Building and Fire Code, (2017), National Energy Code of Canada for Building

Canadian Northern Economic Development Agency. (2016). Building a Strong North Together. Retrieve from: https://www.cannor.gc.ca/eng/1458573988380/1458574067957. June 5th, 2019

Candanedo, L. M., Athienitis, A., & Park, K. W. (2011). Convective heat transfer coefficients in a building-integrated photovoltaic/thermal system. *Journal of Solar Energy Engineering*, *133*(2), 021002.

Carlucci, S., Cattarin, G., Causone, F., & Pagliano, L. (2015). Multi-objective optimization of a nearly zero-energy building based on thermal and visual discomfort minimization using a non-dominated sorting genetic algorithm (NSGA-II). *Energy and Buildings*, *104*, 378-394.

Carlucci, S., Pagliano, L., & Zangheri, P. (2013). Optimization by discomfort minimization for designing a comfortable net zero energy building in the Mediterranean climate. In *Advanced Materials Research* (Vol. 689, pp. 44-48). Trans Tech Publications.

Castro-Lacouture, D., Sefair, J. A., Flórez, L., & Medaglia, A. L. (2009). Optimization model for the selection of materials using a LEED-based green building rating system in Colombia. *Building and environment*, *44*(6), 1162-1170.

Chantrelle, F. P., Lahmidi, H., Keilholz, W., El Mankibi, M., & Michel, P. (2011). Development of a multicriteria tool for optimizing the renovation of buildings. *Applied Energy*, *88*(4), 1386-1394.

Charron, R., & Athienitis, A. K. (2006). Optimization of the performance of double-facades with integrated photovoltaic panels and motorized blinds. *Solar Energy*, *80*(5), 482-491.

Chen, X., & Yang, H. (2017). A multi-stage optimization of passively designed high-rise residential buildings in multiple building operation scenarios. *Applied energy*, *206*, 541-557.

Chen, Y. (2012). *Design and Evaluation of Façade-Integrated Solar Technologies Suitable for* High-Latitude Applications (Doctoral dissertation, Concordia University).

CMHC, (2007), Research report The Northern Sustainable House: An Innovative Design Process

Cvetković, D., & Bojić, M. (2014). Optimization of thermal insulation of a house heated by using radiant panels. *Energy and Buildings*, *85*, 329-336.

Delgarm, N., Sajadi, B., Delgarm, S., & Kowsary, F. (2016). A novel approach for the simulation-based optimization of the buildings energy consumption using NSGA-II: Case study in Iran. *Energy and Buildings*, *127*, 552-560.

Delgarm, N., Sajadi, B., Kowsary, F., & Delgarm, S. (2016). Multi-objective optimization of the building energy performance: A simulation-based approach by means of particle swarm optimization (PSO). *Applied energy*, *170*, 293-303.

Department of Public Works and Services Government of the Northwest Territories, (2011), Good Building Practice for Northern Facilities. Retrieved from: https://www.inf.gov. nt.ca/sites/ inf/files/good_building_practice_for_northern_facilities.pdf

DoE, U. S. (2016). Energyplus engineering reference. *US Department of Energy*.

Echenagucia, T. M., Capozzoli, A., Cascone, Y., & Sassone, M. (2015). The early design stage of a building envelope: Multi-objective search through heating, cooling and lighting energy performance analysis. *Applied Energy*, *154*, 577-591.

Elbeltagi, E., Hegazy, T., & Grierson, D. (2005). Comparison among five evolutionary-based optimization algorithms. *Advanced engineering informatics*, *19*(1), 43-53.

Energy and Mines Ministers' Conference. (2017). Build smart – Canada's Buildings Strategy

Energy Resources Canada. (2019). Energy Use Data Handbook Tables: Total End-Use Sector & Residential Sector (online), available at: http://oee.nrcan.gc.ca/corporate/statistics/neud/dpa/menus/trends/handbook/tables.cfm

Energyhub.org. Solar Energy Maps Canada. Retrieve from: https://energyhub.org/solar-energy-maps-canada/. June 14th 2019

EnergyPlus Weather Data. (2017 September 11). Weather Data Download – Yellowknife 719360 (CWEC). Retrieved from: https://energyplus.net/weather-location/north_and_central_america_wmo_region_4/CAN/NT/CAN_NT_Yellowknife.719360_CWEC

Engineers, R. A. C. (2017). ASHRAE Handbook-fundamental, Chapter 26: Heat, Air, and Moisture Control in Building Assemblies – Material properties. *American Society of Heating, Refrigerating and Air-Conditioning Engineers*.

Fan, Y., & Xia, X. (2017). A multi-objective optimization model for energy-efficiency building envelope retrofitting plan with rooftop PV system installation and maintenance. *Applied energy*, *189*, 327-335.

Futrell, B. J., Ozelkan, E. C., & Brentrup, D. (2015). Bi-objective optimization of building enclosure design for thermal and lighting performance. *Building and Environment*, *92*, 591-602.

Goldberg, D. E. (1989). Genetic Algorithms in Search. Optimization and Machine Learning. Addism1—Wesley. *Reading, MA*.

Gossard, D., Lartigue, B., & Thellier, F. (2013). Multi-objective optimization of a building envelope for thermal performance using genetic algorithms and artificial neural network. *Energy and Buildings*, *67*, 253-260.

Government of Canada, Canada – Heating Degree-Days. Retrieve from: https://open.canada.ca /data/en/dataset/fd8efb83-b73d-5442-ab60-7987c824f5fd. June 19th, 2019

Hailu, G., Dash, P., & Fung, A. S. (2015). Performance evaluation of an air source heat pump coupled with a building-integrated photovoltaic/thermal (BIPV/T) system under cold climatic conditions. *Energy Procedia*, *78*, 1913-1918.

Hamdy, M., Hasan, A., & Siren, K. (2009, July). Combination of optimisation algorithms for a multi-objective building design problem. In *IBPSA: 11th International Building Performance Simulation Association Conference, Glasgow-UK*.

Hamdy, M., Nguyen, A. T., & Hensen, J. L. (2016). A performance comparison of multi-objective optimization algorithms for solving nearly-zero-energy-building design problems. *Energy and Buildings*, *121*, 57-71.

Harish, V. S. K. V., & Kumar, A. (2016). A review on modeling and simulation of building energy systems. *Renewable and Sustainable Energy Reviews*, *56*, 1272-1292.

Hassan, R., Cohanim, B., De Weck, O., & Venter, G. (2005, April). A comparison of particle swarm optimization and the genetic algorithm. In 46th AIAA/ASME/ASCE/AHS/ASC structures, structural dynamics and materials conference (p. 1897).

Holland, J. H. (1992). *Adaptation in natural and artificial systems: an introductory analysis with applications to biology, control, and artificial intelligence*. MIT press.

Hooke, R., & Jeeves, T. A. (1961). "Direct Search" Solution of Numerical and Statistical Problems. *Journal of the ACM (JACM)*, *8*(2), 212-229.

Huang, Y., & Niu, J. L. (2016). Optimal building envelope design based on simulated performance: History, current status and new potentials. *Energy and Buildings*, *117*, 387-398.

Hunker. (2019 January 17). *How Thick Should a Roof Be?* Retrieved from: https://www.hunker. com/13401243/how-thick-should-a-roof-be

Hydro Quebec. (2019). 2019 Electricity Rates.

International Energy Agency. (2018). Key world energy statistics

Jedrzejuk, H., & Marks, W. (2002a). Optimization of shape and functional structure of buildings as well as heat source utilization. Basic theory. *Building and Environment*, *37*(12), 1379-1383.

Jedrzejuk, H., & Marks, W. (2002b). Optimization of shape and functional structure of buildings as well as heat source utilisation. Partial problems solution. *Building and Environment*, *37*(11), 1037-1043.

Junghans, L., & Darde, N. (2015). Hybrid single objective genetic algorithm coupled with the simulated annealing optimization method for building optimization. *Energy and Buildings*, *86*, 651-662.

Karanasions, K., & Parker, P. (2016). Recent Developments in Renewable Energy in Remote Aboriginal Communities, Quebec, Canada. Pap. Can. Econ. Dev. 16, 98-108.

Kativik Regional Government and Makivik Corporation. (2012). Plan Nunavik. Westmount, QC: Avataq Cultural Institute.

Kerdan, I. G., Raslan, R., & Ruyssevelt, P. (2016). An exergy-based multi-objective optimisation model for energy retrofit strategies in non-domestic buildings. *Energy*, *117*, 506-522.

Kayello, A. (2018). Hygrothermal Performance of Structural Insulated Panels and Attics for Inuit Communities (PhD thesis, Concordia University).

Kheiri, F. (2018). A review on optimization methods applied in energy-efficient building geometry and envelope design. *Renewable and Sustainable Energy Reviews*, *92*, 897-920.

Kim, J. H., Ahn, J. G., & Kim, J. T. (2016). Demonstration of the performance of an air-type photovoltaic thermal (PVT) system coupled with a heat-recovery ventilator. *Energies*, *9*(9), 728.

Li, H., Cao, C., Feng, G., Zhang, R., & Huang, K. (2015). A BIPV/T System Design Based on Simulation and its Application in Integrated Heating System. *Procedia Engineering*, *121*, 1590-1596.

Lstiburek, J. W. (2009). Building in extreme cold. ASHRAE Journal, 51(2), 56-60.

Machairas, V., Tsangrassoulis, A., & Axarli, K. (2014). Algorithms for optimization of building design: A review. *Renewable and Sustainable Energy Reviews*, *31*, 101-112.

Magnier, L., & Haghighat, F. (2010). Multiobjective optimization of building design using TRNSYS simulations, genetic algorithm, and Artificial Neural Network. *Building and Environment*, *45*(3), 739-746.

Makivik Corporation. Rise in the Cost of Gasoline. Retrieves from: https://www.makivik.org/rise-in-the-cost-of-gasoline/, July 17th, 2019

National Energy Board of Canada. (2011). Energy Use in Canada's North: An Overview of Yukon, Northwest Territories, and Nunavut. Ottawa.

Natural Resources Canada, (2012), R-2000 Standard. Retrieved from: https://www.nrcan.gc.ca/sites/www.nrcan.gc.ca/files/oee/files/pdf/2012%20R2000%20Standard%20EN.pdf

Nguyen, A. T., Reiter, S., & Rigo, P. (2014). A review on simulation-based optimization methods applied to building performance analysis. *Applied Energy*, *113*, 1043-1058.

Northwest Territories Energy Facts, (2012), Heating in the NWT. Retrieve from: https://www.inf.gov .nt.ca/sites/inf/files/heating_in_the_nwt_0.pdf

Northwest Territories Power Corporation, Rate Schedule, (May. 1st, 2019). Retrieve from: https://www.ntpc.com/customer-service/residential-service/what-is-my-power-rate, Aug. 17th, 2019

Pal, S. K., Takano, A., Alanne, K., Palonen, M., & Siren, K. (2017). A multi-objective life cycle approach for optimal building design: A case study in Finnish context. *Journal of cleaner production*, *143*, 1021-1035.

Palonen, M., Hasan, A., & Siren, K. (2009, July). A genetic algorithm for optimization of building envelope and HVAC system parameters. In *Proc. Of the 11th IBPSA Conference, Glasgow, Scotland*.

Pernodet, F., Lahmidi, H., & Michel, P. (2009, July). Use of genetic algorithms for multicriteria optimization of building refurbishment. In *11th International IBPSA Conference*.

RDH Building Engineering. Energy Efficient Housing Guidelines for Whitehorse, YT: Energy Optimized House. Retrieve from: http://www.energy.gov.yk.ca/pdf/Energy-Efficient-Northern-Housing-Guide-Energy-Optimized.pdf

Roberti, F., Oberegger, U. F., Lucchi, E., & Troi, A. (2017). Energy retrofit and conservation of a historic building using multi-objective optimization and an analytic hierarchy process. *Energy and Buildings*, *138*, 1-10.

RS Means Company. (2017). Residential building cost data. RS Means Company.

Schwartz, Y., Raslan, R., & Mumovic, D. (2016). Implementing multi objective genetic algorithm for life cycle carbon footprint and life cycle cost minimisation: A building refurbishment case study. *Energy*, *97*, 58-68.

Shahsavar, A., & Rajabi, Y. (2018). Exergoeconomic and enviroeconomic study of an air based building integrated photovoltaic/thermal (BIPV/T) system. *Energy*, *144*, 877-886.

Shi, X. (2011). Design optimization of insulation usage and space conditioning load using energy simulation and genetic algorithm. *Energy*, *36*(3), 1659-1667.

Shi, X., Tian, Z., Chen, W., Si, B., & Jin, X. (2016). A review on building energy efficient design optimization rom the perspective of architects. *Renewable and Sustainable Energy Reviews*, *65*, 872-884.

Société D'Habitation Du Québec, (2014), Housing in Nunavik. Retrieve from: http://www. habitation.gouv.qc.ca/fileadmin/internet/documents/English/logement__nunavik_2014.pdf. June 4th, 2019

Tardif, J. M., Tamasauskas, J., Delisle, V., & Kegel, M. (2017). Performance of air based BIPV/T heat management strategies in a Canadian home. *Procedia Environmental Sciences*, *38*, 140-147.

THE RADIANT PROFESSIONALS ALLIANCE. (2018 December 31). Retrieved from: http://www.radiantprofessionalsalliance.org/Pages/FloorCoveringR-ValueChart.aspx

Thirunavukarasu, A. (2016). *Protocol for Low Energy Houses for Northern Canadian Regions* (Masters thesis, Concordia University).

Toffanin R., Ge H., Athienitis A. (2019) Integration of Building Integrated Photovoltaic/Thermal (BIPV/T) System with Heat Recovery Ventilators for Improved Performance Under Extreme Cold Climates. In: Johansson D., Bagge H., Wahlström Å. (eds) Cold Climate HVAC 2018. CCC 2018. Springer Proceedings in Energy. Springer, Cham

Torczon, V. (1992). *PDS: Direct search methods for unconstrained optimization on either sequential or parallel machines* (No. TR-92-9). RICE UNIV HOUSTON TX DEPT OF MATHEMATICAL SCIENCES.

True Professionals, Inc. Typical "Life Expectancy" Table for common building materials & systems. Retreive from: http://weberaccetta.com/wp-content/uploads/2017/04/Life_Expectancy_Table.pdf. Oct. 30th, 2019.

Tuhus-Dubrow, D., & Krarti, M. (2010). Genetic-algorithm based approach to optimize building envelope design for residential buildings. *Building and environment*, *45*(7), 1574-1581.

Wetter, M. (2016). GenOpt(R), Generic Optimization Program, User Manual, Version 3.1.1.

Wetter, M., & Wright, J. (2004). A comparison of deterministic and probabilistic optimization algorithms for nonsmooth simulation-based optimization. Building and Environment, 39(8), 989-999.

World Population Review. Canadian Provinces Population 2019. Retrieve from: http://world populationreview.com/canadian-provinces/, Nov 11th, 2019.

Xu, W., Chong, A., Karaguzel, O. T., & Lam, K. P. (2016). Improving evolutionary algorithm performance for integer type multi-objective building system design optimization. *Energy and Buildings*, *127*, 714-729.

Yang, M. D., Lin, M. D., Lin, Y. H., & Tsai, K. T. (2017). Multiobjective optimization design of green building envelope material using a non-dominated sorting genetic algorithm. *Applied Thermal Engineering*, *111*, 1255-1264.

Yang, T. (2015). *A Numerical and Experimental Investigation of Enhanced Open-Loop Air-Based Building-integrated Photovoltaic/Thermal (BIPV/T) Systems* (PhD thesis, Concordia University).

Yu, W., Li, B., Jia, H., Zhang, M., & Wang, D. (2015). Application of multi-objective genetic algorithm to optimize energy efficiency and thermal comfort in building design. *Energy and Buildings*, *88*, 135-143.

Appendix A Passive design parameters value in Standards and Codes

Table. A-1 Passive design parameters requirements in Codes and Standards

Variables	Building Code
Thermal Resistance for Exterior Wall	**NBCC :** > R 3.85 $m^2 \cdot$K/W (Zone 8) [Division B 9.36.2.6] **ASHRAE 90.2:** < U 0.32 W/$m^2 \cdot$K = > R 3.13 $m^2 \cdot$K/W (Zone 8) [Page 10] **NECB :** < U 0.183 W/$m^2 \cdot$K = > R 5.46 $m^2 \cdot$K/W (Zone 8) [Division B 3-5] **R-2000:** Thermal insulation levels must meet or exceed provincial or local requirements [Page 5] **GBP:** Walls: RSI 5.6 [Architectural Page 11]
Thermal Resistance for Roof/Ceiling	**NBCC :** > R 10.43 $m^2 \cdot$K/W (Ceiling below attic, Zone 8) [Division B 9.36.2.6] **ASHRAE 90.2:** < U 0.15 W/$m^2 \cdot$K = > R 6.67 $m^2 \cdot$K/W (Ceiling, Zone 8) [Page 10] **NECB :** < U 0.121 W/$m^2 \cdot$K = > R 8.26 $m^2 \cdot$K/W (Roof, Zone 8)[Division B 3-5] **R-2000:** Thermal insulation levels must meet or exceed provincial or local requirements [Page 5] **GBP:** Roofs: RSI 8.75 [Architectural Page 11]
Thermal Resistance for Floor	**NBCC :** > 4.44 $m^2 \cdot$K/W (Heated and unheated floors on permafrost, Zone 8)[Division B 9.36.2.8] **ASHRAE 90.2:** < U 0.16 W/$m^2 \cdot$K = > R 6.25 $m^2 \cdot$K/W (Zone 8) [Page 10] **NECB :** < U 0.142 W/$m^2 \cdot$K = > R 7.04 $m^2 \cdot$K/W (Zone 8) [Division B 3-5] **R-2000:** Thermal insulation levels must meet or exceed provincial or local requirements [Page 5] **GBP:** Suspended Floor: RSI 7.0 [Architectural Page 11]
Thermal Resistance for Window/Window type	**NBCC :** <U 1.40 W/$m^2 \cdot$K (Zone 8) [Division B 9.36.2.7] **ASHRAE 90:** <U 1.82 W/$m^2 \cdot$K (Zone 8) [Page 10] **NECB :** <U 1.40 W/$m^2 \cdot$K (Zone 8) [Division B 3-5] **R-2000 :** Windows shall have the following minimum requirements: double-glazed window with a low-emissivity coating, insert gas fill, and an insulated spacer with a wood, vinyl or fiberglass frame. [Page 6] **GBP:** All window are recommended to have as a minimum double-glazed sealed glazing units with low "E" coating, or triple-glazed sealed units [Architectural Page 42]
Window-wall Ratio	**NECB :** < 20% [Division B 3-16]
Ventilation (introduce outside air into room)	**NBCC :** 1) Non-Heating-Season Mechanical Ventilation: (See Table 9.32.2.3) [division B 9.32.3.2] (1) basement areas used for any other purposes that exceed 2/3 of the total basement floor area shall be assigned an air change rate of 10L/s

(2) basement areas used for any other purposes that are 2/3 of the total basement floor area or less shall be assigned an air change rate of 5L/s

(3) other habitable rooms, other than spaces intended solely for access, egress, storage, or service equipment, shall be assigned an air change rate of 5 L/s.

2) Heating-Season (Ventilation system not used in conjunction with forced air heating system) (see Table 9.32.3.3): An outdoor air supply fan shall be installed with a rate capacity within ±10% of the actual normal operating exhaust capacity of the exhaust fan installed to satisfy the requirement for principal ventilation fan. [Division B 9.32.3.5]

3) Indoor air quality required ventilation: the rates at which outdoor air is supplied in buildings by ventilation systems shall be not less than the rates required by ANSI/ASHRAE 62 "Ventilation for Acceptable indoor Air Quality" [Division B 6.3.1.3]

Table 9.32.2.3 Air Change Rate

Room or space	Rate, L/s
Master bedroom	10
Other bedrooms	5
Living room	5
Dining room	5
Family room	5
Recreation room	5
Basement	10
Kitchen	5
Bathroom or water-closet room	5
Laundry room	5
Utility room	5
Other habitable room	5

Table 9.32.3.3 Normal Operating Exhaust Capacity of Principle Ventilation Fan

Number of Bedroom in Dwelling Unit	Normal Operating Exhaust Capacity of Principal Ventilation Fan, L/s	
	Minimum	Maximum
1	16	24
2	18	28
3	22	32
4	26	38
5	30	45
More than 5	System must comply with Clause 9.32.3.1.(1)(a) *	

* good practice such as that described in CAN/CSA-F326-M, "Residential Mechanical Ventilation system"

R-2000 :
Mechanical ventilation rate: [Page 16]
To comply with the R-2000 Standard, the ventilation energy use calculation assumes that a house is ventilated at a monthly average rate of 0.30 normal air changes per hour, with a minimum of 25 L/s and a maximum of 100 L/s, of combined natural and mechanical ventilation.

GBP:
In the interest if economy, designers are encouraged to consider more energy-efficient ventilation strategies while continuing to meet the requirements of ASHRAE 62 (Current Edition) and maintaining optimum occupant comfort levels of indoor air quality. [Mechanical Page 71]

	ASHRAE 62.2:
	1. Ventilation rate:[Page 4] A mechanical exhaust system, supply system, or combination thereof shall be installed to operate for each dwelling unit to provide continuous whole-building ventilation with outdoor air at a rate not less than specified in section 4.1.1 (Total Ventilation Rate) **2. Total Ventilation Rate:** The total required ventilation rate (Q_{tot}) shall be as specified in Table 4.1b, alternatively, calculated using Equation 4.1b $Q_{tot} = 0.15A_{floor} + 3.5\,(N_{br} + 1)$ (SI) (4.1b) where Q_{tot} = total required ventilation rate, L/s A_{floor} = dwelling-unit floor area, m^2 N_{br} = number of bedrooms (not to be less than 1) Table 4.1b (SI) Ventilation Air Requirements, L/s

Floor Area, m^2	Bedrooms				
	1	2	3	4	5
<47	14	18	21	25	28
47-93	21	24	28	31	35
93-139	28	31	35	37	42
140-186	35	38	42	45	49
186-232	42	45	49	52	56
232-279	49	52	56	59	63
279-325	56	59	63	66	70
325-372	63	66	70	73	77
372-418	70	73	77	80	84
418-465	77	80	84	87	91

3) Different Occupant Density:
Table 4.1b and Equation 4.1b assume two person in a studio or one-bedroom dwelling unit and an additional person for each additional bedroom. Where higher occupants' densities are known, the rate shall be increased by 3.5 L/s for each additional person. When approved by the authority having jurisdiction, lower occupant densities may be used.

Air leakage/ Infiltration	**ASHRAE 90.2:** The building or dwelling unit shall have a tested air leakage rate no greater than 5 ACH$_{50}$ in Climate zone 0 through 2 and no greater than 3 ACH$_{50}$ in Climate Zone 3 through 8.[Page 8] **R-2000 :** The building envelope shall be constructed sufficiently airtight such that either the air change rate at 50 Pascals is no greater than 1.5 air changes per hour. [Page 6] **GBP:** Air leakage rates: [Architectural Page 6] 1) 0.15 litre/sec/m^2 @ 75 Pa for all buildings with a low indoor air relative humidity less than 27%. Typically apply to warehouse, large volume stores, low occupant load offices, vehicle storage and repair facilities, and similar. 2) 0.1 litre/sec/m^2 @ 75 Pa for all buildings with a normal indoor air relative humidity between 27 and 55%. Typically apply to schools, community halls, health centre, libraries or higher occupant load offices. 3) 0.05 litre/sec/m^2 @ 75 Pa for all buildings with a normal indoor air relative humidity greater than 55%. Typically apply to homes, student residences, long-term care facilities and humidified of hospitals, indoor pools and spa rooms.

Heating Set-point	**NBCC :** The energy model calculation shall account the following space-heating temperature set point: [Division B 9.36.5.4] 1) 21 ˚C in all living spaces above the basement 2) 19 ˚C in basements and common spaces 3) 15 ˚C in crawl spaces intended to be conditioned spaces **ASHRAE:** Heating systems shall be equipped with controls configured to automatically restart and temporarily operate the system as required to maintain zone temperature above an adjustable heating set point at least 10 ˚F below the occupied heating set point. (= 5.55 ˚C) **R-2000 :** [Page 15] 1) Main floor heating set point : 21.0 ˚C 2) Basement set point 19.0 ˚C **GBP:** The design temperature for indoor occupied space during winter is 21 ˚C [Mechanical Page 50]
Cooling Set-point	**NBCC :** The energy model calculations shall account for a space-cooling temperature set-point of 25 ˚C in all conditioned spaces served by the cooling system [Division B 9.36.5.4] **ASHRAE:** Cooling systems shall be equipped with controls configured to automatically restart and temporarily operate the mechanical cooling system as required to maintain zone temperature below an adjustable heating set point at least 5 ℉ above the occupied cooling set point. (= 2.78 ˚C) **GBP:** The design temperature for indoor occupied space during summer is 24 ˚C [Mechanical Page 50]
Shading Schedule	**GBP:** In residential applications, curtains and blinds are provided both to control outdoor lighting and for privacy considerations. Daylight control is particularly important during the summer months when most northern communities experience 18 – 24 hours of day light for as many as four months of the year [Architectural Page 64]
Heat Recovery	**NBCC:** 1) Heat recovery ventilator with rated capacities of not less than 25L/s and not more than 200L/s. [Division B 6.3.1.4] **R-2000 :** All heat recovery ventilators (HRVs), energy recovery ventilators (ERVs), exhaust fans and kitchen range hoods shall be certified by the Home Ventilating Institute (HVI). [Page 7] **GBP:** When designing new building systems, whether heating, ventilation, and/or services, every effort should be made to incorporate energy recovery and/or control systems. [Mechanical Page 86]

[1] NBCC – Canadian Commission on Building and Fire Codes, 2015 National Building Code of Canada. Location: Zone 8 HDD > 7000

[2] NECB - Canadian Commission on Building and Fire Codes National Research Council of Canada, National Energy Code of Canada for Building 2017. Location: Zone 8

[3] ASHRAE 90 - ANSI/ASHRAE/IES Standard 90.2-2018 Energy-Efficient Design of Low-rise Residential Building. Location: Zone 8

[4] ASHREA 62 – ANI/ASHRAE Standard 62.2-2016 Ventilation and Acceptable Indoor Air Quality in Low-Rise Residential Building

[5] R-2000 – Natural Resources Canada, 2012 R-2000 Standard

[6] GBP – Department of Public Works and Services Government of the Northwest Territories, Good Building Practice for Northern Facilities 2011

Appendix B Construction cost of studied house

Table. B-1 Construction cost of envelope in details (RSMeans, 2017)

COST PER S.F.			
	MAT.	**INST.**	**TOTAL**
Wall			
1. Exterior Wall Wood Siding System			
Prefinished structural smart panel siding [1]	0.99	1.39	2.38
Air space - Wood strip, 1x3 @ 16" O.C. [2]	0.42	0.51	0.93(1.31)
Dupont home wrap Tyvek membrane [3]	0.17	0.13	0.30
Trim [4]	0.12	0.29	0.41
Paint, primer & 2 coats [5]	0.23	0.83	1.06
2. 2"x6" Wall Wood Framing System			
Sheathing - OSB [6]	0.38	0.47	0.85(1.20)
2x6 stud @ 16" O.C. [7]	0.69	0.94	1.63
Plates, 2x6, double top, single bottom [8]	0.26	0.35	0.61
Corner bracing, let-in, 1x6 [9]	0.05	0.20	0.25
with mineral fiber insulation in stud cavity [10]	1.10	0.17	1.27(1.50)
3. Gap - Insulation Filled			
Mineral fiber insulation [11] 1"	0.52	0.28	0.80(1.04)
1-1/2"	0.78	0.28	1.06(1.33)
2"	1.05	0.31	1.36(1.69)
2-1/2"	1.10	0.35	1.45(1.79)
3"	1.59	0.35	1.94(2.33)
Polyethylene air and vapor barrier [12]	0.03	0.08	0.11(0.16)
4. 2"x4" Wall Wood Framing System			
2x4 stud @ 16" O.C. [13]	0.44	0.85	1.26
Plates, 2x4, double top, single bottom [14]	0.17	0.32	0.49
Corner bracing, let-in, 1x6 [9]	0.05	0.20	0.25
with mineral fiber insulation in stud cavity [15]	0.70	0.17	0.87(1.06)
5. Interior Drywall Wall System			
1/2 in Gypsum board [16]	0.37	0.47	0.84
Finish, taped & finished joints [17]	0.05	0.47	0.52
Corner, taped & finished, 32 L.F. per 12'x12' room [18]	0.01	0.08	0.09
Painting, primer & 2 coat [19]	0.22	0.51	0.73
Trim, baseboard [20]	0.60	0.33	0.93
The cost in above system is based on the square foot of wall			
Roof/Ceiling			
1. Truss Roof Framing System			
Truss 40# loading, 16" O.C., [21] 8/12 pitch, 28' span	3.59	1.52	5.11
4/12 pitch, 28" span	2.84	1.41	4.25
Fascia board, 2x6 [22]	0.08	0.33	0.41
Sheathing - 1/2" Plywood [23]	0.92	0.89	1.81
Furring, 1x3, 16" O.C. [24]	0.46	1.34	1.80
2. Roofing System			
3/8 in Roofing shingles [25]	2.26	1.63	3.89
Drip edge, metal, 5" wide [26]	0.10	0.18	0.28
Self-sealing-membrane type eave [27]	0.08	0.10	0.18
Ridge shingles, asphalt [28]	0.10	0.06	0.16
Soffit & fascia, white painted aluminum, 1' overhang [29]	0.41	0.71	1.12
Rake trim, 1"x6" [30]	0.06	0.18	0.24
Gutter, seamless, aluminum painted [31]	0.26	0.34	0.60
Downspouts, aluminum painted [32]	0.05	0.09	0.14

3. Ceiling insulation	Equipment			
Mineral fiber insulation [33] 5.5"	0.10	0.19	0.17	0.46(0.59)
6"	0.12	0.26	0.22	0.60(0.78)
8.8"	0.16	0.33	0.30	0.79(1.04)
10"	0.20	0.38	0.36	0.94(1.25)
11.5"	0.24	0.46	0.44	1.14(1.49)
13"	0.26	0.53	0.47	1.26(1.64)
16"	0.32	0.68	0.57	1.57(2.05)
20"	0.39	0.89	0.71	1.99(2.60)
4. Interior Drywall Ceiling System				
Polyethylene air and vapor barrier [12]		0.03	0.08	0.11(0.16)
1/2 in Gypsum board [34]		0.37	0.47	0.84
Finish, taped & finished [35]		0.05	0.47	0.52
Corner, taped & finished, 12'x12' room [36]		0.04	0.32	0.36
Paint, primer & 2 coat [37]		0.22	0.51	0.73

The cost in above system is based on the square foot of plan area (ceiling area)

Floor

1. Floor system	Equipment			
Wood flooring [38]	-	5.20	1.64	6.84(8.45)
5 cm Concrete [39] 4"	0.01	1.58	0.68	2.27(2.85)
6"	0.01	2.30	0.69	3(3.67)
Polyethylene air and vapor barrier [12]	-	0.03	0.08	0.11(0.16)
SIPs [40] 3 5/8"	0.28	3.65	0.62	4.55(5.35)
5 5/8"	0.33	4.10	0.74	5.17(6.10)
7 3/8"	0.40	4.45	0.90	5.75(6.85)
9 3/8"	0.51	4.75	1.14	6.40(7.70)

The cost in above system is based on the square foot of floor

Window

			COST PER UNITE	
1. Window Openings	Unit			
Headers, 2"x6" double [41]	L.F.	0.69	2.60	3.29
2. Casement Window System				
Window, 8'-6"x5' [42]	Ea.	675	160	835(1000)
Window frame	L.F.	4.13	-	4.13(4.54)
Trim, interior casing [43]	L.F.	1.54	2.36	4.32
Print, interior & exterior, primer & 2 coat [44]	Face	1.36	43	44.36
Caulking [45]	L.F.	0.25	1.63	1.88
Snap-in grille, 20"x56" [46]	Ea.	51	14.60	65.60
Drip cap, metal [47]	L.F.	0.63	1.17	1.80

The cost in above system is based on the quantity and dimension of window

Other Material

Shading [48]	S.F.	6.70	3.29	9.99(12.90)

* The price with under line is the bared cost of material and labor, the total value in brackets is the total cost with bare cost plus overhead and profit. And if the price provide in standard is not in per square foot, then it changed to the price per square foot, except the window part, window part still remain as the cost per unit.

[1] Page 163 - Southern yellow pine, 3/8" thick
[2] Page 380 - Wood strip, 1"x3", on walls, on wood
[3] Page 162 - Building wrap, spunbonded polypropylene
[4] Page 163 - Trim, White pine
[5] Page 163 - Painting, primer, & 2 coat
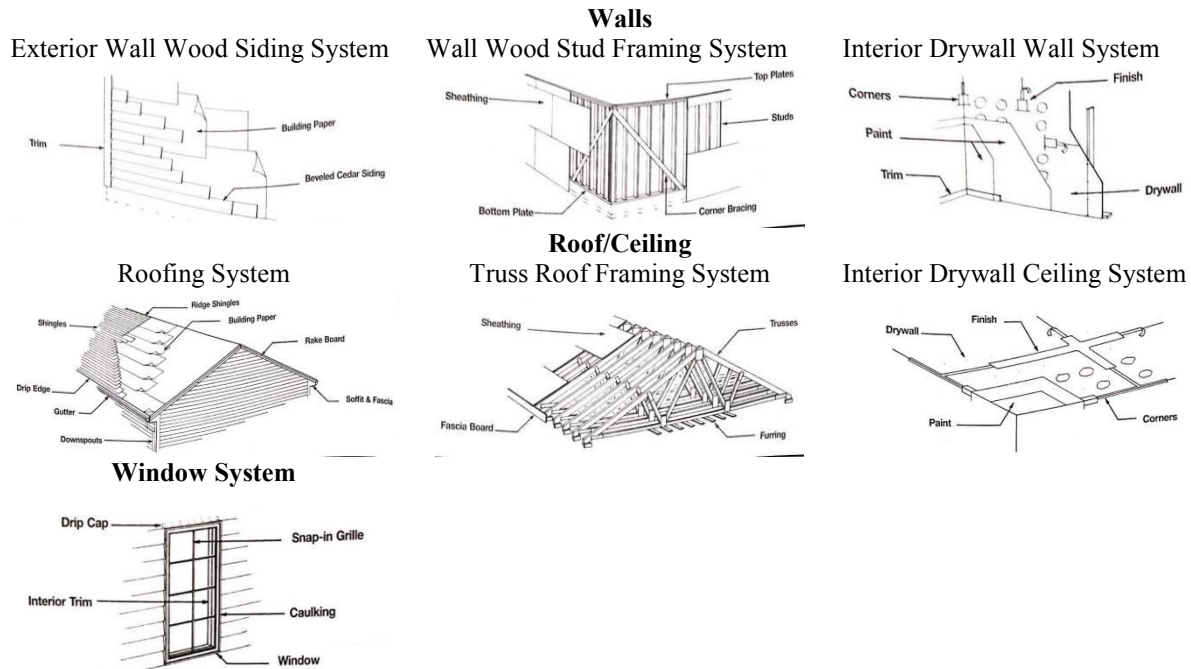[6] Page 386 - Orientated stand board, on wall, 1/2" thick
[7] Page 137 - Studs, #2 or better, 2"x6", 16" O.C.
[8] Page 137 - Pates, #2 or better, double top, single bottom, 2"x6"
[9] Page 137 - Corner bracing, let-in 1"x6" boards, studs, 16" O.C.
[10] Page 419 - Blanket Insulation for Walls - Wall or ceiling insulation, mineral wool batts 5 1/2" thick

[11] Page 418 - Rigid Insulation - Fiberglass, 3#/C.F., unfaced, 1" thick, R4.3; 1-1/2" thick, R6.5; 2" thick, R8.7; 2-1/2" thick, R10.9; 3" thick, R13

[12] Page 424 - Polyethylene vapor barrier, standard, 0.004" thick

[13] Page 137 - Studs, #2 or better, 2"x4", 16" O.C.

[14] Page 137 - Pates, #2 or better, double top, single bottom, 2"x4"

[15] Page 419 - Blanket Insulation for Walls - Wall or ceiling insulation, mineral wool batts 3 1/2" thick

[16] Page 215 - Gypsum wallboard, 1/2" thick standard

[17] Page 215 - Gypsum wallboard, taped & finished

[18] Page 215 - Gypsum wallboard corners, taped & finished, 32 L.F. per 12'x12' room

[19] Page 215 - Painting, primer & 2 coat

[20] Page 215 - Trim, painted or stained, baseboard

[21] Page 141 - Truss 40# loading, including 1' overhang, 8/12 pitch, 28' span, 16" O.C; 4/12 pitch, 28' span, 16" O.C.

[22] Page 141 - Fascia board, #2 or better, 2"x6"

[23] Page 141 - Sheathing, plywood CDX, 8/12 pitch, 1/2" thick

[24] Page 141 - Furring, 1"x3", 16" O.C.

[25] Page 195 - Shingles, asphalt, inorganic, Premium laminated, multi-layered, 260-300 lb./sq., 8/12 pitch

[26] Page 195 - Drip edge, metal, 5" wide

[27] Page 195 - Building paper, #15 asphalt felt

[28] Page 195 - Ridge shingles, asphalt

[29] Page 195 - Soffit & fascia, aluminum, vented, 1' overhang

[30] Page 195 - Rake trim, 1"x6"

[31] Page 195 - Gutter, 5" box, aluminum, seamless, painted

[32] Page 195 - Downspouts, 2"x3", aluminum, one story house

[33] Page 420 - Blown Insulation - Fiberglass, 5.5" thick, R11; 6" thick, R12; 8.8" thick, R19; 10" thick, R22; 11.5" thick, R26; 13" thick, R30; 16" thick, R38; 20" thick, R49

[34] Page 217 - Gypsum wallboard ceilings, 1/2" thick standard

[35] Page 217 - Gypsum wallboard ceilings, taped & finished

[36] Page 217 - Corners, taped & finished, 12'x12' room

[37] Page 217 - Painting, primer & 2 coat

[38] Page 499 – Prefinished, white oak, prime grade, 2-1/4" wide

[39] Page 315 - Slab on grade (3500 psi), incl. troweled finish, not incl. forms or reinforcing, over 10,000 S.F., 4" thick; 6" thick

[40] Page 381 - Structural insulated panels - 7/16" OSB both faces, EPS insul, 3 5/8" thick; 5 5/8" thick; 7 3/8" thick; 9 3/8" thick

[41] Page 137 - Headers, 2"x6" double, 2' long

[42] Page 463 - Wood sash (including glazing but not trim) - 8'-6"x5' high, 1" thick, triple glazed

[43] Page 173 - Trim, interior casing, window 2'x4'

[44] Page 173 - Paint or stain, interior or exterior, 2'x3' window, primer & 2 coat

[45] Page 173 - Caulking, window 2'x3'

[46] Page 173 - Grills, glass size, to 20"x56"

[47] Page 173 - Drip cap, metal, 2' long

[48] Page 535 - Shades - Solar screening, fiberglass

Walls

Exterior Wall Wood Siding System	Wall Wood Stud Framing System	Interior Drywall Wall System

Roof/Ceiling

Roofing System	Truss Roof Framing System	Interior Drywall Ceiling System

Window System

*Figures all from Rsmeans Residential Cost Data (RSMeans, 2017)

Figure. B-1 the envelope system illustration

Table. B-2 Location factors of city in Canada list in RSMeans reference book (RSMeans, 2017)

Yellowknife (NT)	Montreal (QC)	Toronto (ON)	Whitehorse (YT)
1.13	1.05	1.10	1.04

Table. B-3 The modified parameter value in the algorithm

Wall insulation thickness	Ceiling insulation thickness	Floor insulation thickness	Window width	Window height	Floor concrete thickness	Walls gypsum board layers
X_1	X_2	X_3	X_4	X_5	X_6	X_7

Table. B-4 The area of each construction part (m^2)

Wall Framing area	Wall exterior area	Wall interior area	Roof/Ceiling area	Floor area	Window area
118.33	$143.36 - X_4 \times X_5$	$118.33 - X_4 \times X_5$	130	130	$X_4 \times X_5$

The Total Construction Cost is:

C_{total} = Location factor × [Walls (frame + exterior facade + interior finish + gap insulation)

+ Roof/Ceiling (Roof truss + interior finish + Roofing + Ceiling insulation)

+ Floor (Concrete + SIP) + Window

= 1.13 ×   - Location factor
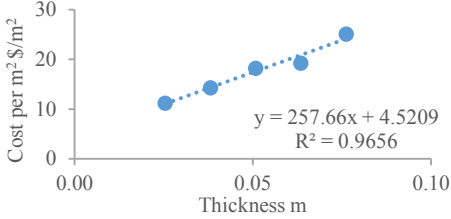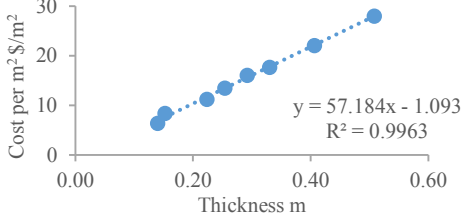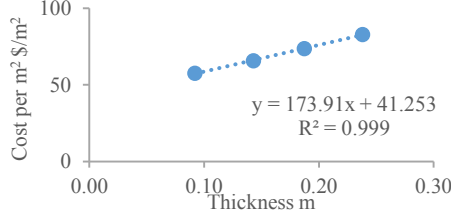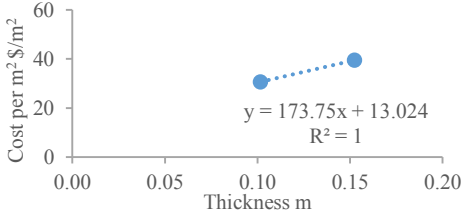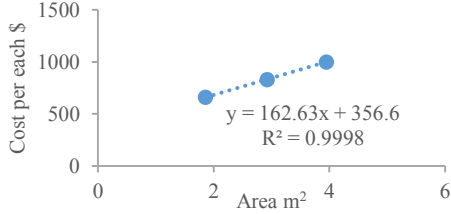
$[10497.02+58.71×(143.36–X_4×X_5)+(9.03×X_7+26.13+F(X_1))×(118.33–X_4×X_5)$ - Wall part

+ $(192.69 + F(X_2+0.2858)) × 130$ - Ceiling part

+ $(1.72 + F(X_6) + F(X_3)) × 130$ - Floor part

$+F(X_6,X_7) +91.11×(X_4×X_5)+88.72+27.49×X_4+35.24×2×(X_4+X_5)]$ - Window part

Table. B-5 The function of modified insulation cost

Cost of walls insulation	Cost of ceiling insulation
$F(X_1) = 257.66X_1 + 4.52$	$F(X_2) = 57.18X_2 − 1.09$
Cost of floor insulation	**Cost of window**
$F(X_3) = 173.91(X_3+0.0254)+41.25$	$F(X_6) = 173.75X_6 + 13.02$
Cost of window	
$F(X_4,X_5) = 162.63X_4X_5+356.6$	

The Utility Fees/Operation Cost is:

U = energy consumption (simulation output) × energy price

Table. B-6 Energy price in Yellowknife (NWT)

Electricity (NWT Rate Schedule, 2019)	Gas (Energy Facts, 2012)	Fuel oil - regular gasoline (NRC)
29.81 ₵/kWh	37 $/GJ = 13.3 ₵/kWh	136.4 ₵/Liter = 14.5 ₵/kWh

Table. B-7 Energy price in Kuujjuaq (QC)

Electricity (Hydro Quebec, 2019)	Fuel oil - gasoline (Makivik Corporation. 2018)
6.08 ₵/kWh	2.03 $/Liter = 21.7 ₵/kWh

Appendix C   The calculation and explanation of add-on costs in Kuujjuaq to support labor working in the north

Table. C-1 Information about the location factors and local cost of the studied house

	Calculated construction cost range – the reference house based on code*	Construction cost presents in Altus Group (2017)	HDD (2018) (CWS, 2019)
	Total $/m^2	Total $/m^2	
US national average	514.76	-	-
Montreal (QC)	540.50	969-1,238	4,356
Kuujjuaq (AC)	2,500-4,200	-	8,888
Iqaluit (NU)	-	2,713-5,167	9,950
Yellowknife (NT)	581.68	1,921-3,660	8,140
Remote communities	-	3,108-5,920	-
	Note: construction only includes the envelope part, without considering the site work, foundation, mechanical, electrical, etc. According to the RSMeans single-story house example, the envelope takes around 60% of the total construction cost. The cost in Yellowknife is 652.55 $/m^2 by using the location factor given in RSMeans. Location factors: Montreal (1.05); Yellowknife (1.13)	City Index: Refer to cost in GTA as 100 Yellowknife:170 Iqaluit: 240 Remote Communities: 275 other northern big cities/areas use the index as Iqaluit	

*the reference house based on code is the reference house presented in Chapter 3

The US national average condtruction cost is calculated based on the cost in RSMeans (2017) and follows the envelope detail set-up in EnergyPlus. Then the cost in Montreal is converted using the location factor (1.05) from RSMeans. The result is a basic cost for calculating construction costs in northern cities.

Costs in northern cities are converted using the city index given by Canadian Cost Guide – Altus Group (2017). As the construction cost for Montreal provided by Altus Group is 969-1,238 $/m^2, compared to a cost calculated by RSMeans of 606/0.6 = 1,010 $/m^2, a preliminary conclusion could be that the two references provide similar cost values.

Calculations based on RSMeans include only the cost of constructing the envelope. The total construction cost, however, is presented in the Canadian Cost Guide and other documents, which also includes the site work, mechanical, electrical, and so on. As these costs remain the same in a given location, they will not influence the optimization results, thus they are excluded during the calculations. Based on the single-story house example in RSMeans, the cost for the envelope accounts for approximately 60% of the total construction cost.

When building a house in the north, the construction cost includes not only the material cost and labor cost, as in the south, but also includes high logistics expenses. As the north lacks skilled labor, all laborers come from the south, and their travel, food and lodging fees account for a large portion of the total cost.

As a reference cost provided by Housing in Nunavik (SHQ, 2014), in 2008, a house with approximately 98 m^2 cost almost \$345,000, which is 3,520 \$/m^2. As the average inflation rate for the last 10 years is 1.6% (Canada infiltration rate, 2019), converting this cost for 2017 makes it around 4,061 \$/m^2. Combining this with the range of 5,000-7,000 \$/m^2 provided by Daniel Baril, who has experience with construction costs in Kuujjuaq, the total construction cost in Kuujjuaq (Nunavik) is 4,100-7,000 \$/m^2.

The cost of supporting laborers from the south to work in the north remains roughly the same whether they are building a high-performance building or a general building based on the code. A basic house is used to calculate the logistic fees for labor working in the northern area. This basic house has the envelope thermal resistance following the Good Building Practice for the Northern Facilities, which has R-value similar to the reference house presented in Housing in Nunavik,

The construction cost of a building that meets the GBP envelope standard in Kuujjuaq, calculated using the city index (240) presented in Altus Group, is 1,297.20 \$/m^2 (540.50 \$/m$^2 \times 2.4 = 1,297.20$ \$/m^2; 1,297.20 \$/m^2/0.6 = 2,162 \$/m^2), which is still lower than the reference range of 4,100-7,000 \$/m^2. Excluding the material cost and the construction labor cost – primarily the salaries paid to the laborers – the remaining portion of 1,200-2,900 \$/m^2 is the range of costs for the logistics for laborers. During the optimization, the median cost value, 2,100 \$/m^2, is used. Costs in other cities are calculated using the same method (4,100 $\times$ 0.6 - 1,297.20 $\approx$ 1200 \$/m^2; 7,000 * 0.6 - 1,297.20 $\approx$ 2900 \$/m^2).

The construction cost is calculated based on RSMeans and converted to the studied city by first converting the cost to a Montreal cost using the location factor and then multiplying by the city index to convert the cost from Montreal to a given northern city. The logistics cost calculated in the previous paragraph is then added to get the total construction cost.

Appendix D   BIPV/T Matlab code discussion

There are four factors studied in the BIPV/T Matlab code that might influence the outputs: time step, Nusselt number correlations, exterior convection coefficient and control volume of panels.

The case used to compare factors uses one array of PV panels, which is 4.8 m², with the cavity height at 0.5 m and the airflow rate at 0.027 m³/s.

1. Compare BIPV/T outputs with time step in hourly and every 10 minutes

For the two time-step models, the weather data for the models is extracted from EnergyPlus weather file separately for 1-hour steps and 10-minute steps, which means the 10-minute data is not based on a linear interpolation from hourly data.

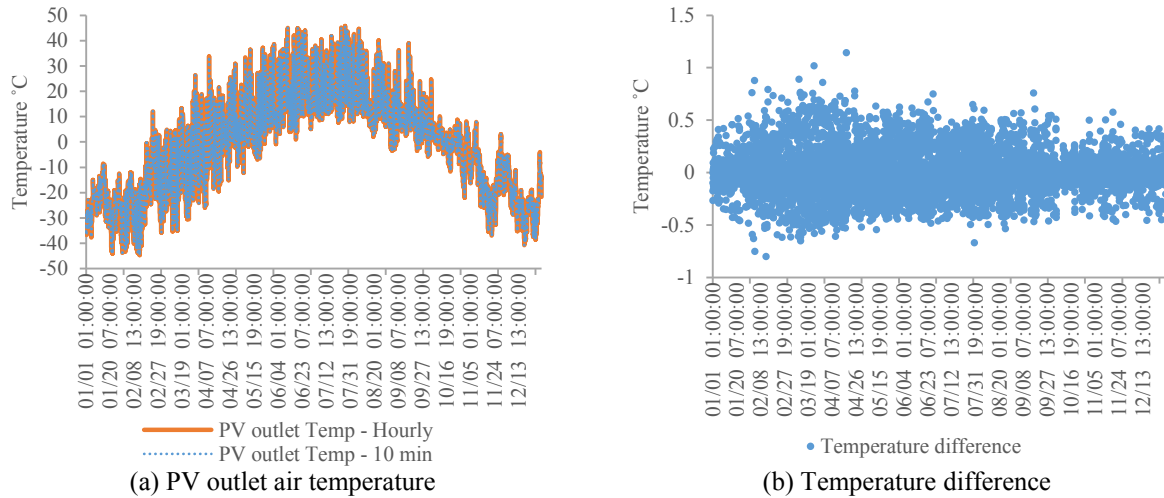(a) PV outlet air temperature   (b) Temperature difference
Figure. D-1 BIPV/T temperature outputs by Matlab under hourly and every 10 min time steps

Figure. D-1 (a) shows that the graphs of the output temperature in hourly time steps and 10-minute time steps overlap with each other throughout the year. When it comes to the temperature difference between the two time steps, Figure. D-1 (b) shows that the temperature difference is within 1 ˚C, and most often is less than 0.5 ˚C. This implies that the time step chosen for this BIPV/T calculation does not make a significant difference in the outputs. Furthermore, the efficiencies for PV panels show in Table. D-1 are the same for both time-step models.

Table. D-1 BIPV/T panels efficiency in hourly and 10 min time steps

	Thermal efficiency	Electric efficiency	Exterior heat loss efficiency
Hourly	0.102	0.153	0.701
10 min	0.102	0.153	0.701

2. Compare BIPV/T outputs with average and local Nusselt number correlations

Average Nusselt number on both surfaces:

$$Nu_{pv} = 0.052 \cdot Re^{0.78} \cdot Pr^{0.4} \quad 250 \leq Re \leq 7{,}500$$

$$Nu_{bot} = 1.017 \cdot Re^{0.471} \cdot Pr^{0.4} \quad 800 \leq Re \leq 7{,}100$$

Local Nusselt number on both surfaces:

$$Nu_{pv} = 8.188 \cdot Re^{0.77} \cdot Pr^{3.85} \cdot e^{-\frac{x^{0.2}}{2.8 \cdot D_h}} + 0.061 \cdot Re^{0.77} \cdot Pr^{3.85} \quad 2{,}300 < Re < 9{,}500$$

$$Nu_{bot} = 4.02 \cdot Re^{1.09} \cdot Pr^{19.3} \cdot e^{-\frac{x^{0.2}}{14 \cdot D_h}} + 0.005 \cdot Re^{1.09} \cdot Pr^{19.3} \quad 2{,}300 < Re < 9{,}500$$

Under the average Nusselt number correlations, the Nu remains the same along the PV panels. When using local Nusselt number correlations, the Nu changed alone the cavity. The controlled section is set as 0.1 m and in each section the Nu remains constant and refers to the value calculated by the middle point of the section.

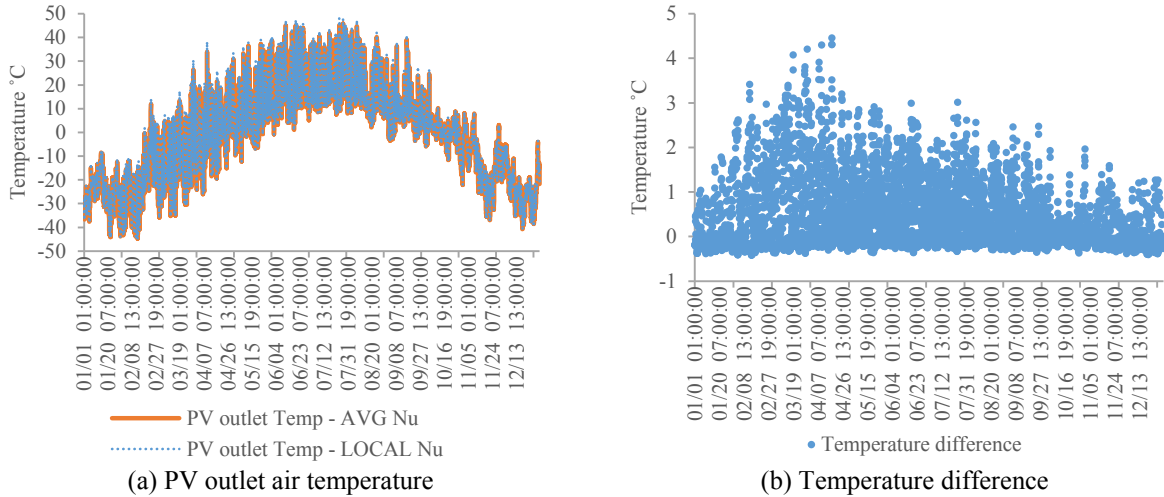(a) PV outlet air temperature   (b) Temperature difference
Figure. D-2 BIPV/T temperature outputs by Matlab under average and local Nusselt number correlations

Figure. D-2 (a) shows that the graphs of the output temperature by average and local Nu correlations almost overlap with each other throughout the year. When it comes to the temperature difference between two kinds of correlations, Figure. D-2 (b) shows that the temperature difference

is less than 5 ˚C, which indicates that at some points there is a significant temperature difference between the two types of correlations. The number of hours for each temperature difference are shown in Table. D-2. For more than 96% of the year, the temperature difference between the two correlations is less than 2 ˚C. Table. D-3 shows that the case with local Nu correlations has a slightly higher thermal efficiency and a slightly lower exterior heat loss efficiency. This is because the local Nu correlations give a somewhat higher value at the entrance and then decrease sharply before become flat along the cavity, as shown in Figure. D-3, which graphs the curves for average and local Nu at the top surface with the air at 20 ˚C and the Reynolds number in the cavity at 3,142. With a higher Nu value at the section right after the entrance, namely a higher convection coefficient, a larger amount of heat would transfer from the PV panels to the cavity air, contributing to a relatively higher thermal efficiency under local Nu correlations.

Table. D-2 Hours at each temperature difference between average and local Nusselt number correlations

Hours that temperature difference less than	1˚C	2˚C	3˚C	4˚C	5˚C
Value [hr]	7,543	8,488	8,716	8,754	8,760
%	86.11	96.89	99.50	99.93	100
Hours that temperature difference between	0-1˚C	1-2˚C	2-3˚C	3-4˚C	4-5˚C
Value [hr]	7,543	945	228	38	6
%	86.11	10.79	2.60	0.43	0.07

Table. D-3 BIPV/T panels efficiency in average and local Nusselt number correlations

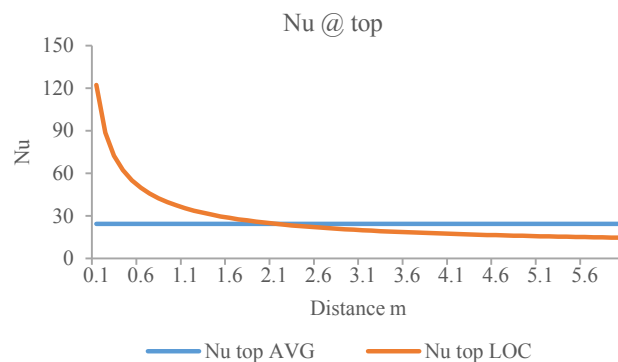|	Thermal efficiency	Electric efficiency	Exterior heat loss efficiency
AVG	0.102	0.153	0.701
LOCAL	0.113	0.153	0.690

Figure. D-3 Local and average Nu correlation curves

3. Compare BIPV/T outputs with different exterior air film convection coefficient correlations

The different exterior convection coefficient correlations are shown as follows. All the results from different correlations are compared with the first one – the reference equations for exterior convection from EnergyPlus engineering reference. The values for D, E and F in the correlations are listed in the table at right also refer to Table 4-3.

1. $h_o = D + EV_{wind} + FV_{wind}^2$	
2. $h_o = 8.55 + 2.56V_{wind}$	
3. $h_o = 11.9 + 2.2V_{wind}$	
4. $h_o = 5.7 + 3.8V_{wind}$	

Roughness Index	D	E	F	Example material
1 (Very Rough)	11.58	5.894	0.0	Stucco
2 (Rough)	12.49	4.065	0.028	Brick
3 (Medium Rough)	10.79	4.192	0.0	Concrete
4 (Medium Smooth)	8.23	4.0	-0.057	Clear pine
5 (Smooth)	10.22	3.1	0.0	Smooth Plaster
6 (Very Smooth)	8.23	3.33	-0.036	Glass

As shown in Figure. D-4, the wind speed on the south-facing roof through the year is mostly between 0.5 m/s and 2 m/s. Within this range, correlation 3 gives the highest convection coefficient, and correlation 4 gives the lowest. The largest exterior convection coefficient leads to a large portion of the heat loss to the environment. A large heat loss to the environment lowers the panel temperature, although it increases the panel electricity generation efficiency, and the left portion of thermal transfer to the air becomes smaller. Thus, as Table. D-4 shows, the model with correlation 3 has the highest exterior heat loss efficiency and electricity efficiency, while it has the thermal efficiency.
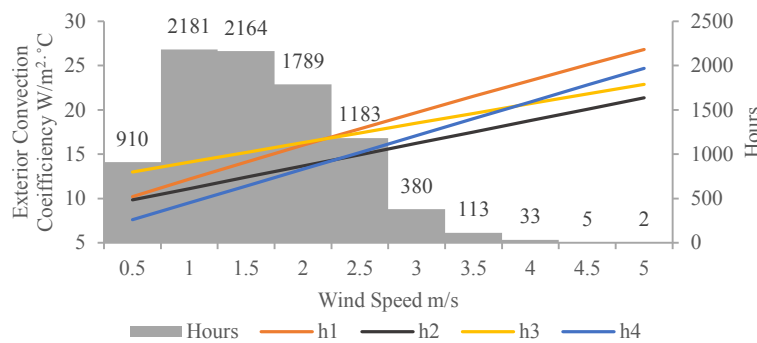

Figure. D-4 Figure of four exterior convection coefficient correlations

Table. D-4 BIPV/T panels efficiency in four exterior convection correlations

	Thermal efficiency	Electric efficiency	Exterior heat loss efficiency
1	0.102	0.153	0.701
2	0.110	0.152	0.694
3	0.098	0.153	0.704
4	0.114	0.152	0.689

132

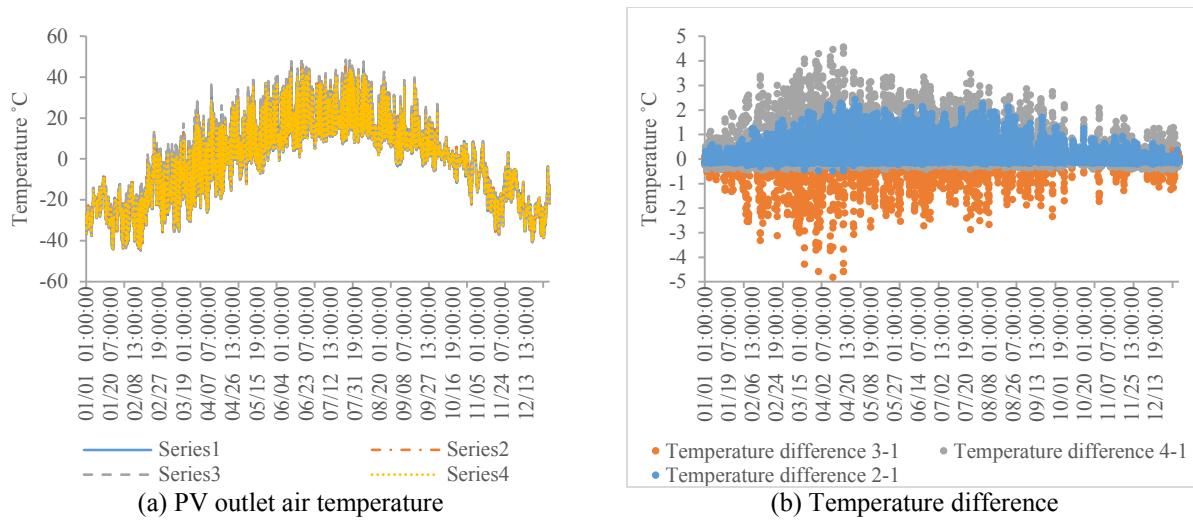(a) PV outlet air temperature　　　　　(b) Temperature difference

Figure. D-5 BIPV/T temperature outputs by Matlab under different exterior air film convection coefficient correlations

Figure. D-5 (a) shows that the output temperatures from different exterior air film convection coefficient correlations are similar to each other throughout the year. When it comes to the temperature differences between correlation 1 and correlations 2, 3 or 4, Figure. D-5 (b) shows that the temperature difference is between -5 ˚C and 5 ˚C. The temperatures of correlations 1 and 2 are quite similar to each other. The temperature calculated by correlation 4 is generally higher than that of correlation 1, while the temperature calculated by correlation 3 is generally lower than that of correlation 1.

Table. D-5 Hours at each temperature difference for different exterior air film convection coefficient correlations

Hours that temperature difference less than [hr(%)]	1˚C	2˚C	3˚C	4˚C	5˚C
Correlation 2-1	8,103 (92.50)	8,729 (99.65)	8,760 (100)		
Correlation 3-1	8,308 (94.84)	8,636 (98.58)	8,740 (99.77)	8,754 (99.93)	8,760 (100)
Correlation 4-1	7,333 (83.71)	8,274 (94.45)	8,672 (99.00)	8,753 (99.92)	8,760 (100)
Hours that temperature difference between [hr(%)]	0-1˚C	1-2˚C	2-3˚C	3-4˚C	4-5˚C
Correlation 2-1	8,103 (92.50)	626 (7.15)	31 (0.35)		
Correlation 3-1	8,308 (94.84)	328 (3.74)	104 (1.19)	14 (0.16)	6 (0.07)
Correlation 4-1	7,333 (83.71)	941 (10.74)	398 (4.54)	81 (0.92)	7 (0.08)

The counts of hours representing each temperature difference are shown in Table. D-5, Although the temperature difference is as high as 5 ˚C at certain times, for most of the year the temperature

difference is less 2 ˚C. Comparing correlation 2 with correlation 1, 99.7% of the time the temperature difference is less than 2 ˚C, and when comparing correlation 1 to correlation 3 and correlation 4, this value becomes 98.6% and 94.5%, respectively.

4. Compare BIPV/T outputs with different control volume of panels

Dividing panels into different control volumes is considering the PV surface temperature differently. As Figure. D-6 shows, when under one control volume, the air temperatures inside the cavities are calculated by each small section, while the temperature at the PV surface is considered as one constant temperature within each time step. When moving to the multi-control-volume for panels, the PV surface temperature varies in each control volume in one time step, which is a more realistic situation. In a realistic situation, the air is colder at the entrance and can absorb much heat from the panels and cool down the panel surface. After the heat exchange along the cavity, the air is warmed at the outlet, which means the heat exchange between the air and the panel surface is less, which leads to the panel surface temperature remaining higher near the outlet.
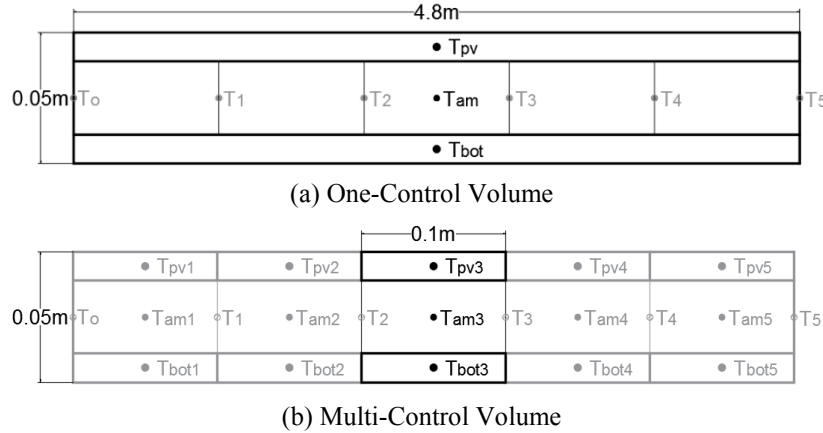

(a) One-Control Volume

(b) Multi-Control Volume
Figure. D-6 Illustration of control volume for PV panels

Evenly dividing the panels into sections to vary the surface temperature within time steps, the Nu correlations, especially the local Nu correlations, introduced above are also related to the control volume separation. Hence, two types of correlations are studied separately to show the influence of control volume in the panels.

4.1 Use average Nu correlations in different panel control volume cases

Average Nusselt number on both surfaces:

$$Nu_{pv} = 0.052 \cdot Re^{0.78} \cdot Pr^{0.4} \quad 250 \leq Re \leq 7{,}500$$

$$Nu_{bot} = 1.017 \cdot Re^{0.471} \cdot Pr^{0.4} \quad 800 \leq Re \leq 7{,}100$$

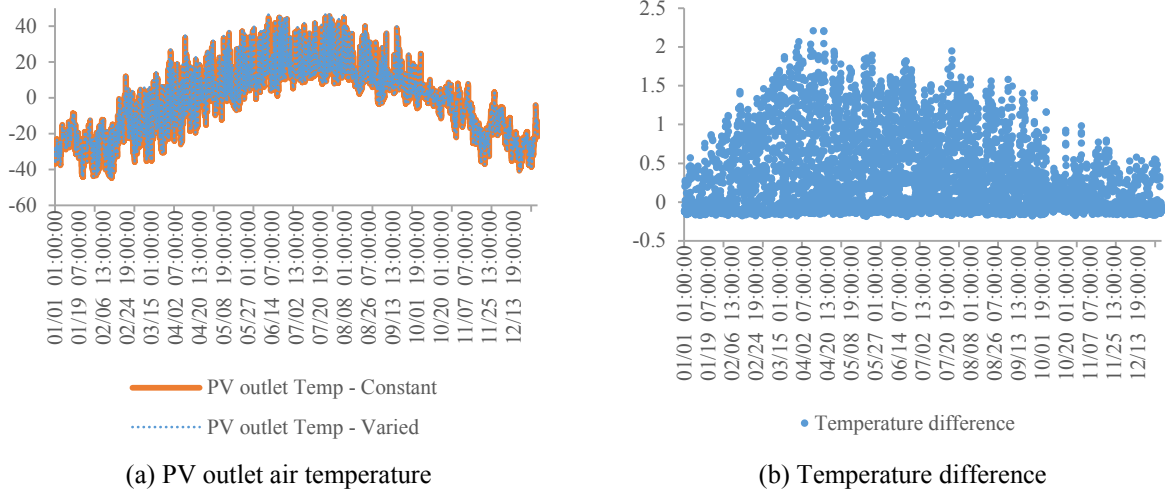(a) PV outlet air temperature　　　　　　(b) Temperature difference

Figure. D-7 BIPV/T temperature outputs by Matlab under different control volumes in panels (avg Nu correlations)

Figure. D-7 (a) shows that the output temperatures of different PV panel control volume cases using average Nu correlations are much the same throughout the year. When it comes to the temperature difference between two models, Figure. D-7 (b) shows that the difference is less than 2.5 ˚C; during the majority of the year, the temperature difference is less than 1 ˚C, as shown in Table. D-6.

Table. D-6 Hours at each temperature difference between different control volumes in panels (avg Nu correlations)

Hours that temperature difference less than	1 ˚C	2˚C	3˚C
Value [hr]	7,987	8,753	8,760
%	91.18	99.92	100
Hours that temperature difference between	0-1˚C	1-2˚C	2-3˚C
Value [hr]	7,987	766	7
%	91.18	8.74	0.08

As Table. D-6 shows, when using the Nu average correlations, the case of the panel with multi-control-volume gives higher thermal efficiency and lower heat-loss efficiency. One hour of temperature data is captured in Figure. D-8 to illustrate how the panel control volume number influences the efficiency. The weather condition data for this one-hour simulation is taken from

135

noon on March 25th in the EnergyPlus weather data file, with the ambient air temperature at -16.59 ˚C and the incident solar radiation on the south-facing roof at 918 W/m².

Table. D-7 BIPV/T panels efficiency in different control volumes in panels (avg Nu correlations)

	Thermal efficiency	Electric efficiency	Exterior heat loss efficiency
One CV	0.102	0.153	0.701
Multi-CV	0.110	0.152	0.694

In the case of the panel with one control volume, within a one-hour time step, the temperature at the PV surface and the bottom surface are constant, which leads to the temperature difference between surfaces and cavity air being larger at the entrance and smaller at the outlet. As the Nu number does not change along the cavity, as indicated by the Nu average correlation, the heat convection coefficients between surfaces and cavity air are kept the same in one time-step. The cavity air absorbs a large amount of heat from the PV surface at the entrance, and heat flux from the PV surface to the cavity air becomes less as the air moves further along the cavity. Therefore, the cavity air temperature rises quickly at first, and when it reaches the end of the cavity the speed of temperature rise is quite slow. Additionally, the constant bottom surface temperature contributes to the cavity air temperature's change pattern, as at the entrance the bottom surface has a higher temperature and heats up the air; after the cavity air becomes warmer, the bottom surface temperature is lower than the air, and the surface extracts heat from the air.

In the case of the panel with multi-control-volume, within a one-hour time step, the temperature at the PV surface and the bottom surface vary in sections – namely, the control volumes. The PV surface temperature is lower at the inlet and higher at the outlet. Compared with the PV surface temperature in the one-CV case – Tp – 1-CV, shown by the solid orange line – the PV surface temperature in the multi-CV case – Tp – multi-CV, shown by the dashed orange line – is lower in first half of the cavity and higher in the latter part of the cavity, which leads to cavity air in the multi-CV case capturing less heat than the in the one-CV case in the first part of the cavity and receiving more heat in the second part of the cavity. As the red dashed line shows, it rises more steadily. Likewise, the bottom surface temperature also changes from a lower point at the entrance to a higher temperature at the outlet. Unlike the bottom surface temperature in the one-CV case – Tb – 1-CV, shown by the solid blue line – this bottom surface temperature – Tb – multi-CV, shown by the dashed blue line – is always higher than the cavity air temperature, which means it will not affect the air temperature change pattern, as it does in the one-CV case. Comparing the results of

the cavity air outlet temperature shows that the one in the multi-CV case is higher than the one in one-CV case – 4.2 ˚C compared with 2.8 ˚C. Thus the multi-CV case provides a slightly higher thermal efficiency.
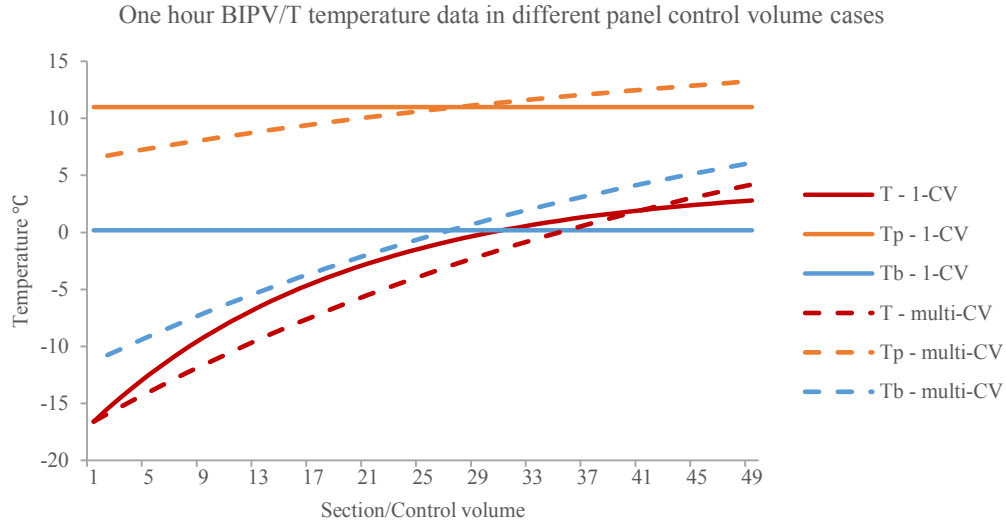

Figure. D-8 One hour BIPV/T temperature data in different panel control volume cases (average Nu correlations)
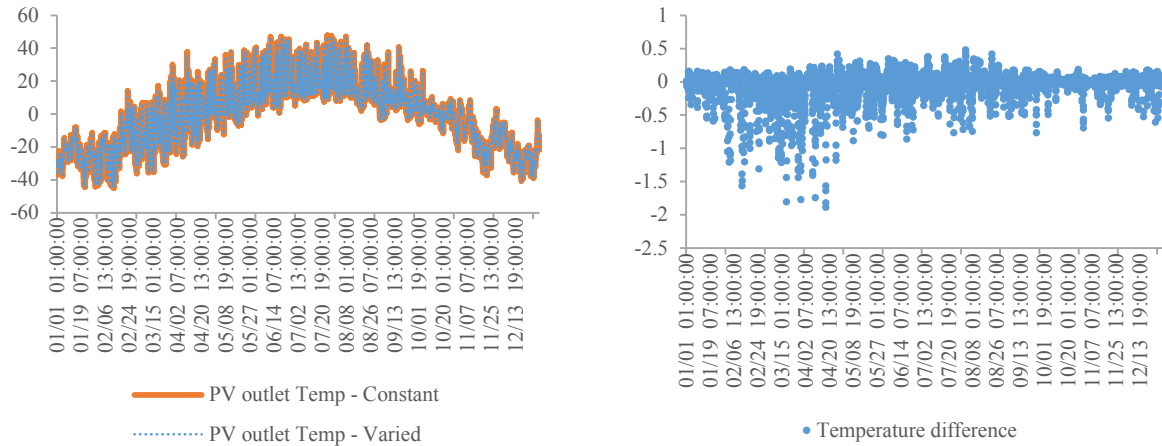
4.2 Use local Nu correlations in different panel control volume cases

Local Nusselt number on both surfaces:

$$Nu_{pv} = 8.188 \cdot Re^{0.77} \cdot Pr^{3.85} \cdot e^{-\frac{x^{0.2}}{2.8 \cdot D_h}} + 0.061 \cdot Re^{0.77} \cdot Pr^{3.85} \quad 2{,}300 < Re < 9{,}500$$

$$Nu_{bot} = 4.02 \cdot Re^{1.09} \cdot Pr^{19.3} \cdot e^{-\frac{x^{0.2}}{14 \cdot D_h}} + 0.005 \cdot Re^{1.09} \cdot Pr^{19.3} \quad 2{,}300 < Re < 9{,}500$$

Figure. D-9 (a) shows that the output temperature of the separate control volumes for PV panels using local Nu correlations are much the same throughout the year. When it comes to the temperature difference between the two models, Figure. D-9 (b) shows that the temperature difference is less than 2 ˚C. During most of year, the temperature difference is less than 1 ˚C, as shown in Table. D-8. Compared to the temperature differences seen when using average Nu correlations (Figure. D-7 (b)) the outlet air temperature is less influenced by dividing the PV panels into smaller control volumes when local Nu correlations are used. The obvious temperature differences occur in February, March and April.

| (a) PV outlet air temperature | (b) Temperature difference |

Figure. D-9 BIPV/T temperature outputs by Matlab under different control volume in panels (local Nu correlations)

Table. D-8 Hours at each temperature difference between different control volumes in panels (local Nu correlations)

Hours that temperature difference less than	1 ˚C	2˚C
Value [hr]	8713	8760
%	99.46	100
Hours that temperature difference between	0-1˚C	1-2 C
Value [hr]	8713	47
%	99.46	0.54

Table. D-9 BIPV/T panels efficiency in different control volumes in panels (local Nu correlations)

	Thermal efficiency	Electric efficiency	Exterior heat loss efficiency
Constant	0.113	0.153	0.690
Varied in Sections	0.112	0.152	0.692

138

Appendix E   Reviewed optimization papers

Table. E-1 The summary of reviewed building optimization papers

Year/ Author	Building Location	Algorithm	Building Performance Software	Optimization Tools	Objective Functions	Studied Parameters
2009 Hamdy et al.	Jyväskylä (Finland)	PR-GA, GA-RF, GA	IDA ICE 3.0	Matlab	●Energy Consumption ●Initial Investment Cost	(Variable No.: 5) ●Insulation thickness of wall, ceiling and floor ●U-value of window ●Heat recovery efficiency
2009 Palonen et al.	N/A	GA, GA+Hooke−Jeeves	IDA ICE 3.0	Genopt 2.0	●Life Cycle Cost	(Variable No.: 5) ●Additional insulation thickness of wall, roof and floor ●Window type ●Heat recovery type
2009 Pernodet et al.	Trappes (France) Agen (France)	GA	Trnsys	Real-Coded Genetic Algorithm, GenetikSol ver V4.1 by Turkkan	●Energy Consumption ●Investment Cost of Refurbishment ● Economic Global Cost	(Variable No.: 8) ●Thermal resistance of walls, roof and windows ●Glazing ratio ●Solar factor of window ●Airtightness ●Artificial lighting power ●Lighting regulation [Switch, occupancy sensor, daylight sensor]
2010 Magnier et Haghighat	Campus of National Research Council Canada, Ottawa[1] (Canada)	ANN, NSGA-II	Trnsys	GenOpt	●Thermal Comfort ●Energy Consumption	(Variable No.: 12) ●Setpoint of heating and cooling temperature and RH ●Starting and stopping delay time ●Supply airflow rate ●Window area on 1st floor north and south, and 2nd floor north, south-east and southwest ●Thickness of concrete
2010 Tuhus-Dubrow et Krarti	Boulder, CO (USA) Phoenix, AZ (USA) Chicago, IL (USA) Miami, FL (USA) San Francisco, CA (USA)	GA, PSO	DOE-2	Matlab	●Life Cycle Cost	(Variable No.: 9) ●Building shape and orientation ●Insulation level in walls, roof and foundation ●Window type and area ●Air leakage level ●Thermal mass - ceiling drywall thickness

2011 Chantrelle et al.	Nice (France)	NSGA-II	Trnsys	MultiOpt	●Environment Impact ●Investment Cost ●Energy Consumption ●Thermal Comfort	(Variable No.: 6) ●Different envelope type of exterior walls, ground floor, roof, intermediate floor, internal partitions wall and window
2011 Shi	Nanjing (China)	MOGA	EnergyPlus	modeFRONTIER	●Life-cycle Cost ●Life-cycle Environmental Impact	(Variable No.: 6) ●Thermal insulation thickness on six different orientation walls
2012 Asadi et al.	Central region of Portugal (Portugal)	MOO	Matlab	Tchebychff programming technique	●Energy Saving ●Retrofit Cost	(Variable No.: 4) ●Window type ●Insulation material type of exterior wall and roof ● Solar collector type
2013 Carlucci et al.	Mascalucia (Italy)	PSO	EnergyPlus	GenOpt	●Seasonal thermal discomfort	(Variable No.: 7) ●Different construction type for walls, floor and roof ●Different construction type for windows ●Shading control strategies ●Night opening pivoted window and double-leaf windows options
2013 Gossard et al.	Nancy (France) Nice (France)	ANN, NSGA-II	Trnsys	GenOpt	●Energy Consumption ●Summer Comfort Degree	(Variable No.: 4) ●Thermal conductivity of wall and roof ●Volumetric specific heat of wall and roof
2014 Bojić et al.	Kragujevac (Serbia)	Hooke−Jeeves	EnergyPlus	GenOpt	●Embodied Energy ●Energy Consumption	(Variable No.: 2) ●Insulation thickness in exterior wall and roof and material type
2014 Cvetković et al.	Belgrade (Serbia)	Hooke−Jeeves	EnergyPlus	GenOpt	●Embodied Energy ●Energy Consumption	(Variable No.: 2) ●Insulation thickness ●Heating panel location - walls, floor, ceiling and floor&ceiling
2014 Asadi et al.	Coimbra (Portugal)	ANN with GA	Trnsys	GenOpt	●Energy Consumption ●Retrofit Cost ●Total Percentage of Discomfort Hours	(Variable No.: 5) ●Insulation material type for exterior wall and roof ●Window type ●Solar collector type ●HVAC system type
2015 Ascione et al.	Naples (Italy)	MOGA	EnergyPlus	Matlab	●Energy Consumption ●Discomfort Hours	(Variable No.: 9) ●Solar radiation absorption coefficient ●Insulation thickness of walls and roof ●Free cooling options ●Heating and cooling setpoint

						●Window type ●Boiler and chiller type
2015 Carlucci et al.	Mascalucia (Italy)	NSGA-II	EnergyPlus	GenOpt	●Thermal Comfort ●Visual Comfort	(Variable No.: 9) ●Thermal resistance of walls, floor and roof ●Glazing parameters for different orientation window (U-value, G-value, visible transmittance) ●Shading control strategies ●Night opening pivoted window and double-leaf windows options
2015 Echenagu cia et al.	Palermo (Italy) Torino (Italy) Frankfurt (Germany) Oslo (Norway)	NSGA-II	EnergyPlus	Python	●Heating Energy ●Cooling Energy ●Lighting Energy	(Variable No.: 3) ●Thickness of masonry wall ●Number, shape and placement of windows ●Glazing characteristics of the window
2015 Futrell et al.	Charlotte, North Carolina (USA)	Hybrid Hooke–Jeeves and PSO (GPSPSOC CHJ)	EnergyPlus	GenOpt	●Thermal Performance ●Daylight Evaluation	(Variable No.: 11) ●Ceiling height ●The light and solar transmittance of clerestory window, daylight window and view window ●Window width of clerestory window and daylight/view window ●Exterior shading length ●Light shelf length
2015 Junghans et Darde	San Francisco, California (USA) Miana, Florida (USA)	GA combined with SA	EnergyPlus	C++	●Life Cycle Cost	(Variable No.: 8) ●Window U-value, SHGC and light transmittance ●Wall insulation U-value ●Airtightness ●Overhang-wing-wall dimensions
2015 Yu et al.	Chongqing (China)	GA-BP, NSGA-II	EnergyPlus	Matlab	●Energy Consumption ●Thermal Comfort	(Variable No.: 14) ●Layout plan, Floor area, Shape coefficient, Orientation and Stories ●Window wall ratio on North, South, East and West ●Heat transfer coefficient of wall, roof and window ●Heat inertia index of wall and roof
2016 Ascione et al.	Madrid (Spain) Nice (France)	NSGA-II	EenrgyPlus (DesignBuilder as interface)	N/A	●Heating Load ●Cooling Load	(Variable No.: 6) ●Glazing type and WWR

	Naples (Italy) Athens (Greece)					●Local shading and window blind type ●different type of walls and roof
2016 Azari et al.	Seattle, Washington (USA)	GA, NSGA-II	eQuest 3.65, Athena IE (for LCA)	Lazarus 1.2.4 FPC 2.6.2	●Operational Energy ●Global Warming Potential ●Acidification Potential ●Ozone Depletion Potential ●Eutrophication Potential ●Smog Formation Potential	(Variable No.:6) ●WWR on south & north facade ●Window type and window frame material ●Wall thermal resistance and insulation material
2016 Bre et al.	Paraná (Argentina)	GA	EnergyPlus 8.4.0	DEAP	● Thermal Discomfort Degree-Hours with Energy Consumption	●Different type of exterior walls, roof, window, internal walls and floor (first floor)
2016 Delgarm et al.	Tabriz (Iran) Tehran (Iran) Kerman (Iran) Bandar Abbas (Iran)	NSGA-II	EnergyPlus V8.4.0	jEPlus, Matlab	●Cooling Consumption ●Lighting Consumption	(Variable No.: 5) ●Building orientation ●Window length and height ●Overhang tilt angle and depth
2016 Delgarm et al.	Tehran (Iran) Kerman (Iran) Bandar Abbas (Iran) Tabriz (Iran)	MOPSO	EnergyPlus	Matlab	●Heating Demand ●Cooling Demand ●Lighting Demand	(Variable No.:12) ●Building rotation ●Window length and height ●Glazing conductivity, solar and visible transmittance ●Wall conductivity, thermal, solar and visible absorptance ●Overhang tilt angle and depth
2016 Delgarm et al.	Tehran (Iran) Kerman (Iran) Bandar Abbas (Iran) Tabriz (Iran)	MOABC	EnergyPlus	Matlab, jEPlus	●Energy Consumption ●Thermal Confort	(Variable No.:12) ●Building rotation ●Window length and height ●Glazing conductivity, solar and visible transmittance ●Wall conductivity, thermal, solar and visible absorptance ●Heating and cooling setpoint temperature

142

2016 Hamdy et al.	Helsinki (Finland)	pNSGA-II, MOPSO, PR_GA, ENES, evMOGA, spMODE-II and MODA	IDA-ICE 4.6	Matlab (Mathwork, optimizatio n toolbox)	●Primary Energy Consumption ●Life Cycle Cost	(Variable No.:16) ●Building envelope package ●Lighting and appliances: efficiency ●Heat recovery: type(efficiency) ●Auxiliary system: fans and pumps ●Buffer tank: size and insulation level ●Solar thermal collector: area ●Photovoltaic: area, efficiency, slope angle and azimuth angle ●Heating Unit: type, size, supply water temperature, start and stop operating hour
2016 Kerdan et al.	London (UK)	NSGA-II	EnergyPlus, ECB IEA Annex 49	jEPlu+EA	●Exergy Efficiency ●Energy Use ●Thermal Comfort Hour	(Variable No.: 7) ●HVAC system type ●Walls, roof and ground insulation type and thickness ●Sealing (cracks, joints and holes percentage) ●Glazing type ●Heating and Cooling set-point ●Lighting type ●Electric equipment retrofit to different efficient
2016 Schwartz et al.	Manchester (UK)	MOGA (NSGA-II)	EnergyPlus	jEPlu+EA	●Life-cycle Cost ●Life-cycle Carbon Footprint	(Variable No.: 9) ●Insulation thickness of Panel, Street and exterior ●Brick thickness ●Thermal bridges insulation thickness ●WWR on each floor with different orientation
2016 Xu et al.	Pittsburgh, Pennsylvania (USA)	NSGA-II, aNSGA-II, ammNSGA-II	EnergyPlus	Java	●Initial Investment Cost ●Operation Cost	(Variable No.: 6) ●Exterior walls and roof type ●Window type ●Lighting type ●Daylight control ●HVAC system type
2017 Ascione et al.	Naples (Italy)	CAMO, SLABE, ANN	EenrgyPlus	Matlab	●Primary Energy Consumption ●Discomfort Hours ●Globle Cost	(Variable No.: 48) ●Orientation ●Number of floors, area of each floor, form ration and floor height ●Window wall ratio on South, North, East and West ●Walls each layers' materials and their thickness, conductivity, density and specific heat

143

Year/Author	Location	Algorithm	Model	Tool	Objectives	Variables
						●Concrete thickness - partitions ●Roof and floor material type and their thickness, conductivity, density and specific heat ●External walls' and roof's solar absorptance ●Type of window glasses and frame ●Internal heat gain: people density, artificial light and equipment load ●Infiltration rate ●Heating and cooling setpoint temperature ●HVAC type
2017 Chen et Yang	Hong Kong (China) Los Angeles (USA)	NSGA-II	EnergyPlus, Model*: (MLR), (MARS) and (SVM)	jEplus, R program	●Heating Demand ●Cooling Demand ●Lighting Demand	(Variable No.: 9) ●Building orientation and external obstruction angle ●Exterior wall thermal resistance and specific heat ●Window solar heat gain coefficient and U-value ●Window to ground ratio ●Overhang projection factor ●Infiltration air mass flow coefficient
2017 Fan et al.	South African	GA	N/A	N/A	●Energy Saving ●Net Present Value ●Payback Period of Investment	(Variable No.: 6) ●Window type ●Exterior wall and roof insulation material type and thickness ●Solar panel type
2017 Roberti et al.	Bolzano (Italy)	NSGA-II	EnergyPlus 7.2	original C	●Heating Demand ●Cooling Demand ●Thermal Comfort	(Variable No.: 8) ●Facade insulation location (interior/exterior), partly or fully extent and thickness ●Roof insulation location (interior/exterior), partly or fully extent and thickness ●Glazing or window replacement ●Cooling system (Yes/NO)
2017 Pal et al.	Helsinki (Finland)	NSGA-II	IDA ICE, Excel	MOBO	●Life Cycle Energy ●Life Cycle Cost	(Variable No.: 4) ●Insulation thickness of exterior walls, roof and floor ●Window type
2017 Yang et al.	Chiayi (Taiwan, China)	NSGA-II	MOPBEM	MOPBEM	●Envelope Construction Cost ●Envelope Energy Performance	(Variable No.: 9) ●Window number, size (length and width), material type ●Walls and roof material type

144

					●Window Opening Rate	●Glass curtain material type ●Sunshade type and size
aNSGA-II - Adaptive Operators with NSGA-II						
ANN - Artificial Neural Network						
ammNSGA-II - Adaptive Meta-model with NSGA-II						
BP - Back Propagation						
CAMO - Cost-optimal Analysis by Multi-objective Optimization						
DEAP - Distributed Evolutionary Algorithms in Python						
ENSES - Elitist Non-dominated Sorting Evolution Strategy						
evMOGA - Multi-Objective Evolutionary Algorithm Based on the Concept of Epsilon Dominance						
GA - Genetic Algorithm						
GA-RF - Genetic Algorithm with Refine Process						
LCA - Life Cycle Assessment						
MARS - Multivariate adaptive regression splines						
MLR - Multiple linear regression						
MOABC - Multi-Objective Artificial Bee Colony						
MOBO - Multi-Objective Building Optimization						
MODA - Multi-Objective Dragonfly Algorithm						
MOGA - Multi-Objective Genetic Algorithm						
MOO - Multi-Objective Optimization						
MOPBEM - Multiobjective Optimal Model on Building Envelope design						
MOPSO - Multi-Objective Particle Swarm Optimization						
NSGA-II - Non-dominated-and-crowding Sorting Genetic Algorithm II						
pNSGA-II - Controllrf Non-dominated Sorting Algorithm with a Passive Archive						
PR-GA - Preparation Process and Genetic Algorithm						
PR_GA - Two-phase Optimization Using the Genetic Algorithm						
PSO - Particle Swarm Optimization						
SA - Simulated Annealing Optimization						
SLABE - Simulation-based Large-scale Uncertainty/Sensitivity Analysis of Building Energy Performance						
spMODE-II - Multi-Objective Differential Evolution Algorithm						
SVM - Support vector machine						